uOttawa

L'Université canadienne
Canada's university

FACULTÉ DES ÉTUDES SUPÉRIEURES ET POSTOCTORALES

uOttawa

L'Université canadienne
Canada's university

FACULTY OF GRADUATE AND POSDOCTORAL STUDIES

Jing Zhang

AUTEUR DE LA THÈSE / AUTHOR OF THESIS

M.Sc. (Cellular and Molecular Medicine)

GRADE / DEGREE

Department of Cellular and Molecular Medicine

FACULTÉ, ÉCOLE, DÉPARTEMENT / FACULTY, SCHOOL, DEPARTMENT

Role of Hedgehog Signaling in Branching Morphogenesis and Patterning of the Fin Ray during Zebrafish Fin Regeneration

TITRE DE LA THÈSE / TITLE OF THESIS

Dr. M-A. Akimenko

DIRECTEUR (DIRECTRICE) DE LA THÈSE / THESIS SUPERVISOR

CO-DIRECTEUR (CO-DIRECTRICE) DE LA THÈSE / THESIS CO-SUPERVISOR

EXAMINATEURS (EXAMINATRICES) DE LA THÈSE / THESIS EXAMINERS

Dr. M. Ekker

Dr. M. Hincke

Gary W. Slater

Le Doyen de la Faculté des études supérieures et postdoctorales / Dean of the Faculty of Graduate and Postdoctoral Studies

Role of Hedgehog signaling in branching morphogenesis and patterning of the fin ray during zebrafish fin regeneration

Jing Zhang

Thesis submitted to the
Faculty of Graduate and Postdoctoral Studies
in partial fulfillment of the requirements for the degree of

Master of Science

In Cellular and Molecular Medicine

Department of Cellular and Molecular Medicine
Faculty of Medicine
University of Ottawa

Your file Votre référence
ISBN: 978-0-494-25847-7
Our file Notre référence
ISBN: 978-0-494-25847-7

Dedicated to my parents, Jianguo Zhang and Yue-e Wang,
the reason for my existance

Abstract

Zebrafish have the capability to regenerate their fins after injury. Previous studies from our laboratory showed that fin regeneration triggers the re-expression of genes involved in the hedgehog (hh) signaling pathway. One member of the hh family, *sonic hedgehog (shh)* was suggested to regulate bone patterning based on its expgression pattern and functional analysis. Another member of the hh family, *indian hedgehog (ihha)* is expressed in the differentiating scleroblasts, the bone-matrix releasing cells, of each fin ray, and may have a more direct role on bone formation based on its expression pattern and known function in other vertebrates. The present study is aimed at investigating the role of hh signalling in patterning the fin ray regenerate and more specifically its role in ray branching morphogenesis. In a first approach, we used the zebrafish *2.2shh:gfp:ABC* transgenic line, in which GFP expression recapitulates the endogenous expression of *shh,* to ablate the *shh*-expressing cells using a laser beam. Results show that such ablation leads to a delay of ray bifurcation suggesting that the *shh*-expressing cells play an important role in branching morphogenesis. In a second approach, we cloned the zebrafish *hedgehog interacting protein (hip)*, a hedgehog antagonist, to investigate the effects of its overexpression on ray patterning. Analysis of *hip* expression during fin regeneration suggests its involvement in limiting hh signaling on the lateral sides of the dermal bones and in their medial region during branching morphogenesis. Overexpression of *hip* via *in vivo* cell transfection in the regenerating fin causes a branching delay, possibly as a result of the altered expression of *patched1,* the hh receptor and *type X collagen,* a component of the fin ray. These results suggest that hh signaling is involved in patterning the ray branching during zebrafish fin regeneration. Based on the distinct

role of shh and ihha suggested by studies in other systems, ihha may be more involved in the scleroblast proliferation and differentiation, and shh is likely to be responsible to pattern the bone formation by directing the site of scleroblast differentiation or possibly mediating scleroblast migration.

Table of content

List of figures

List of Abbreviations

Bmp	Bone morphogenetic protein
bp	Base pairs
BrdU	Bromo-2'-deoxy-uridine
cDNA	Complementary deoxyribonucleic acid
CMV	Cytomegalovirus
col10	Type X Collagen
col2	Type II Collagen
DEPC	diethylpyrocarbonate
Dhh	Desert hedgehog
DiI/Di-I	1.1'-dioctadecyl-3,3,3'3'-tetramethyl indocarbocyanine perchlorate
DNA	Deoxyribonucleic Acid
dpa	Days post amputation
EGFP	Enhanced Green Fluorescent Protein
Ehh	Echidna hedgehog
Fgf	Fibroblast growth factor
Fgfr	Fibroflast growth factor receptor

GFP	Green Fluorescent Protein
Hh	Hedgehog
Hip	Hedgehog-interacting protein
Ihh	Indian hedgehog
Ihha	Indian hedgehog a
kDa	kilo Daltons
Lef1	Lymphoid Enhancer Factor 1
mRNA	Messenger ribonucleic acid
PBS	Phosphate buffered saline
PBST	Phosphate buffer saline/ 0.1%Tween-20
PFA	Paraformaldahyde
Ptc	Patched
RA	Retinoic acid
RAR	Retinoic acid receptor
RARE	Retinoic acid response element
Shh	Sonic hedgehog
Shh-N	N-terminal fragment of shh

Smo	Smoothened
tRNA	Transfer ribonucleic acid
Twhh	Tiggy winky hedgehog
ZPA	Zone of polarizing activity

Acknowledgement

I would like to express my sincere appreciation to my supervisor Dr. Marie-Andreé Akimenko for giving me the opportunity to to pursue my Master degree in her lab and for her dedicated instruction, which helps me learn not only knowledge and skills but also scientific attitude. I would also like to thank my advisory committees, Dr. Marc Ekker, Dr. Cristofre Matin and Dr. Valerie Wallace for their advice and help. To Amanda Smith and Fabien Avaron, I owe you many thanks for helping me with the lab techniques and skills and I wish you all the best and good luck in the future. To Danielle Guay, I thank you for your kindness and hard work and for the organized lab and fish facility; you are the best lab technician I ever know. For other members of the Ekker and Akimenko labs, I thank you for the assistance and laugh. I would also thank other members in the Ottawa Health Research Institute and in the Department of Cellular and Molecular Medicine, University of Ottawa for their contribution. I would like to express my great gratitude to my parents for their trust and support and for always granting me the freedom to pursue whatever I truly want. To my boyfriend Yanwei Xi, thank you for your love and care and everything that is more than I can say. To my friends, thank you for the weekends and the enjoyment; I wish you guys all the happiness in the world

Introduction

1. Significance of regeneration studies

Damaged vertebrate organs heal through one of two mechanisms: repair or regeneration. Repair is characterized by heavy inflammation and permanent scar, while regeneration is the process by which damaged or lost structures are replaced almost perfectly. Based on cellular mechanisms, regeneration can be categorized into two types: morphallaxis and epimorphosis. Morphallaxis refers to the type of regeneration in which lost body parts are replaced by the remodeling of the remaining tissue. This process of regeneration involves little or no cellular proliferation. In contrast to morphallaxis, epimorphosis requires active cellular proliferation and formation of a blastema prior to the replacement of the lost body part (Morgan, 1901). For example, when the limb of a newt is amputated, epidermal cells from the remaining stump migrate to cover the wound surface, forming the wound epidermis. This single-layered structure is required for the regeneration of the limb. Then the cells beneath it, including bone cells, cartilage cells, fibroblasts, myocytes, and neural cells, undergo a dramatic dedifferentiation. These cells will subsequently enter the cell cycle and proliferate to form an undifferentiated cell mass, called the regeneration blastema (Tanaka, 2003; Odelberg, 2005). This blastema is necessary for proper regeneration. As the regeneration proceeds, the blastema cells re-differentiate into all the cell types required for the reestablishment of the lost part (Butler, 1935). Epimorphosis depends on the limb innervation (Singer, 1954).

Teleost fishes, as well as several aquatic urodele amphibians, master the art of

epimorphic regeneration. This regenerative capability has been lost through evolution. Regeneration in mammals during adulthood only occurs in rare cases, such as the deer antlers, the cartilage of the rabbit ear, and the membrane (but not the bones) of bat wings (Akimenko et al., 2003). Therefore, investigation of the mechanisms of regeneration in lower vertebrate model systems will give promising prospect: if we understand how regeneration occurs naturally in these organisms, we may learn how to activate the regenerative process in mammals including in humans.

2. The zebrafish caudal fin is a good model for studying regeneration

a. Advantage of the zebrafish as a model for regeneration

Zebrafish, *Danio rerio*, is widely used as a research model for developmental biology and human disease (Berghmans et al., 2005; Drummond, 2005). Zebrafish is a freshwater teleost fish that is originally found in slow streams and rice paddies and in the Ganges River in East India and Burma. In 1981, Dr. George Streisinger published methods for mutational and genetic analysis of zebrafish embryos (Streisinger et al., 1981), initiating the use of zebrafish as research model for developmental biology. Since then, the use of the zebrafish in research has spread to over 300 developmental and genetics laboratories in over 30 countries. Zebrafish became one of the ideal research model for developmental biology and human disease for several reasons (Westerfield, 1995): 1) their small size and adaptation to many environments make it easy to maintain a large number of zebrafish; 2) females lay large quantity of eggs every few days and the eggs are externally fertilized; 3) the embryos develop outside the mother's body and are transparent during early development allowing the visualization of developing organs; 4) they develop rapidly and reach sexual maturity

in 3 months; 5) zebrafish embryos are easily amenable to physical manipulation; 6) many studies have been conducted on zebrafish embryonic development at the cellular and genetic levels and various methods and tools have been developed for molecular research using zebrafish; 7) the sequencing of the zebrafish genome is almost finished.

Zebrafish is capable of regenerating several parts of its body after lesion including the optic nerve, scales, heart, spinal cord and all fins. The caudal fin is adopted here as a model because this organ is easily accessible for surgery, its injury does not compromise survival, the regenerated portions are relatively transparent, and the caudal fin possesses a relatively simple, symmetric structure with limited cell types. These advantages, as well as a rapid regeneration process make zebrafish an ideal model to study limb regeneration.

b. Structure of the zebrafish fin

The zebrafish fins are composed of skeletal elements, epidermis, blood vessels, nerves and connective tissue. The skeleton of a caudal fin is made of a protruding visible exoskeleton, connected to the endoskeleton by ligaments. The endoskeleton is made of endochondral bones termed "hypurals" on which articulate the fin rays (Mabee and Bird, 2001). The endoskeleton will not regenerate following amputation. The exoskeleton, which is the part capable of regeneration, consists of bony fin rays (Figure1B), also known as lepidotrichia, and soft unmineralized collagenous fibrils, named actinotrichia. The lepidotrichia ontogenesis occurs by direct mineralization of a collagenous matrix without passage through a cartilage precursor and therefore

corresponds to the definition of dermal bones or intramembranous bones (Geraudie and Landis, 1982; Sire and Akimenko, 2004; Haas, 1962). However, the recent finding of the expression of cartilage markers, such as *ihha* and *col10a1*(Avaron et al., 2006), as well as *col2a1*, *sox9a* and *sox9b* (Smith et al, submitted), suggest that the lepidotrichia present an intermediate phenotype between cartilage and dermal bone. A lepidotrichium consists of a pair of symmetrical concave hemirays, surrounded by a monolayer of bone-secreting cells, called scleroblasts. Blood vessels, nerves, pigment cells and fibroblast-like cells are sheltered within the space between the two hemirays as well as in the interray tissue. Each hemiray is made of multiple successive segments joined end-to-end by ligaments (Figure1C). A fin grows in length throughout the entire life of the fish by sequential addition of bone segments of constant length to the end of the rays, rather than by an increase in the length of a fixed number of segments. There are 18 lepidotrichia in each zebrafish caudal fin, and except for the two most lateral ones, all the other lepidotrichia bifurcate periodically along the proximo-distal axis of the fin to form sister branches (Akimenko et al., 2003; Poss et al., 2003).

A

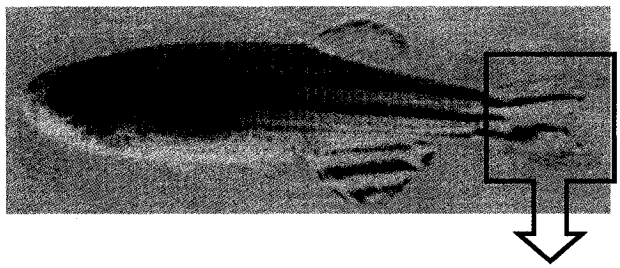

B

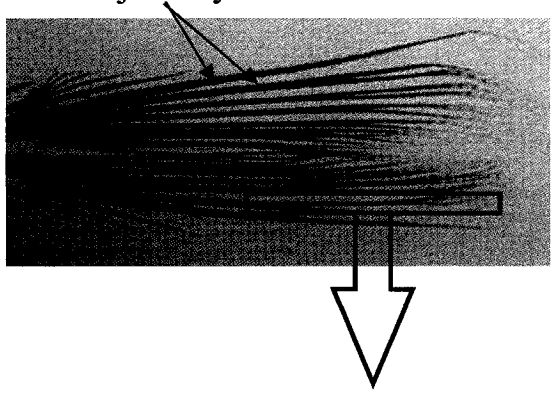
Major Rays

C

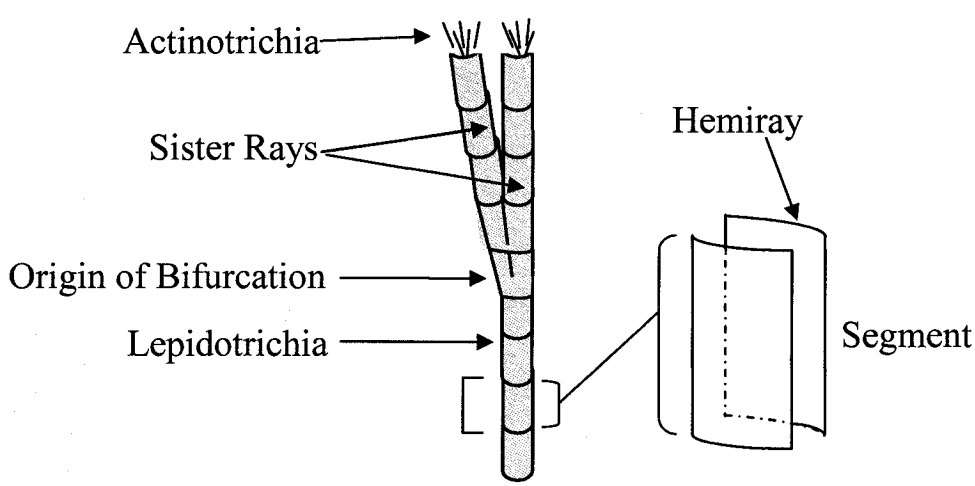
Actinotrichia
Sister Rays
Origin of Bifurcation
Lepidotrichia
Hemiray
Segment

Figure 1

Figure 1: Structure of the zebrafish caudal fin.

A: an adult zebrafish. **B:** the skeleton of zebrafish caudal fin. **C:** schematic representation of a fin ray (lepidotrichia). A fin ray comprises soft unmineralized actinotrichia and bony lepidotrichia, also called bony fin ray which consists of two symmetrical hemirays. Each hemiray is made of successive segments, connected to each other by ligaments.

3. A brief review of the process of regeneration and of the genes involved in regeneration

Zebrafish fin regeneration is a very rapid process (Figure 2A). The lost part of the fin can be replaced in three weeks. The early regenerative events after amputation include four major stages (Figure 2B-E): 1) covering of the cut stump by the wound epidermis, 2) disorganization and migration of mesenchymal cells to the wound, 3) formation of a blastema and 4) outgrowth of the fin regenerate. In the following parts or sections, the four stages will be described in more details and genes that are found involved in these processes will be briefly reviewed.

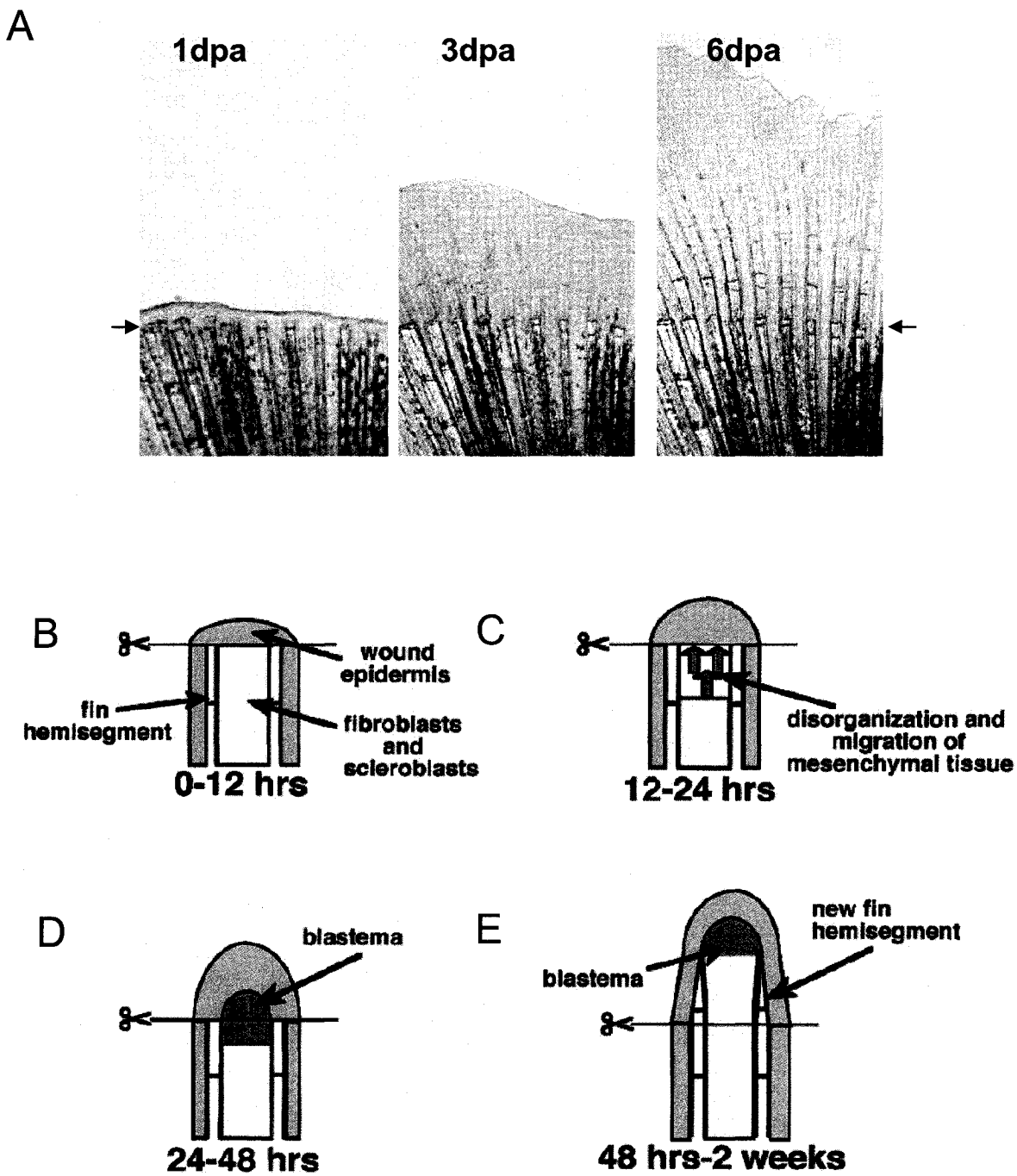

Poss, K. D., J. Shen, et al. (2000). Dev Biol 222(2): 347-58.

Figure 2

Figure 2: The process of zebrafish fin regeneration.

A: zebrafish caudal fin regeneration is a rapid process. The three panels show the same regenerate at 1dpa, 3dpa and 6dpa. The arrows indicate the level of amputation.

B-E: schematic representation of longitudinal sections (top, posterior; bottom, anterior) of caudal fin regenerates at different stages. **B**, During the first 12 h, epidermal cells migrate to cover the stump. **C**, Within the next 12 h, the wound epidermis thickens, while cells located within one or two bone segments proximal to the amputation plane lose their dense organization and show signs of distal migration. **D**, Next, these mesenchymal cells proliferate to form a blastema, a mass of undifferentiated tissue, just distal to the ray stumps. **E**, During the outgrowth stage, proximal cells of the regeneration blastema differentiate while distal cells divide and maintain outgrowth. The time course represents the regenerative events at 33℃.

a. Wound healing and formation of the wound epidermis

Remarkably, there is little bleeding after fin amputation. The stump is covered by epithelial cells that migrate to the wound within a few hours after amputation. A multilayered epidermal cap forms and this process involves little or no cell proliferation (Poleo et al., 2001; Santos-Ruiz et al., 2002) (Figure 2B). Little is known about the mechanisms of the migration of epithelial cells to form an epidermal cap. *β-catenin* is expressed in the wound epidermal cells (Poss et al., 2000) and is presumed to be part of a cascade involved in the maintenance of cell-cell interactions to facilitate migration (Poss et al., 2003). *Lef1* is markedly up-regulated in the newly formed wound epidermis of the fin regenerate (Poss et al., 2000). However the role of Lef1 in the formation of the epidermal cap has not been investigated.

During wound healing and formation of the wound epidermis following newt limb amputation, *9-cis* retinoic acid (*9-cis* RA) is synthesized and released by the wound epidermis. This creates a concentration gradient of RA in the regenerative blastema (Viviano et al., 1995). Such analysis has not been repeated in zebrafish, but RA receptors are expressed in the early fin ray blastema at 2 days post amputation (dpa) and in the distal blastema at later stage (White et al., 1994). In addition, treatments with retinoic acid during fin regeneration can result in multiple fusions of adjacent lepidotrichia (White et al., 1994) and disruption of the expression of many genes, including *shh, ptc1* and *bmp2b* (Laforest et al., 1998), suggesting a regulatory role of RA in morphological patterning of the fin regenerate.

b. Initiation of blastema formation

While the epidermal cap is forming, the fibroblast-like cells located close to the wound (up to two segments) reorganize and migrate distally toward the epidermal cap (Figure 2C). Analyses of BrdU incorporation show that a large number of these cells start to proliferate (Poleo et al., 2001; Santos-Ruiz et al., 2002). As they continue to proliferate, a blastema forms under the epidermal cap (Figure 2D) (Poleo et al., 2001; Santos-Ruiz et al., 2002). Studies in newt revealed that cell dedifferentiation is a crucial step leading to the formation of a blastema. This was suggested by the observation that when mature multi-nucleate myocytes are labeled with a fluorescent dye, the fluorescent labeling is later observed during limb regeneration in mono-nucleate cells (Lo et al., 1993). At a later stage of the regeneration process, labeling is also observed in cartilage cells suggesting a mechanism of transdifferentiation (Lo et al., 1993). Dedifferentiation is presumed to be involved in the formation of the blastema during zebrafish fin regeneration as well, but to date there is no convincing evidence for the existence of such process. Alternatively, blastemal cells could originate from a pool of progenitor cells present in the normal fin ray, but this proposal still remains to be tested.

During blastema formation, expression of *msxB* and *msxC* is induced in the blastema cells at the tip of each fin ray, while cells of the overlying epithelium express *msxD* (Akimenko et al., 1995). *Msx* genes are homeobox genes proposed to be involved in epithelial-mesenchymal interactions required for the growth of the vertebrate developing limb/fin buds (Coelho et al., 1992; Akimenko et al., 1995). In addition, *msx* genes have been shown to be responsible for maintaining the cells in an undifferentiated state, as suggested by the finding that forced expression of *Msx1* in

determined mouse myogenic cells blocks their terminal differentiation in vitro (Song et al., 1992). Furthermore, expression of *Msx1* in mouse myotubes induces *in vitro* dedifferentiation of these cells ((Muneoka and Sassoon, 1992; Song et al., 1992; Odelberg et al., 2000). These results suggest that during limb and fin regeneration, the *msx* genes may be involved in the dedifferentiation step and initiation of blastema formation.

Fibroblast growth factor (fgf) signaling is required for blastema formation. *Fibroblast growth factor receptor 1 (fgfr1)* is expressed in mesenchymal cells underlying the wound epidermis, and specific inhibition of Fgfr1 immediately following fin amputation blocks blastema formation without obvious effects on wound healing, cell proliferation and onset of *msx* gene expression (Poss et al., 2000). *Fgf20a* is expressed during initiation of fin regeneration in the mesenchymal cells underneath the wound epidermis and later its expression overlaps with the blastema marker *msxb*. Furthermore, *fgf20a* null mutant fails to form a blastema suggesting that this factor is required for the initiation of the regeneration and formation of a blastema (Whitehead et al., 2005). The heat-shock protein 60 (hsp60) is also required for blastema formation and maintenance, as suggested by the finding that fin regeneration fails in *hsp60* null mutant due to a defective blastema formation (Makino et al., 2005).

c. Outgrowth of the blastema

Soon after the formation of a blastema, the regenerate enters the outgrowth phase (Figure 2E). This phase is characterized by the presence of a mature blastema and proximally-positioned differentiating tissue, which consists of scleroblasts and

fibroblast-like cells. At the onset of this outgrowth phase, the blastema is subdivided into two zones: the distal blastema and the proximal blastema (Nechiporuk and Keating, 2002) (Figure 3A and B).

Cells of the distal blastema are characterized by their slow cell-cycling and the expression of fibroblast growth factors family (fgf) such as *fgf8* (unpublished data of our lab) and the receptor *fgfr1* (Poss et al., 2000), the bone morphogenetic proteins, *bmp4* (Murciano et al., 2002) and *bmp6* (Smith et al, submitted), *msxb* and *msxc* (Akimenko et al., 1995). Inhibition of Fgfr1 during fin regeneration prevents further outgrowth of the regenerates and down-regulates the expression of blastemal *msx* genes (Poss et al., 2000).

The proximal blastema is localized immediately beneath the distal blastema. In contrast to the distal blastema, cells of the proximal blastema are highly proliferative. *Bmp6* is expressed in cells of the proximal blastema too. No defined boundary is present between these two zones. Based on the difference in the cell cycling rate and gene expression between the two blastema cell populations, it has been proposed that the distal blastema may serve as a pool of pluripotent progenitor cells for the proximal blastema.

The cells located more proximally than the proximal blastema are entering the zone of differentiation which consists of differentiating mesenchymal cells and scleroblasts (Poss et al., 2003). How the different zones of the regenerate are set and maintained is not clear yet.

A

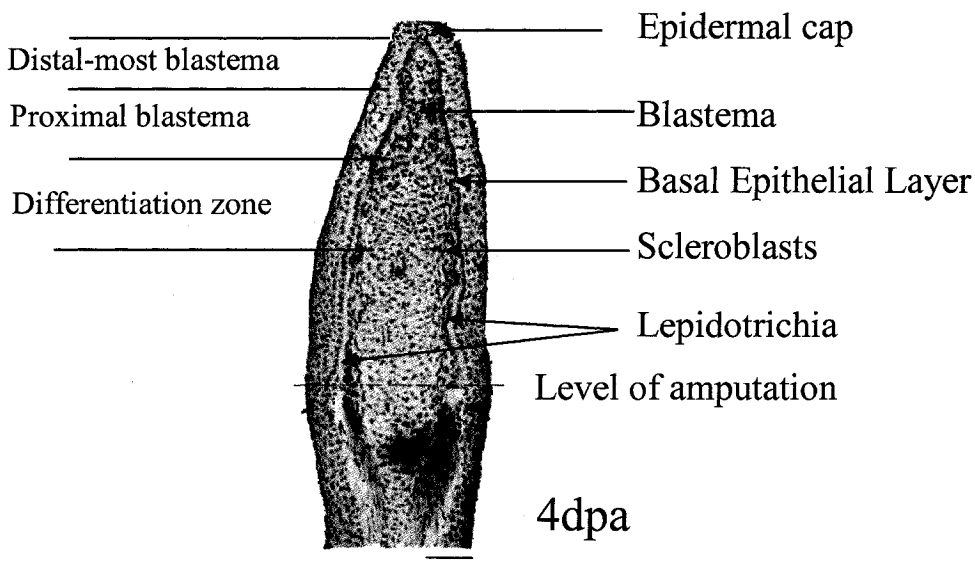
Epidermal cap
Distal-most blastema
Proximal blastema
Blastema
Basal Epithelial Layer
Differentiation zone
Scleroblasts
Lepidotrichia
Level of amputation
4dpa

B

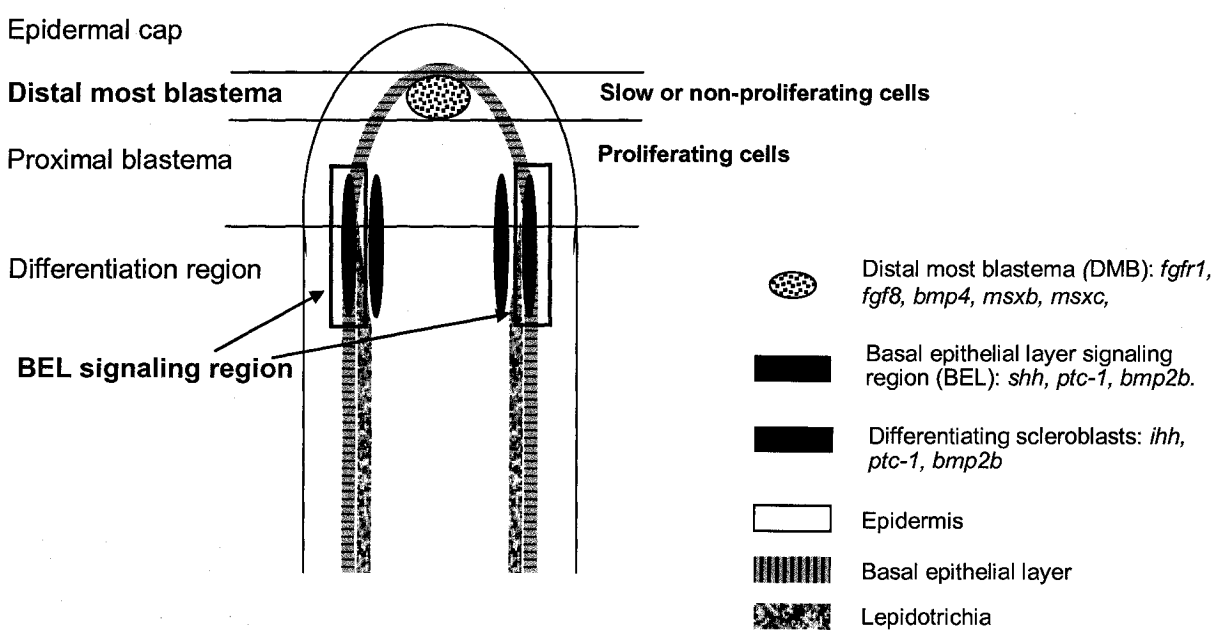
Epidermal cap
Distal most blastema
Slow or non-proliferating cells
Proximal blastema
Proliferating cells
Differentiation region
BEL signaling region
Distal most blastema (DMB): fgfr1, fgf8, bmp4, msxb, msxc,
Basal epithelial layer signaling region (BEL): shh, ptc-1, bmp2b.
Differentiating scleroblasts: ihh, ptc-1, bmp2b
Epidermis
Basal epithelial layer
Lepidotrichia

Figure 3

Figure 3: The blastema during the outgrowth phase.

A: A longitudinal section of a regenerate at 4dpa, indicating the histological structure of the regenerate. B: Schematic representations of the various regions of the fin regenerate during the outgrowth phase.

d. Differentiation of the blastemal cells

Studies on cell differentiation during fin regeneration have been mainly focused on the analysis of the regeneration of the lepidotrichia. The bone matrix of the lepidotrichia is secreted by a specific type of cells, termed scleroblasts (Figure 3A and B). Blastema cells located in the proximal part of the blastema and lining the epidermis differentiate into scleroblasts (Santamaria and Becerra, 1991). These cells release the bone matrix in the epithelial-mesenchymal interface. As the lepidotrichia matures and grows, some scleroblasts migrate around the already deposited matrix into the epithelial-mesenchymal interface where they continue to secrete the bone matrix contributing to the thickening of the lepidotrichia (Santamaria and Becerra, 1991). Scleroblasts express cartilage markers such as *Type II Collagen* (*col2a1*) (Johnson and Weston, 1995) and *Type X Collagen* (*col10a1*) (Avaron et al., 2006), as well as *Indian Hedgehog a (ihha)* (Avaron et al., 2006) and its receptor *Patched1 (ptc1)* (Laforest et al., 1998). A subset of cells in the basal epithelial layer, located at the same level along distal-proximal axis as the newly differentiating scleroblasts, express the morphogen *Sonic Hedgehog (shh)*, its receptor *ptc1*, and *bmp2b* (Laforest et al., 1998). As it will be discussed further later, the expression patterns of these genes and functional analyses suggest their possible role in the differentiation of the scleroblasts or patterning of the regenerating lepidotrichia.

4. Hedgehog signaling

First identified (Nusslein-Volhard and Wieschaus, 1980) and cloned (Lee et al., 1992; Mohler and Vani, 1992; Tabata et al., 1992; Tashiro et al., 1993) in *Drosophila*, Hedgehog (Hh) has interested many developmental biologists. Hh and its vertebrate

homologs (see below) are secreted proteins involved in cell-cell communication and play important roles in coordinating cell differentiation thus regulating tissue formation during invertebrate and vertebrate development (Ingham and McMahon, 2001). Three members of the Hh family have been identified in mammals, *sonic hedgehog (shh), indian hedgehog (ihh),* and *desert hedgehog (dhh).* Shh is a very important morphogen that is involved in morphogenesis of many organs and patterning of many tissues (reviewed in Ingham and McMahon, 2001). In the following sections the functions, transmission and reception of Hh proteins will be briefly reviewed.

a. A brief review of the functions of Shh and Ihh

Shh is expressed in three key signaling centers in the vertebrate embryo: the notochord, the floor plate of the neural tube, and the zone of polarizing activity (ZPA) of the limb/fin bud (reviewed in Ingham and McMahon, 2001). Ectopic expression of *shh* in the neural tube results in the inappropriate activation of genes normally expressed in the floor plate, in the dorsal CNS (Echelard et al., 1993; Krauss et al., 1993; Roelink et al., 1994). Shh is expressed in the ZPA, a region located in the posterior mesenchyme in the limb and fin buds, which is essential for patterning the antero-posterior axis of the bud. Ectopic expression of Shh in the anterior limb mesenchyme produces a mirror-image duplication of the digits, implicating shh in the anterior-posterior patterning of the limb (Riddle et al., 1993; Chang et al., 1994). Shh is also required for patterning of the eyes. Targeted disruption of the *shh* gene in mouse results in embryos with severe anterior neural tube defects and a single fused primitive optic vesicle (Chiang et al., 1996). Overexpression of *shh* in zebrafish

embryos causes eye malformations (Ekker et al., 1995; Macdonald et al., 1995).

Shh has also been shown to be an essential factor for the regulation of branching morphogenesis in different organs such as the lungs (van Tuyl and Post, 2000; Hu and Rosenblum, 2003; Miller et al., 2004), prostate (Pu et al., 2004), and salivary glands (Jaskoll et al., 2004). Shh regulates branching morphogenesis by mediating epithelial-mesenchymal interactions. When acting as a branching morphogen, *shh* is expressed in the epithelial cells, and patterns the tissue via its transmembrane receptor ptc1, which is expressed in the adjacent mesenchymal cells. Formation of branches involves interactions between Shh signaling pathways and Fgf and Bmp signaling pathways (Affolter et al., 2003; Warburton et al., 2005).

Shh functions as a morphogen probably by its capability of regulating cell proliferation, differentiation and cell survival as evidenced in the following examples. In $Shh^{-/-}$ mouse or cyclopamine-treated wild-type mouse, lung mesenchymal cells proliferation and differentiation are defective (Li et al., 2004). Inactivation of hedgehog signal leads to regression of basal cell carcinoma accompanied by reduced tumor cell proliferation and increased apoptosis (Hutchin et al., 2005). In cultured mouse muscle satellite cells, Shh inhibits caspase-3 activation and apoptosis induced by serum deprivation, and these effects are reversed by simultaneous treatment with cyclopamine, a specific inhibitor of the Hh pathway (Koleva et al., 2005). In $Smo^{n/c}$; $Nestin^{cre}$ mouse in which Shh signaling is removed, the number of neural progenitors is dramatically reduced in both the postnatal subventricular zone and hippocampus. This is partially attributable to a marked increase in programmed cell death in the

subventricular zone (Machold et al., 2003). Interestingly, Shh regulates cell differentiation both positively and negatively. Shh maintains the enteric neural crest cells in an undifferentiated state *in vitro* (Fu et al., 2004). However, Shh also induces differentiation of osteoblasts *in vitro* (Yuasa et al., 2002). What factor(s) regulates the different regulatory potentials of Shh in cell differentiation is not clear yet.

Ihh was shown to be involved in the development of chondrocytes in developing endochondral bones (St-Jacques et al., 1999; Long et al., 2004; Colnot et al., 2005; Avaron et al., 2006), and in hematopoiesis and vasculogenesis (Dyer et al., 2001; Byrd et al., 2002; Colnot et al., 2005). In the appendicular skeleton of the mouse, Ihh is secreted by pre-hypertrophic and early hypertrophic chondrocytes (Bitgood and McMahon, 1995). Functional analyses in mouse embryos have shown that Ihh slows down the differentiation of proliferative chondrocytes into hypertrophic chondrocytes through a negative feedback loop involving the parathyroid hormone related peptide (PTHrP) (Vortkamp et al., 1996). In the forelimb cartilage of $Ihh^{-/-}$ mutant mice, chondrocyte proliferation is markedly reduced, chondrocyte maturation is delayed and mature osteoblasts are absent (St-Jacques et al., 1999). During gastrulation of the mouse embryo, blocking Ihh function in primitive endoderm inhibits activation of hematopoiesis and vasculogenesis in the adjacent epiblast (Dyer et al., 2001). $Ihh^{-/-}$ mice have fewer and smaller blood vessels in the yolk sac, and show a substantial decrease in the expression of hemangioblast markers and angiogenesis markers (Byrd et al., 2002).

Dhh is involved in maturation of the testes, male germ line development,

masculinization (Bitgood et al., 1996; Clark et al., 2000) and the formation of peripheral nerve sheath (Parmantier et al., 1999; Umehara et al., 2000).

b. Transmission and reception of hedgehog proteins

The mouse *shh* gene encodes a protein of 47.8kDa with a signal peptide of 24 amino acids. The Shh precursor protein undergoes an intramolecular cleavage after translation, generating a C-terminal and an N-terminal products of 30kDa and 19kDa, respectively (Bumcrot et al., 1995). The C-terminal peptide has no other known function than catalyzing the autocleavage reaction (Porter et al., 1995), while the secreted N-terminal fragment (termed Shh-N) is sufficient for all the known biological activities of Shh (Ingham and McMahon, 2001). During the auto-processing, a cholesterol molecule is covalently attached to the C-terminal of Shh-N (Porter et al., 1996). In addition, the Shh protein is palmitoylated at the Cys-24 site (Pepinsky et al., 1998).

Shh functions via a combination of short- and long-range signaling. Three models, which are not necessarily mutually exclusive, have been proposed to mediate long-range signaling (Goetz et al., 2002): 1) simple diffusion of Shh-N, 2) transport of the Shh protein by other factors and 3) direct delivery of Shh to target cells via cytonemes, a thin, actin-based cell extensions. Consistent with the simple diffusion model, a native freely diffusible form of Shh which is cholesterol-modified, multimeric and biologically potent has been characterized (Zeng et al., 2001). Such free diffusion creates a Shh gradient, and cells closest to the *shh*-expressing cells are exposed to the highest concentration of Shh. Many recent studies support the presence

of proteins modulating the extracellular transport of hh proteins. In the mutant *Drosophila* that lacks shifted (shf), a glypican Dally-like (Dlp) protein, or lacks the transferase that adds heparan-sulphate side chains to Dlp, the movement and distribution of hh proteins are restricted while *hh* transcription is not affected (Desbordes and Sanson, 2003; Bornemann et al., 2004; Han et al., 2004; Glise et al., 2005; Gorfinkiel et al., 2005). Shf binds to both Hh and heparan-sulphate proteoglycans, suggesting the presence of an Hh protein complex (Glise et al., 2005; Gorfinkiel et al., 2005). The cytoneme model proposes that Hh may be transported to the distant cells via extremely fine cell membrane protrusions, termed cytonemes (Ramirez-Weber and Kornberg, 1999). However, there is not yet evidence supporting the requirement of cytoneme for Shh signaling.

Shh acts on its target cells by direct binding with its receptor Patched (Ptc), a 12-pass transmembrane protein receptor (Goodrich et al., 1996). Mutation or deletion of the extracellular domains of Ptc reduces or abolishes the responsiveness of cells to Hh (Mullor and Guerrero, 2000; Briscoe et al., 2001). The prevailing model of Hh signaling reception (reviewed in Ingham and McMahon, 2001) is that Ptc forms a receptor-complex with Smoothened (Smo), a 7-pass transmembrane protein that belongs to the superfamily of G-protein-coupled receptor (GPCR), and whose activity is repressed by Ptc within the plasma membrane. Binding of Hh to Ptc induces a conformation change of Ptc, releasing the inhibition of Smo. However, recent studies have revealed that in the *Drosophila* wing imaginal disc, expression of *ptc* and *smo* does not colocalize (Denef et al., 2000) and that in response to hh signal, Ptc and Smo undergo endocytosis separately (Denef et al., 2000; Incardona et al., 2002). These

recent findings suggest a more complex mechanism of Hh signaling reception and transduction. The intracellular signal induced by Hh binding is then mediated through a protein complex composed of Costal-2 (Cos2), Fused (Fu), Suppressor of fused (Su(fu)), and Cubitus interruptus (Ci), termed Ci complex. Hh signaling causes the dissociation of the Ci complex from microtubules and the simultaneous inhibition of Ci cleavage. This converts Ci from a transcriptional repressor to an activator, leading to target gene activation (reviewed in Ingham and McMahon, 2001). The direct targets of hh signaling include *Ptc*, the interacting hedgehog protein *(Hip)* (Chuang and McMahon, 1999), the zinc finger transcription factors Gli1 and Gli3 (Marigo et al., 1996; Lee et al., 1997) (Figure4). Gli1 was shown to be an activator of Hh target gene transcription, since ectopic expression of *Gli1* in transgenic mice induces transcription of the Hh target genes in the absence of Hh protein (Hynes et al., 1997; Sasaki et al., 1997). Gli2 acts both as a positive and negative regulatory factor for the transcription of Hh target genes. Gli2 is a weak transcriptional factor, but deletion of the C-terminal domain of Gli2 results in a protein with repressive activities while deletion of N-terminus converts Gli2 into a strong activator. Gli3 mediates Hh signaling with a similar mechanism as Gli2 (Sasaki et al., 1999).

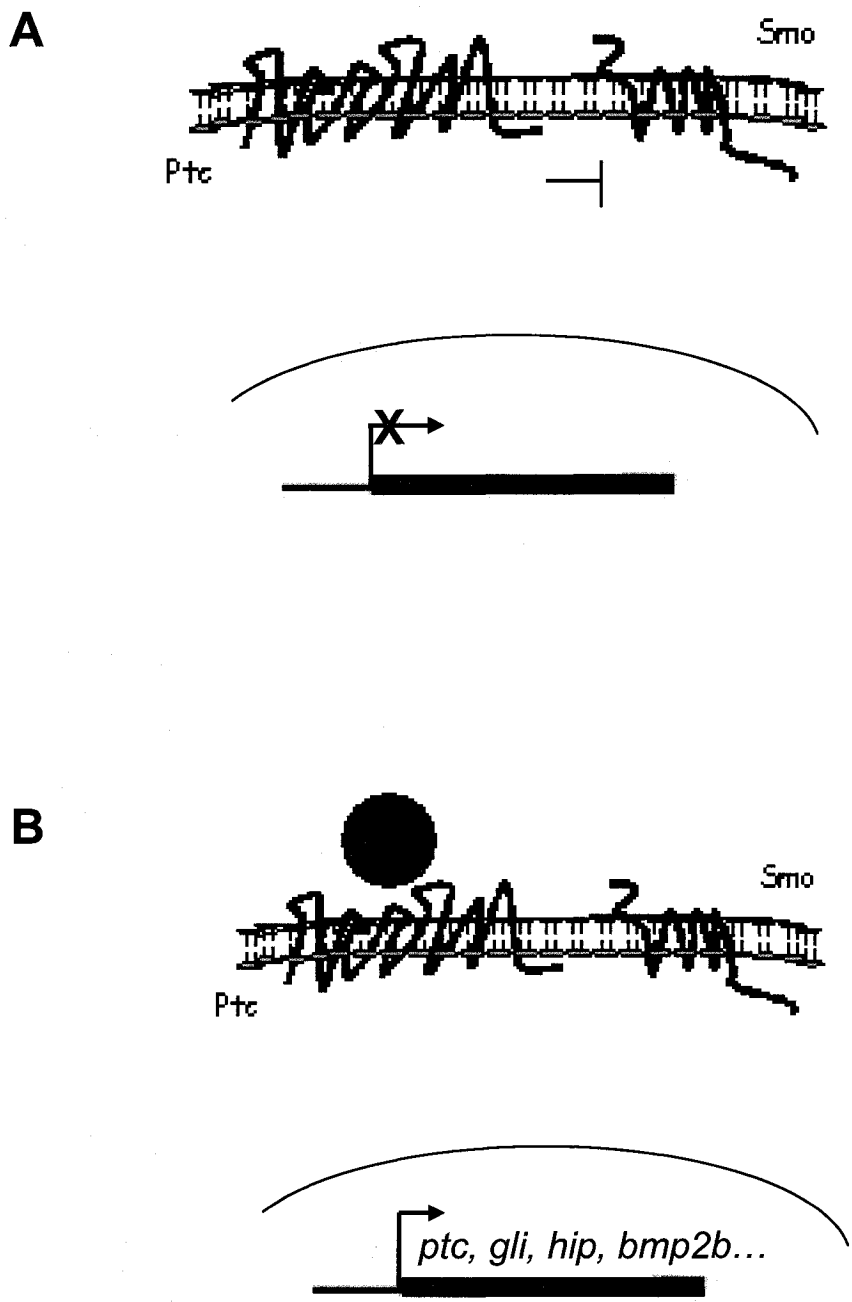

Figure 4

Figure 4: Model of Hedgehog signal reception.

A: Smo (blue) has an intrinsic intracellular signaling activity that is repressed by Ptc (green). **B**: Upon the binding of Hh (red) to Ptc, the repression on Smo is lifted which allows to activate the transcriptional targets, including members of the Gli family, *ptc1*, *hip*, etc..

c. Hedgehog-interacting protein (Hip), an hedgehog antagonist

In order to identify the regulatory factors that can transduce or modulate hh signaling in vertebrates, Chuang and McMahon (1999) performed a biochemical screen for the cell membrane proteins that can directly bind to Shh-N. A biologically active fusion protein of Shh-N and alkaline phosphatase (Shh-N::AP) was used to screen a cDNA expression library from a 10 days postcoitum mouse limb bud. A positive clone that promotes cell-surface binding of Shh-N::AP was identified. The protein encoded by this clone was named hedgehog-interacting protein (Hip, also named Hip1 in some publications (Chuang et al., 2003)).

In vitro analysis showed that Hip can bind to all three mammalian hedgehog proteins (Chuang and McMahon, 1999). In mouse, *Hip*-expressing cells are located next to cells that express each *hedgehog* gene (Chuang and McMahon, 1999; Cobourne and Sharpe, 2002; Olsen et al., 2004). *Hip* is a transcriptional target of Hedgehog signaling. In transgenic mouse embryos ectopically expressing *Shh, Hip* expression is ectopically induced immediately adjacent to the *Shh*-expressing region. In *Shh* and *Dhh* mutant mice, *Hip* expression is absent in hedgehog responsive cells. Overexpression of *Hip* in the developing endochondral skeleton of mouse, which is a target of ihh signaling, leads to a shortened skeleton that resembles the phenotype of the *Ihh* mutant. These results support the hypothesis that Hip attenuates Hedgehog signal by binding to Hedgehog proteins (Chuang and McMahon, 1999).

The mouse *Hip* cDNA is 2669bp long and it encodes a protein of 700 amino acids.

The first 15 amino-acid residues of Hip constitute a signal peptide and the first hydrophobic stretch of the protein, while the last 22 amino-acid residues of the protein are predicted to form a hydrophobic membrane-spanning domain. Deletion of the C-terminal 22 aa generates a soluble form of Hip that can still bind to Shh and blocks its activities (Chuang and McMahon, 1999). However, a native soluble form of Hip in which the putative transmembrane domain is not cleaved, is also found in mouse brain (Coulombe et al., 2004). This observation suggests that the release of Hip soluble form involves other mechanisms than the simple cleavage of the C-terminal domain.

Loss of Hip function in mouse results in specific defects in lungs and endochondral skeleton, which are some of the target tissues of Shh and Ihh signaling, respectively (Chuang et al., 2003). *Hip*$^{-/-}$ mice show defects in secondary lung branching and therefore die of respiratory failure. *Ptc1* expression is up-regulated in *Hip*$^{-/-}$ lung, further supporting the role for Hip in negatively regulating Hh signaling. *Fgf10* expression is down-regulated in the *Hip*$^{-/-}$ defective lung, suggesting an interaction of Shh signaling and Fgf10 in branching morphogenesis during lung development (Chuang et al., 2003).

5. Hedgehog signaling during zebrafish fin regeneration

Five members of the Hh family have been identified in zebrafish: *sonic hedgehog (shh)* (Krauss et al., 1993; Roelink et al., 1994), *indian hedgehog a (ihha)* (Avaron et al., 2006), *desert hedgehog (dhh)* (Avaron et al., 2006), *echidna hedgehog (ehh)* (Currie and Ingham, 1996) and *tiggy-winkle hedgehog (twhh)* (Ekker et al., 1995).

Twhh is a duplicate of the *shh* gene. Both *twhh* and *shh* are expressed in the ventral midline of the embryonic zebrafish neural tube and brain, whereas *shh* is also expressed in the notochord (Krauss et al., 1993; Ekker et al., 1995; Currie and Ingham, 1996). *Shh,* and *ehh* are both expressed in the notochord and participate in myogenesis (Ekker et al., 1995; Currie and Ingham, 1996; Schauerte et al., 1998; Coutelle et al., 2001). *Ehh* is related in sequence to the mammalian *Ihh* although it did not retain the role played by mammalian Ihh in chondrogenesis (Zardoya et al., 1996; Zardoya et al., 1996; Amores et al., 1998). *Ihha* is expressed in the hypertrophic chondrocytes of cartilaginous elements of the craniofacial and fin endoskeleton, suggesting that it probably plays a similar role in bone formation as its counterpart in mammalian embryonic development (Avaron et al., 2006). The function of the zebrafish Dhh is not known yet.

During fin regeneration, *shh* expression initiates at 30 hours post amputation (hpa) in a few dispersed cells at the distal end of each fin rays and by 2 days post amputation (dpa), a strong expression of *shh* is detected distal to the level of amputation in each fin ray. As the regenerates grow, the *shh*-expressing domain remains distally located. Analysis of sections of fin regenerates reveals that *shh* is expressed in a subset of cells in the basal epithelial layer and the *shh*-expressing cells are always located adjacent to the site of new bone matrix deposition along the distal-proximal axis (Figure 5A). Beginning at 4dpa, *shh* expression domain in each fin ray, except the two lateral rays, separates into two subdomains, prefiguring the position of the future ray branches (Figure 5B) (Laforest et al., 1998).

Ihha is expressed in the scleroblasts (Figure 6A and B) of fin regenerates at the same level along the distal-proximal axis as *shh* (Figure 6D). The expression domain of *ihha* splits into two as *shh* before a ray bifurcation can be detected (Figure 6C) (Avaron et al., 2006), suggesting a potential role of ihha in bone formation during fin regeneration as during embryogenesis in mammals (St-Jacques et al., 1999; Long et al., 2004; Colnot et al., 2005).

The Hh receptor *ptc1* is expressed in the same cells as *shh* plus in the adjacent *ihha*-expressing scleroblasts. In chick limb bud, bmp2, a member of the TGF-b family, has been shown to be a downstream target of shh signaling (Laufer et al., 1994). In the regenerating fins of zebrafish, *bmp2b* is expressed in the same cells of the basal layer of the epidermis as *shh*, as well as in the *ptc1*-expressing cells of the blastema. (Figure 5A) (Laforest et al., 1998). Altogether, these observations suggest the involvement of hh signaling in the formation of lepidotrichia during fin regeneration.

The role of shh was investigated by the analysis of the effect of the ectopic expression of *shh*. Microinjection of a *shh-N* DNA construct between the two branches of a fin regenerate, a region where *shh* is not normally expressed, induced an ectopic bone deposition which lead to bone fusion (Figure 7). This effect suggested that shh is a regulator of bone deposition. A similar result was observed after injection of a construct expressing *bmp2b*. However, co-injection of *shh* and *chordin*, an inhibitor of bone morphogenetic protein (bmp) signaling, did not induce ectopic bone formation demonstrating that bmp2b acts downstream of shh signaling (Quint et al., 2002).

Inhibition of Hh signaling in the regenerates with cyclopamine leads to an inhibition of fin outgrowth (Quint et al., 2002). This result suggests the participation of Hh signaling in the regulation of the regenerate outgrowth. In addition, while less lepidotrichia segments were regenerated, bone matrix deposition by already differentiated scleroblasts continued in the absence of Hh signaling as evidenced by the increase bone thickness (Quint et al., 2002). This latter observation suggests that Hh signaling is not required for bone matrix formation and secretion but would be more likely necessary for new scleroblast differentiation or defining the position of scleroblasts differentiation.

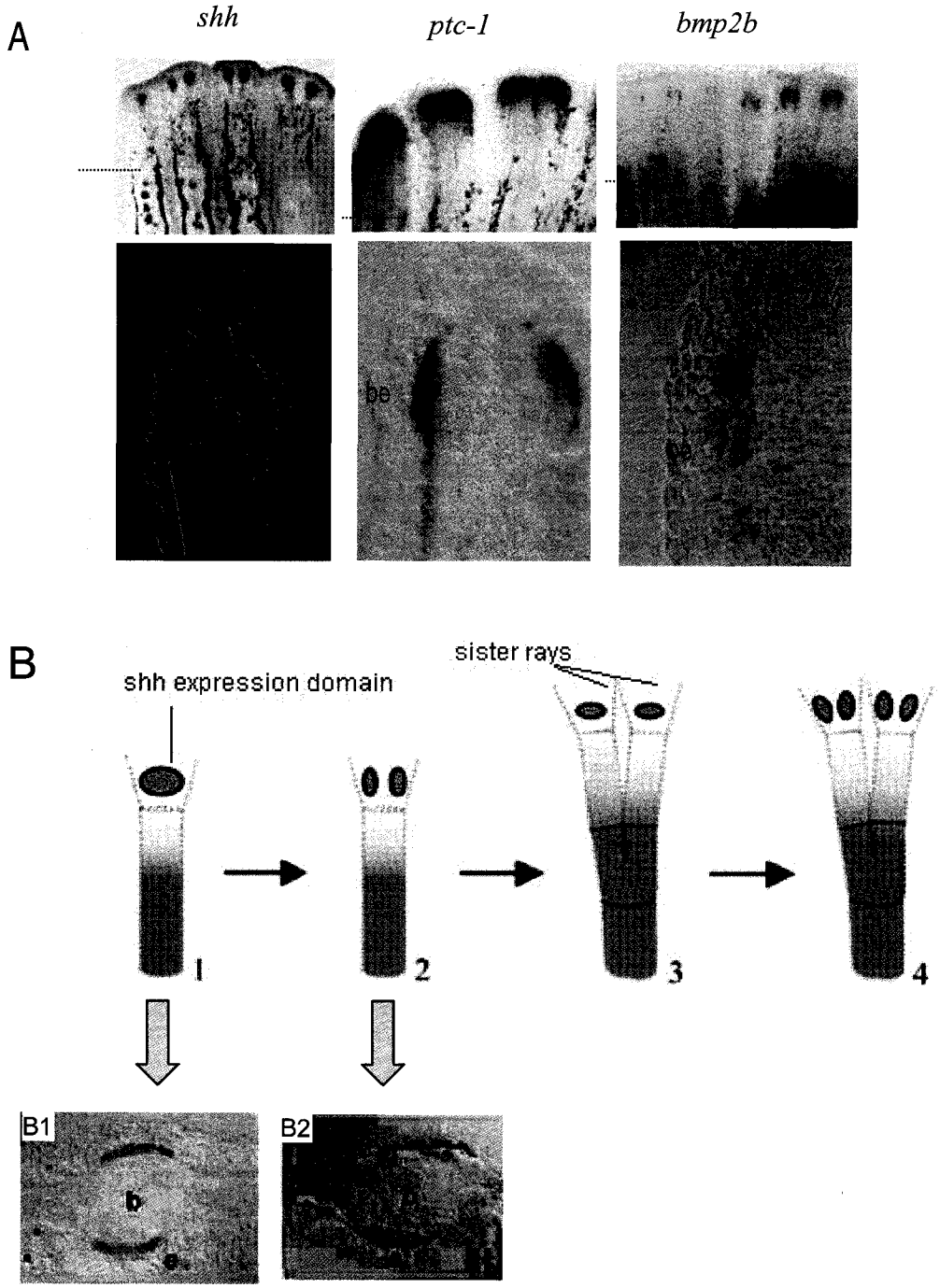

Laforest et al, *Development* 125:4175-4184

Figure 5

Figure 5: Expression of *shh*, *ptc1* and *bmp2b* in zebrafish fin regeneration.

A: *In situ* hybridization on whole mount (upper panels) and longitudinal sections (lower panels) with *shh* (left panels), *ptc1* (middle panels) and *bmp2b* (right panels) anti-sense RNA probes. *Shh* is expressed in a subset of cells of the basal epithelial layer located just at the level of newly formed bone in each fin ray. *Ptc1* is expressed in the same cells as *shh* plus adjacent scleroblasts, the bone matrix-releasing cells. *Bmp2b* is expressed in the *shh*-expressing cells and in a subset of *ptc1*-expressing scleroblasts. **B**: schematic representation of the expression pattern of *shh* during the regeneration process. *Shh*-expressing domains separate into two before ray bifurcation, prefiguring the position of the future sister branches. Once branches are made, *shh* is transiently expressed in only one domain until another subdivision occurs. B1 and B2 show the *in situ* hybridization with *shh* anti-sense RNA probe on transverse sections, indicating that shh-expressing domain on each side of the ray remains unique (B1) and split into two sub-domains (B2). b: blastema; be: basal epidermis; s: scleroblast. The dashed lines in A indicate the level of amputation.

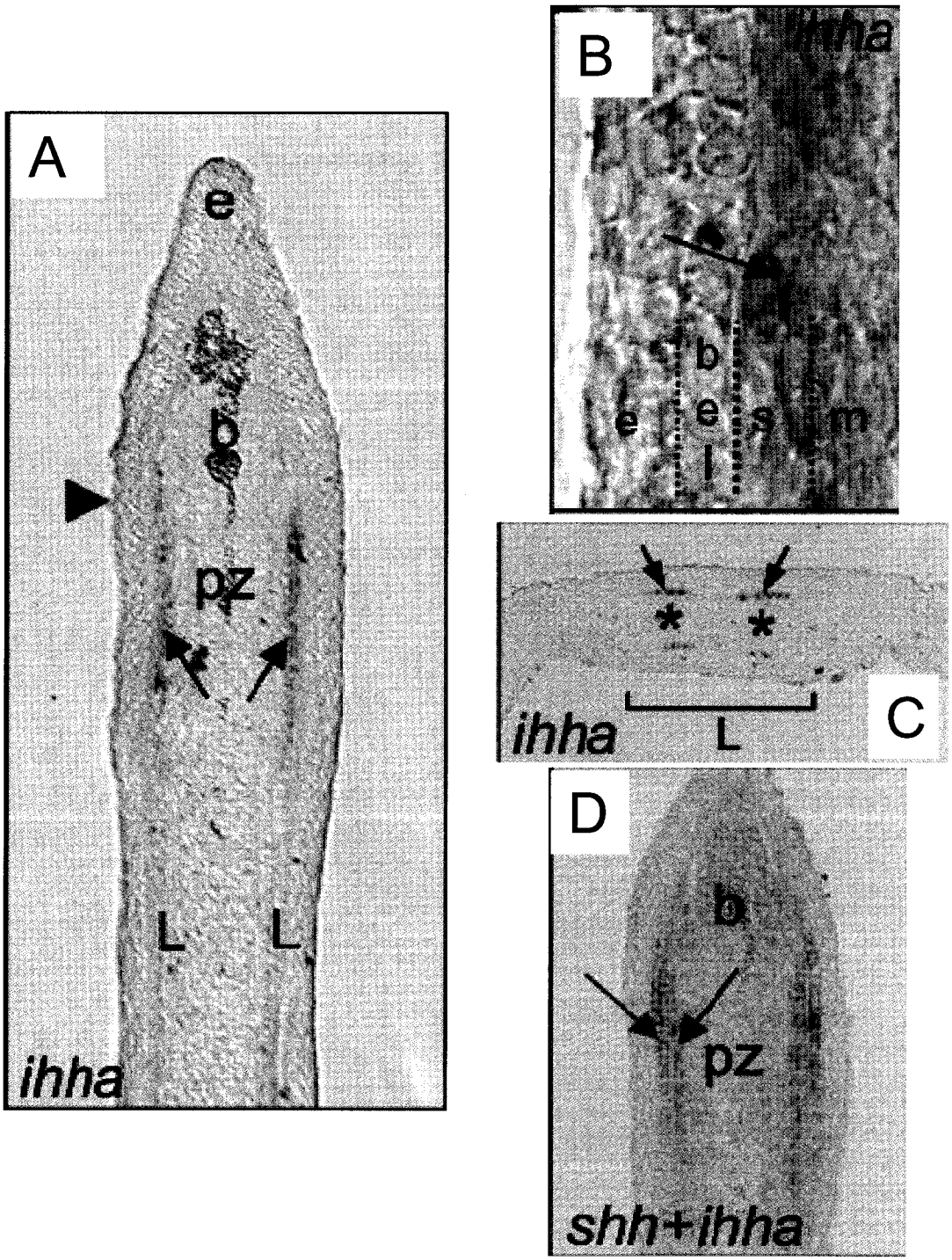

Avaron et al, Dev Dyn 235:478-489

Figure 6: Expression of *ihha* during zebrafish fin regeneration.

A: *ihha* is expressed in two rows of mesenchymal cells lining the epithelium. **B:** closer view of the epithelial-mesenchymal interface reveals that *ihha* is expressed in the newly differentiated scleroblasts.**C:** The expression domain of *ihha* splits into two as that of *shh* before ray bifurcation can be detected. **D:** Double in situ with both *shh* and *ihha* probes showing that *ihha* is expressed in the scleroblasts located at the same level along the proximal-distal axis as *shh*, and colocalizes with the expression domain of *ptc1* (Avaron et al., 2006). The black and red arrows indicate the expression domain of *ihha,* and *shh*, respectively.

bel, basal epidermal layer; e, epidermis; ec, epidermal cap; l, lepidotrichia; m, blastema mesenchyme; pz, patterning zone; *, presumptive sister rays.

A

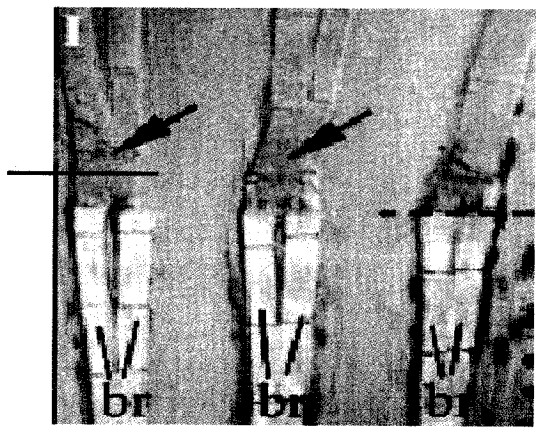

B

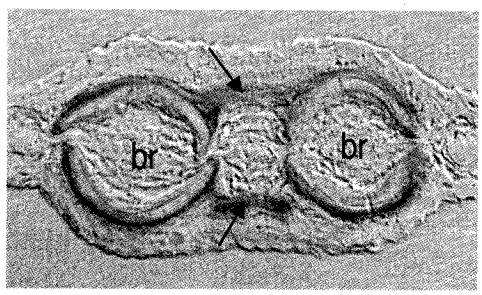

Laforest et al, Development 125:4175-4184

Figure 7

Figure 7: Ectopic expression of shh induces ectopic bone deposition.

A. Ectopic expression of N-shh by plasmid injection into the regenerating fin (Arrow: injection site) results in ectopic bone deposition in the inter-ray region. **B:** Tansverse section of the injected ray at the level of the red line shown in (A). Alcian blue staining showing the ectopic bone deposition in the interface between the epithelial and mesenchymal tissues (arrows). br: ray branches.

6. The zebrafish *2.2shh:gfp*ABC transgenic line

a. The zebrafish *shh* promoter and the *cis*-acting regulatory elements A, B, and C

Dr. Uwe Strähle's group investigated the regulation of *shh* expression in zebrafish embryos by analyzing the promoter and the *cis*-acting regulatory elements of this gene. Analysis of the genomic sequence revealed binding motifs for HNF3β (named Axial in zebrafish) and RAR (retinoic acid receptor) proteins in the upstream region of the zebrafish *shh* gene. Axial is a transcription regulator of the winged helix family that is co-expressed with *shh* in the notochord and the floor plate during embryogenesis but its onset of expression precedes that of *shh* (Strahle et al., 1993; Strahle et al., 1996). Ectopic expression of *axial* in zebrafish embryos induces the ectopic expression of *shh*. In cultured cells, axial activates the expression of a reporter construct containing a fragment of 2.2kb upstream of the *shh* coding region. Altogether, these studies indicate that axial regulates *shh* expression in the midline structures of the zebrafish embryo.

Similarly, a retinoic acid responding elements (RARE) was also identified in the 2.2kb *shh* promoter fragment. *In vitro* analysis showed the binding of the retinoic acid receptor (RAR) and retinoic X receptor (RXR) to this element and cell culture experiments showed that such binding can activate the expression of a reporter construct (Chang et al., 1997). These results suggest a potential direct role of retinoic acid in the regulation of *shh* expression.

The regulatory mechanisms of the spatial expression of *shh* were further explored *in vivo* using a transient transgenesis approach (Muller et al., 1999). A DNA construct containing a genomic fragment covering the 2.2kb promoter sequence and intron1, or intron2 of the *shh* gene and the *lacZ* reporter gene were injected into zebrafish embryos at the one-cell stage. *lacZ* expression was then examined at later stages to reveal the regulatory activities of these regions. Three activator regions, ar-A, ar-B and ar-C, were identified in the introns of the zebrafish *shh* gene (Figure 8A). The three regulatory elements are conserved in human, mouse, fugu and zebrafish. Ar-A and ar-C, identified in introns 1 and 2, respectively, mediate *shh* expression mostly in notochord and floor plate cells, while ar-B, identified in intron 1, drives *shh* expression in the floor plate. Ar-B harbors a sequence with significant homology to a Gli-1 binding site, consistent with the finding that Gli-1 mediates the transcription of the *shh* gene (Hynes et al., 1997; Sasaki et al., 1997). Ar-C contains a sequence with homology to a monomer-binding site of the T-box transcriptional factor Brachyury (*no tail* (*ntl*) in zebrafish), suggesting that this regulatory element may function via its direct binding with this transcription factor (Muller et al., 1999).

b. The *2.2shh:gfp*ABC transgene

Based on the above findings, Dr. Uwe Strähle's group made zebrafish transgenic lines using the transgene, shown in Figure 8B, and which is composed of: the 2.2kb genomic fragment containing the *shh* promoter inserted upstream of the coding region of the *green fluorescent protein* (GFP), followed by the genomic fragment covering the region from intron1 to exon3, which contains the ar-A, ar-B and ar-C elements. Two transgenic lines were obtained: 2.2*shh:gfp*ABC#15 and 2.2*shh:gfp*ABC#28, in

which GFP expression recapitulates the expression observed in the transient transgenic embryos injected with the different regulatory elements (Muller et al., 1999, and personal communication from Dr. Uwe Strähle). In collaboration with Dr. Strähle's lab, I used these transgenic lines to study the role of the *shh*-expressing cells during fin regeneration.

A

Zebrafish *shh* gene

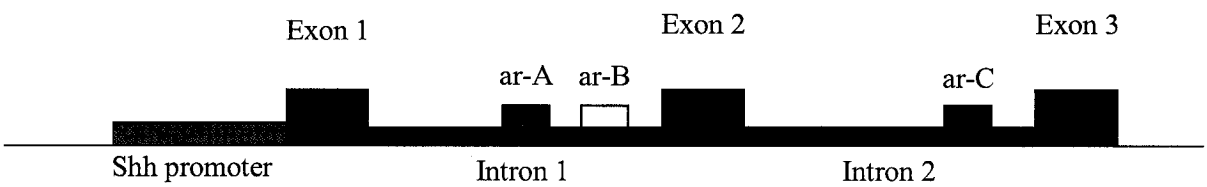

B

Zebrafish transgenic line *2.2shh:gfpABC*

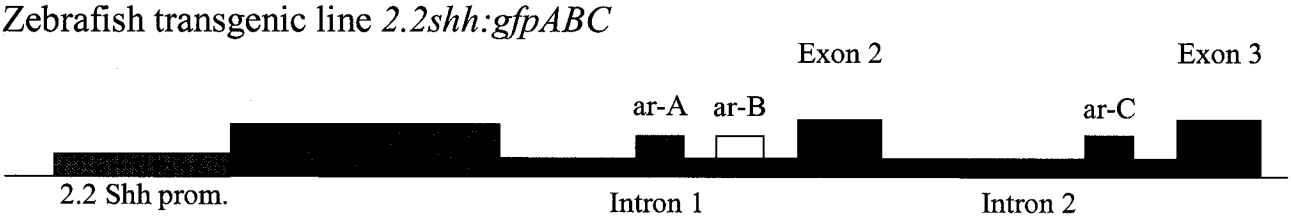

Figure 8

Figure 8: Schematic representation of the regulatory elements of *shh* and the *2.2shh:gfp*ABC transgene.

A: schematic representation of the *shh* gene. The activator regions, ar-A, ar-B and ar-C, were identified in the *shh* introns, and are responsible for proper spatial expression of *shh*. **B:** The *2.2shh:gfpABC* transgene construct is composed of the 2.2 kb upstream promoter sequence of *shh*, inserted upstream of *gfp* cDNA with a polyA signal followed by a 5 kb fragment of the *shh* locus containing intron 1, exon 2, intron 2 and exon 3.

Objective

Our laboratory previously showed that fin regeneration triggers the re-expression of genes involved in the hedgehog (hh) signaling pathway. During fin regeneration, transcripts of one of the zebrafish *indian hedgehog* orthologs, *ihha*, are found in the differentiating scleroblasts of each fin ray. These cells are lining the lateral side of the blastema and are releasing the bone matrix in the subepidermal space. Another member of the *hh* family, *sonic hedgehog* (*shh*), is expressed in a subset of cells of the basal epithelial layer adjacent to the *ihha*-expressing cells. The *hh* receptor *patched1* (*ptc1*) is expressed in both *shh*- and *ihha*-expressing cells. Based on their expression patterns and their known function in other vertebrates, ihha is probably involved in bone formation, probably scleroblasts proliferation and/or differentiation, and may play a more direct role in this process than shh. A time course analysis of shh expression during fin regeneration suggests a possible role of hedgehog signaling in patterning the ray branching. Indeed, the fin rays periodically bifurcate along their proximal-distal axis and, before branching of the regenerating ray, the *shh*-expressing domain separates into two, prefiguring the position of the future ray branches. In addition, ectopic expression of *shh* in the tissue between two ray branches induces ectopic *ptc1* expression and ectopic bone deposition, suggesting a role for hh signaling in bone patterning.

Therefore, the present study is aimed at investigating the role of hh signaling in patterning the fin ray regenerate and more specifically, ray branching, by analyzing the morphological and molecular consequences on the regeneration of the

lepidotrichia of: : 1) the removal of *shh*-expressing cells in regenerating fin rays and 2) the inhibition of hedgehog signaling in fin regenerates by overexpression of hip, a hedgehog antagonist.

Material and Methods

1. Animals

The zebrafish *2.2shh:gfp*ABC#15 and *2.2shh:gfp*ABC#28 transgenic lines were kindly provided by Dr. Uwe Strähle. Fish are maintained at 28.5°C with a photo period of 14 hours of light and 10 hours of darkness, and fed regularly (Westerfield, 1995).

2. Fin amputation

Adult zebrafish of at least 10 weeks of age were anesthetized by immersion in system water containing 0.17 mg/ml tricaine (ethyl-maminobenzoate; Westerfield, 1995) to immobilize the fish and minimize possible pain and discomfort caused by the procedure. Caudal fins of adult fish were amputated, using a scalpel, proximal to the first branch point of the lepidotrichia, and fish were then returned to their tanks where they recover rapidly with very little bleeding and no sign of obvious pain. At various time points afterwards, the regenerating fins were processed for excision, injection or laser ablation, depending on the experiments.

3. Preparation of RNA probes

Antisense RNA probes were synthesized *in vitro* from a linearized DNA template. The synthesis reaction contained 1 μg of linearized DNA template, 2μl NTP labelling mix (10mM ATP, 10mM CTP, 10mM GTP, 6.5mM UTP, 3.5mM DIG-11-UTP (Roche)), transcription buffer (40mM Tris pH 8.0, 6mM $MgCl_2$, 10mM DTT, 10mM

NaCl, 2mM spermidine (Roche)), 20 units RNAsin (Fermentas), and 20 units of the appropriate RNA polymerase (Roche) (refer to Appendix I). This mixture was incubated at 37°C for two hours. This reaction produced approximately 10μg of RNA. The synthesized probe was then precipitated by the addition of lithium chloride (LiCl) to a final concentration of 0.5M and ethanol to 75% final volume and incubated for 30 minutes at –80°C. The precipitated probe was pelleted for 30 minutes in a microcentrifuge (Heraeus Instruments) at high speed, washed with 70% ethanol and dried. The probe was resuspended in DEPC treated water (0.1% Diethyl pyrocarbonate (DEPC) in water stirred overnight) to a final concentration of approximately 100ng/μl.

4. Whole mount *in situ* hybridization

In situ hybridizations experiments on whole mount fins were performed as described in Laforest et al., (1998). Fins were fixed overnight in a solution of PBS containing 4% paraformaldehyde (PFA) at 4°C. The samples were washed twice in PBS, twice in 100% methanol and were stored in methanol for at least 2 hours at -20°C. The samples were subsequently rehydrated in a series of 5-minute washes in dilutions of methanol and PBS (75% MeOH:25% PBS, 50% MeOH:50% PBS, 25% MeOH:75% PBS). The samples were washed 3 times for 5 minutes each in PBST (1x PBS, 0.1% Tween-20). Fins were permeabilized in 20μg/ml proteinase K (Invitrogen) for 30 min. The samples were then washed twice for 5 minutes in PBST, fixed for 20 minutes in 4% PFA and washed twice for 5 minutes in PBST. Samples were then incubated in acetylation solution consisting of 125μl triethanolamine and 27μl acetic anhydride in 10ml of water for 10 minutes, followed by two 10-minute washes in PBST. Next,

embryos were prehybridized at 65°C for 3-4 hours in a solution containing 50% deionized formamide, 5x SSC (20x SSC stock solution; 3.0M NaCl, 0.3M citric acid), 0.1% Tween-20, 50 μg/ml heparin, 9.2mM citric acid and 200 μg/ml yeast tRNA. After incubation for 3-4 hours, the hybridization solution was replaced with a fresh prehybridization solution containing 1 ng/μl DIG-labelled antisense RNA probe and the samples were allowed to hybridize overnight at 65°C.

The next day, the hybridized samples were washed at 65°C for 15 minutes in a series of dilutions of hybridization mix (hyb mix) and 2x SSC (75% hyb mix:25% 2x SSC, 50% hyb mix:50% 2x SSC, 25% hyb mix:75% 2x SSC and 100% 2x SSC). This was followed by two 30-minute washes in 0.2x SSC. The samples were successively washed at room temperature in serial dilutions of 0.2x SSC and PBST (75% 0.2x SSC:25% PBST, 50% 0.2x SSC:50% PBST, 25% 0.2x SSC:75% PBST and 100% PBST) for 10 minutes each. The samples were then preincubated for 1 hour at room temperature in PBST containing 10% calf serum and 40mg/ml BSA. Fins were subsequently incubated at room temperature for 2-4 hours in a solution consisting of a preabsorbed anti-DIG antibody conjugated to Alkaline Phosphatase (AP) (Roche). Preabsorption of the antibody was performed during the first day of the in situ hybridization where 2-3 of nonhybridized fins were placed in a solution containing 20μl calf serum, 20μl BSA, and 2μl antibody and 960μl PBST for 2-4 hours at room temperature and then placed at 4°C overnight. Following incubation with the preabsorbed anti-DIG AP antibody the hybridized embryos were washed twice for 5 minutes and then placed at 4°C overnight.

The hybridized fins were subsequently put through 6 washes of 15 minutes each in PBST. Prior to the chromogenic reaction, the fins were equilibrated in three 5-minute washes in equilibration buffer (100mM Tris pH 9.5, 50mM $MgCl_2$, 100mM NaCl) plus 0.1% Tween-20 and 1mM levamisol at room temperature. Then, staining buffer was made by dissolving 5% Polyvinyl Alcohol (PVA) in equilibration buffer in a boiling water bath. Fins were stained in a solution containing 0.175 mg/ml 5-Bromo-4-Chloro-3-Indolyl phosphate (BCIP) and 0.337mg/ml Nitro Blue Tetrazodium (NBT) in the staining buffer at room temperature until a suitable color was visualized. After staining, the sample were washed in PBST and post fixed in 4% PFA for 2 hours. Fins were then washed in PBS and stored at 4°C in PBS containing 5mM EDTA. The entire in situ hybridization procedure was carried out in six well plates (NUNC Brand Products) with the fins placed in plastic "baskets". The prehybridization and hybridization steps were however performed in eppendorf tubes. Fins were observed and photographed using a Leica microscope equipped with Eclipse software.

5. Cryostat sectioning

Collected fins that were fixed in 4% PFA were rehydrated in a series of 5 minute washes in dilutions of methanol and PBS (75% MeOH:25% PBS, 50% MeOH:50% PBS, 25% MeOH:75% PBS). The samples were washed 3 times for 5 minutes each in PBST. Fins were then embedded in a molten 50°C solution of PBS containing 1.5% agar and 5% sucrose. After solidification, a block enclosing the tissue to be sectioned was trimmed with a scalpel. These blocks were placed in a 30% sucrose PBS solution

and stored at 4°C overnight. The blocks were mounted on the cryostat chuck in a layer of cryomatrix (VWR) and then frozen in 2-methyl butane (-80°C). Sections between 14 and 18μm thick were made using a cryostat sectioner (Leica CM3050S). Sections were collected on glass slides and stored at –20°C until used.

6. *In situ* hybridization on cryostat sections

Sections were defrosted at room temperature for at least one hour prior to use. DIG-labelled antisense RNA probe was diluted (1:200) in the hybridization buffer consisting of 1x Salt solution (10x Salt stock solution; 1.95M NaCl, 0.12M Tris HCl, 0.01M Tris base, 0.05M NaH_2PO_4-H_2O, 0.05M Na_2HPO_4, 0.5M EDTA, pH 7.5), 50% deionized formamide, 10% dextran sulphate, 1mg/ml yeast tRNA and 1x Denhardt's solution (50x stock Denhardt's solution contains 1% Ficoll type 400, 1% polyvinylpyrolidone and 1% bovine serum albumin. The solution is sterile filtered.). The hybridization solution was denatured at 70°C for 5-10 minutes and 500μl of this solution was added to each section. Sections were subsequently hybridized overnight at 65°C in a sealed plastic container containing a Whatman paper soaked with 1x salt solution/50% formamide.

The next day the slides were transferred to a heated Coplin jar containing solution A (1x SSC, 50% formamide, 0.1% Tween-20). The slides were washed twice for 30 minutes in solution A at 65°C, followed by two 30-minute washes at room temperature in 1x TBST (10x TBST stock solution: 1.4M NaCl, 27mM KCl, 0.25M Tris HCl pH 7.5, 1% Tween-20). Next, the slides were blocked in 10%

heat-inactivated calf serum in 1x TBST for one hour at room temperature. Following incubation, the slides were dried one slide at a time making sure the area around the sections was dry. To each slide 500µl of 1:2000 dilution of anti-Dig AP Fab fragment (Roche) in 10% heat-inactivated calf serum and 1x TBST was added. Slides were incubated overnight in a humidified chamber at 4°C.

The following day the slides were washed 4-5 times for 20 minutes in 1x TBST. The slides were then washed twice for 10 minutes at room temperature in 1x NTMT (100mM NaCl, 100mM Tris HCl pH 9.5, 50mM $MgCl_2$, 0.1% Tween-20). Sections were stained in NTMT containing 0.175 mg/ml BCIP and 0.337mg/ml NBT at room temperature. Once a suitable color was visualized the reaction was stopped in 2 washes in 1x PBS. Sections were then fixed in 4% PFA for 20 minutes after which they were washed with distilled water. Slides were dried and then mounted by applying 3 drops of aquatex (VWR) along each slide and placing a glass cover over the sections. Slides were allowed to dry overnight and observed using a Zeiss Axioskop compound microscope.

7. Fluorescence imaging

A dissection microscope (Leica MZ FLIII) with integrated FLUOIII filtersystem is used to visualize the samples. A digital camera (Sony 3CCD Color Video Camera) and Eclipse software were used to photograph the samples. Fluorescent pictures of whole-mount caudal fin require an average exposure time of 55msec.

8. Laser cell ablation

A VSL-337ND-S laser system (Spectra-Physics) installed on a Zeiss Axioskop compound microscope was used to generate a laser beam of 435nm. 30Hz laser pulses were applied for about 5 seconds on each cell (please refer to Part I (b) in Results for details).

9. Lipophilic Carbocyanine Dye (Di-I) Labeling

Di-I (1,19-dioctadecyl-3,3,39,39-tetramethyl indocarbocyanine perchlorate; Molecular Probes, Eugene, OR) was used to label cells. A 0.25% w/v stock solution of Di-I in ethanol was further diluted tenfold in a 45°C 0.3-M sucrose solution prior to microinjection. The injection of Di-I was performed with the same equipments as DNA injection described below. The capillary pipettes were filled with a pressure of 68.0psi for the desired time. An injection of 30msec and 20psi delivered a small bolus of dye solution in the desired region, whereupon a small pink dot was visible. The lipophilic carbocyanine dye inserts into the membrane of the cells adjacent to the injection site. After 24 hr, when single or small clusters of cells labeled with Di-I were distinguishable, the fin was processed for laser ablation.

10. Cloning of zebrafish ortholog of *hedgehog-interacting protein* (*hip*) and making of the Δ*hip*-expressing construct

Total RNA was extracted from 20 or 40 hpf embryos. Approximately 50 embryos were dechorionated and fixed in 1 ml Trizol overnight. Samples were homogenized

with an insulin syringe and centrifuged at 12,000 x g for 10 minutes at 4°C. The supernatant was chloroform extracted and precipitated with isopropanol. The dried pellet was resuspended in DEPC-treated deionized water.

Messenger RNA (mRNA) was isolated by adding 2 volumes of dilution buffer (Promega) to the total RNA preparation and 1 µl oligo (dT)n (Promega). The mixture was incubated for 5 minutes at 70°C and left to cool to room temperature for 30 minutes. The cooled RNA solution was incubated for 5 minutes in a 200 µl magnetic bead solution (Promega) washed with 0.5X SSC. A magnetic stand was used to capture and wash beads three times with 200 µl 0.5X SSC. mRNA was eluted with 300 µl DEPC-treated deionized water and precipitated with 3M sodium acetate and isopropanol. The dried mRNA pellet was stored in -80°C and used for first strand cDNA synthesis.

First strand cDNA synthesis from mRNA pellet was carried out by a standard Reverse Transcriptase-PCR (RT-PCR) (Sambrook and Russell, 2001) using random hexanucleotides. The synthesized single strand cDNA was then stored at 20°C. Amplification of the *hip* cDNA was accomplished through PCR on these first strand preps with the forward primer: 5' ATGAAGCATTTGAAATTTGTGCT 3' and reverse primer: 5' TTAAACAATATAACTAGTGAGGTCCA 3'. Reactions were carried out on a PTC-225 Peltier Thermal Cycler (MJ Research) for 30 cycles with the following cycling parameters: denaturing at 94°C for 30 seconds, primer annealing at 50°C for 30 seconds, elongation at 72°C for 3 minutes.

RT-PCR products were immediately ligated into the pDrive TA-cloning vector (Qiagen kit). Resulting clones were screened for inserts of the correct size by PCR with the above primers. Clean plasmid preparation of the positive clone was obtained using a Promega Wizard plus SV mini preps DNA purification system. The clone was then sent for sequencing on an Applied Biosystems 3730 DNA analyzer at the Ottawa Health Research Institute Sequencing Service. Sequence analysis and multi-transcript alignments were done through SeqWeb (http://www.uottawa.bioinformatics.org).

To generate a soluble form of hip protein, the fragment without the coding region of the last 22 amino acid was amplified by PCR with the forward primer 5' ATGAAGCATTTGAAATTTGTGCT 3' and reverse primer: 5' GTCTTTCTCACCGTCCCCTT 3'. This fragment was inserted into the pDrive TA-cloning vector (Qiagen kit) The Δ*hip* fragment was then cut off at the restriction sites *Hind*III and *Pst*I and inserted into the "New" vector under the control of CMV promoter (refer to Appendix II).

11. DNA injections into regenerating blastema

DNA injections were performed in the regenerating caudal fins of anesthetized zebrafish at 3 dpa. Plasmid DNA was prepared using the Qiagen Hispeed plasmid midi kit and used for injection. The injection of DNA was performed as described in Quint et al. (2002) using 10 cm borosilicate capillary pipettes with 1.0mm outside

diameter and 0.50mm inside diameter (Sutter Instruments), pulled using a Model p-87 Flaming/Brown micropipette puller (Sutter Instrument Co.). Using a Narishige IM300 Microinjector, the capillary pipettes were filled with the injection solution with a pressure of 68.0psi for the desired time. An injection of 20psi for the desired time delivered DNA into the regenerating blastema. About 30ng of plasmid DNA was injected into each fin ray.

The *Δhip*-expressing construct was injected into the blastema of the 6 ventral regenerating rays, while pEGFP-N1 (refer to Appendix II) was injected into the 6 corresponding dorsal rays (Figure 18B). The EGFP-injected rays were examined 1day post injection (dpi) by fluorescence imaging.

Results

Part I: role of shh-expressing cells in patterning the fin rays during regeneration

a. GFP expression in the zebrafish *2.2shh:gfp*ABC transgenic line recapitulates the endogenous expression of *shh* during fin regeneration

To determine whether the *2.2shh:gfp*ABC transgenic lines could be used to analyze the function of *shh*-expressing cells, a time course analysis of GFP expression was performed starting immediately after amputation. No GFP fluorescence was visible during the first day post amputation (data not shown). In the *2.2shh:gfp*ABC#15 line, at 2dpa, GFP started to be expressed in a group of cells located in the distal part of each fin ray regenerate (Figure 9, A). At 3dpa GFP expression expanded to a larger group of cells always located in the distal part of the regenerate (Figure 9, B). At 6dpa, a cleavage started to become visible in the middle of the GFP-expressing region (Figure 9, C). At 9dpa, the division of the GFP-expressing region was very clear but there was no sign of ray branching yet (Figure 9, D). At 21dpa, the fin showed bifurcated rays and a single GFP-expressing domain was visible in the distal part of each ray branch (Figure 9, E and F). 56 fish of the *2.2shh:gfp*ABC#15 line were examined and all of them showed the same five steps of expression: 1) no expression before 2dpa, 2) expansion of the expression domain (during a 2-4 days period), 3) cleavage of the expression domain (during a 1-2 day period), 4) complete separation of expression domain before ray bifurcation (during a 2-5 day period) and 5) single expression domain in each ray branches. Slight variations of the length of each step were observed in different fish individual.

The expression of endogenous *shh* gene was compared with that of GFP in the *2.2shh:gfp*ABC#15 line. GFP expression of a regenerate at 6dpa was recorded by fluorescent imaging (Figure 10A). Then, the same regenerate was fixed and processed for whole mount *in situ* hybridization with a *shh* anti-sense RNA probe (Figure 10B). The results show that the expression domains of GFP and *shh* overlap, confirming that the *2.2shh:gfp*ABC#15 transgenic line is a reliable model to study *shh*-expressing cells in regenerates *in vivo*.

A faint GFP expression expands beyond the *shh* domain of expression. This can be due to the persistence of the GFP proteins in cells where *shh* transcription has already ceased. This observation could be used to investigate the fate of the *shh*-expressing cells but this possibility has not yet been explored.

The same GFP expression was observed in the second transgenic line *shh:gfp*ABC#28 further confirming that GFP expression is clearly reflecting the endogenous expression of *shh*. However, in addition to this expression, the *shh:gfp*ABC#28 line shows a uniform low background fluorescence which may be due to an effect of the insertion site of the transgene in the zebrafish genome. Because of this background fluorescence, this line was no longer used in our analysis.

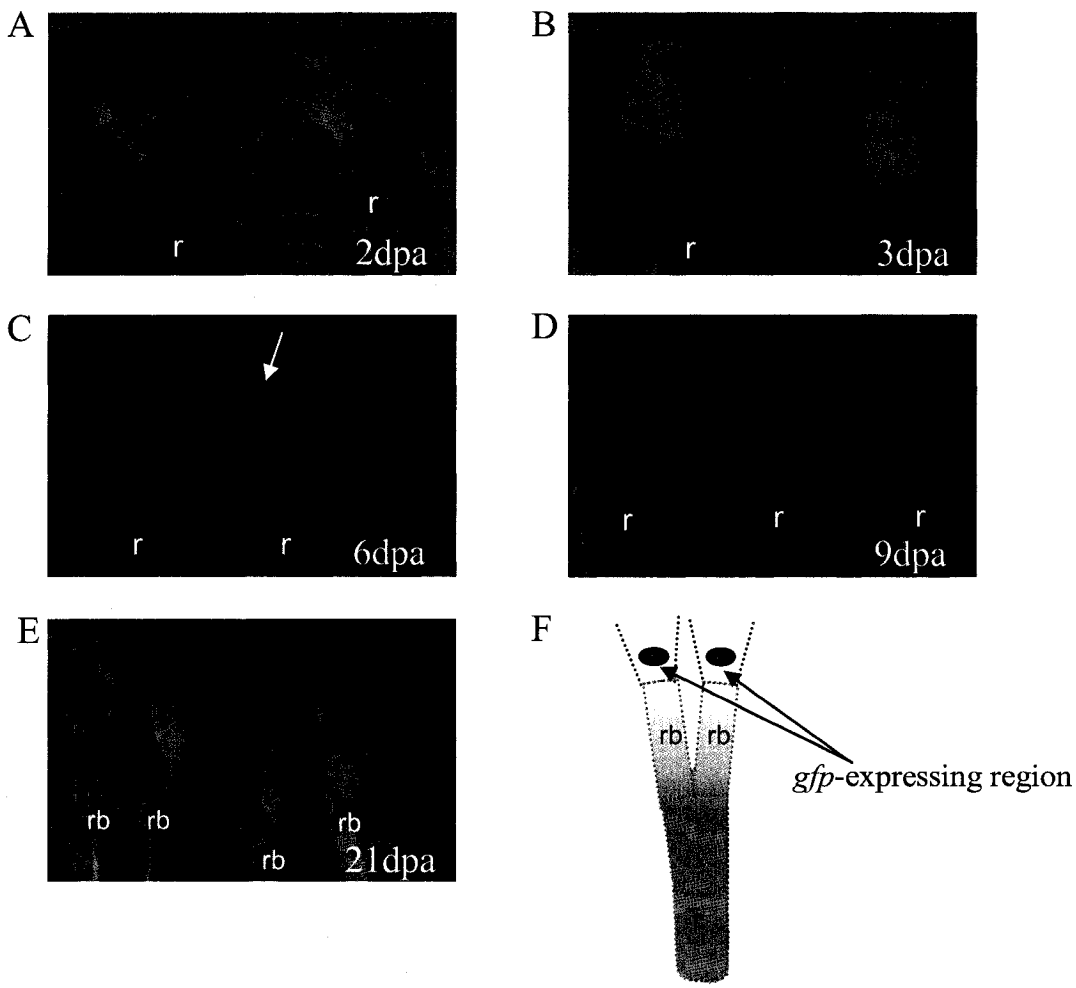
A
r
r
2dpa
B
r
3dpa
C
r
r
6dpa
D
r
r
r
9dpa
E
rb
rb
rb
rb
21dpa
F
rb
rb
gfp-expressing region

Figure 9

Figure 9: Time course analysis of GFP expression in the *2.2shh:gfp:ABC#15* transgenic line.

No GFP expression was observed before 2 dpa. **A**: At 2dpa *shh:gfp* started to be expressed in a group of cells located at the distal part of each fin ray of the regenerates. Through the process of regeneration, *shh:gfp*-expressing domain always remains located in the distal part of the regenerates. **B**: At 3dpa, *shh:gfp*-expressing domain expands. **C**: At 6dpa, cleavage occurs in the middle of *shh:gfp*-expressing domain (white arrow). **D**: At 9 dpa, clear division of *shh:gfp*-expressing domain but no sign of bone branching. **E**: At 21 dpa, unique *shh:gfp*-expressing domain of expression is in each ray branch. **F**: Schematic representation of a bifurcated ray and the GFP-expression domain in each of its branches. rb: ray branch; r: ray

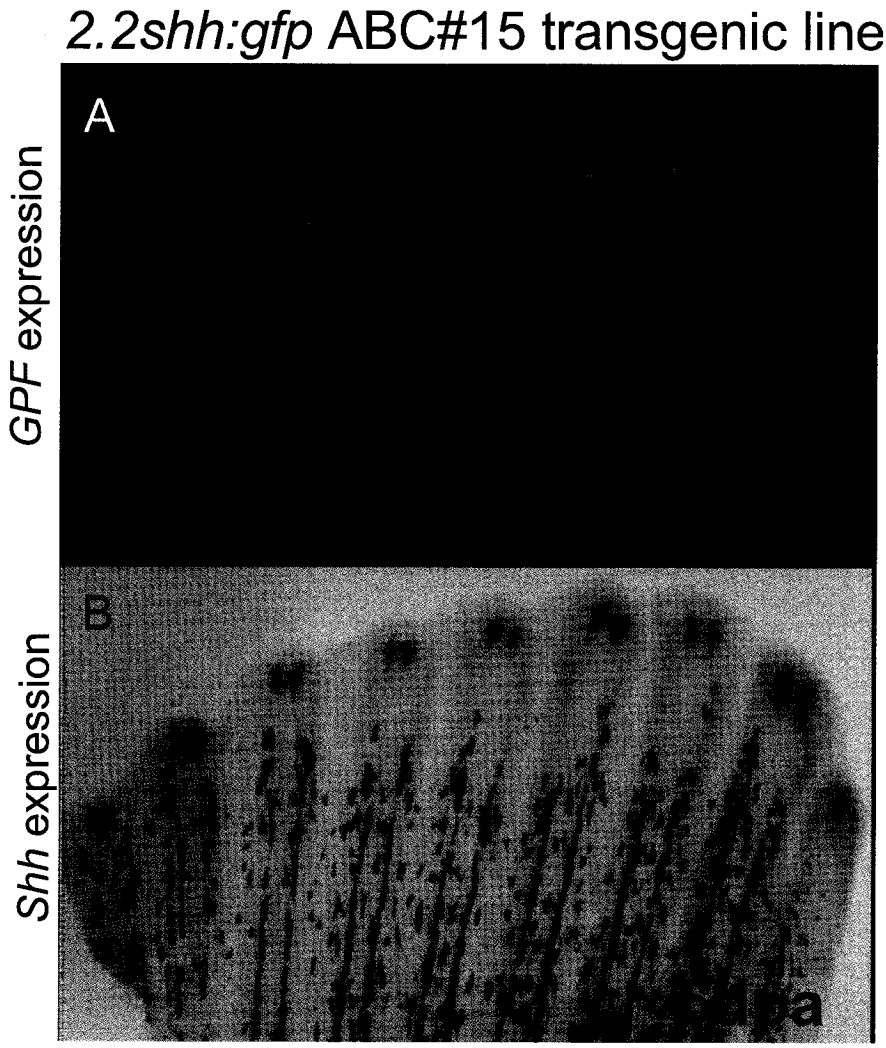
2.2shh:gfp ABC#15 transgenic line
A
GPF expression
B
Shh expression

Figure 10

Figure 10: GFP expression in the *2.2shh:gfp*ABC#15 transgenic line recapitulates the endogenous expression of *shh*.

Expression of GFP and of *shh* in the same fin at 6dpa was detected by fluorescent imaging (A) and by in situ hybridization on whole mount fin with *shh* anti-sense RNA probe (B), respectively. The expression domains of GFP and *shh* overlap, confirming that the line 2.2*shh:gfp*ABC#15 is a reliable model to follow the *shh* expression *in vivo*.

b. Establishment of a method for GFP-guided laser cell ablation in regenerating fin

To investigate the role of the *shh*-expressing cells during fin regeneration, a laser-mediated approach was used to ablate these cells in the *2.2shh:gfp*ABC#15 transgenic line. The *shh*-expressing cells are located in a one-cell thin layer and the epithelium above these cells is of optical clarity, which makes the procedure of laser ablation feasible. By aiming a laser beam of a specific wave length at the *shh*-expressing cells using GFP fluorescence as guidance, these cells can be selectively destroyed without damaging the other cells. The technique of laser cell ablation has been shown to be efficient in determining the function of specific cell types in zebrafish embryos and larvae (Greenspoon et al., 1995; Li et al., 2003; Roeser and Baier, 2003), however, no one has ever applied it to tissue of adult fish such as the fin regenerates. I established the following protocol of laser cell ablation on adult fish regenerates of the *2.2shh:gfp*ABC#15 transgenic line based on the protocol described by T. Roeser and H. Baier (Roeser and Baier, 2003):

Laser cell ablation was performed using a VSL-337ND-S laser system (Spectra-Physics) installed on a Zeiss Axioskop compound microscope. A laser beam of 435nm wave length was aimed via a 20x microscope lens or 40x water immersion lens. Due to the numbers of cells (150~200 cells per ray) to ablate, laser pulse of high frequency (30Hz) were applied for about 5 seconds per cell.

Adult fish were anesthetized with 0.6mM Tricaine for no more than 15 min to avoid

harm by prolonged anesthesia. During the ablation procedure, the fish was placed in a chamber and the regenerating fin was flattened on a small piece of agarose gel to facilitate focusing. It took from 10 to 15min to completely ablate the group of *shh:gfp*-expressing cells in one fin ray.

Laser cell ablation was performed on two rays per fin at 2dpa and the tissue condition was verified before and after ablation (Figure 11 A, B, C, D). GFP fluorescence disappeared after laser ablation while no sign of damage to the tissues surrounding the targeted area was visible.

To verify that laser cell ablation is effective under these conditions and does not simply photobleach GFP fluorescence, I targeted two distinct cell types that are easily distinguishable by their specific pigmentation from other cell types: melanocytes located in the mesenchymal compartment and the immobile blood cells that were trapped in the newly formed plexus in the regenerate (Figure 11, E, F, G, and H). Both cell types were successfully ablated even though they are deeper located in the regenerate tissue than the *shh:gfp*-expressing cells.

The efficiency of the laser cell ablation was further verified by the successful ablation of epithelial cells labeled with DiI. The fluorescent vital dye, DiI, integrates in the cell membrane and does not diffuse from cell to cell but is transferred to daughter cell membranes during cell divisions. A 0.25% w/v stock solution of DiI in ethanol was diluted tenfold in a 0.3-M sucrose solution prior to microinjection. DiI solution was

microinjected into the epithelial layers of fin regenerates at 3dpa. At this time point, a huge cluster of cells were labeled with DiI. Laser cell ablation was performed 1 day later on single cell or small clusters of cells that were distinguishable at this time point due to cell migration and cell division. DiI fluorescence of the targeted cells disappeared within 5 seconds once given laser pulses (Figure 11, I and J).

Finally, to further verify the successful ablation of *shh*-expressing cells, *shh* expression was examined after laser ablation. Laser cell ablation was performed on 3dpa regenerates and pictures were taken before and after ablation (Figure 12, A and B). Immediately after ablation, the regenerates were amputated, fixed, and processed for *in situ* hybridization with a *shh* anti-sense RNA probe. *Shh* expression was undetectable in the fin rays in which cells were ablated, while the other rays used as controls showed a normal expression of *shh* (Figure 12C). This was the final evidence that the technique of laser cell ablation is effective in fin regenerates.

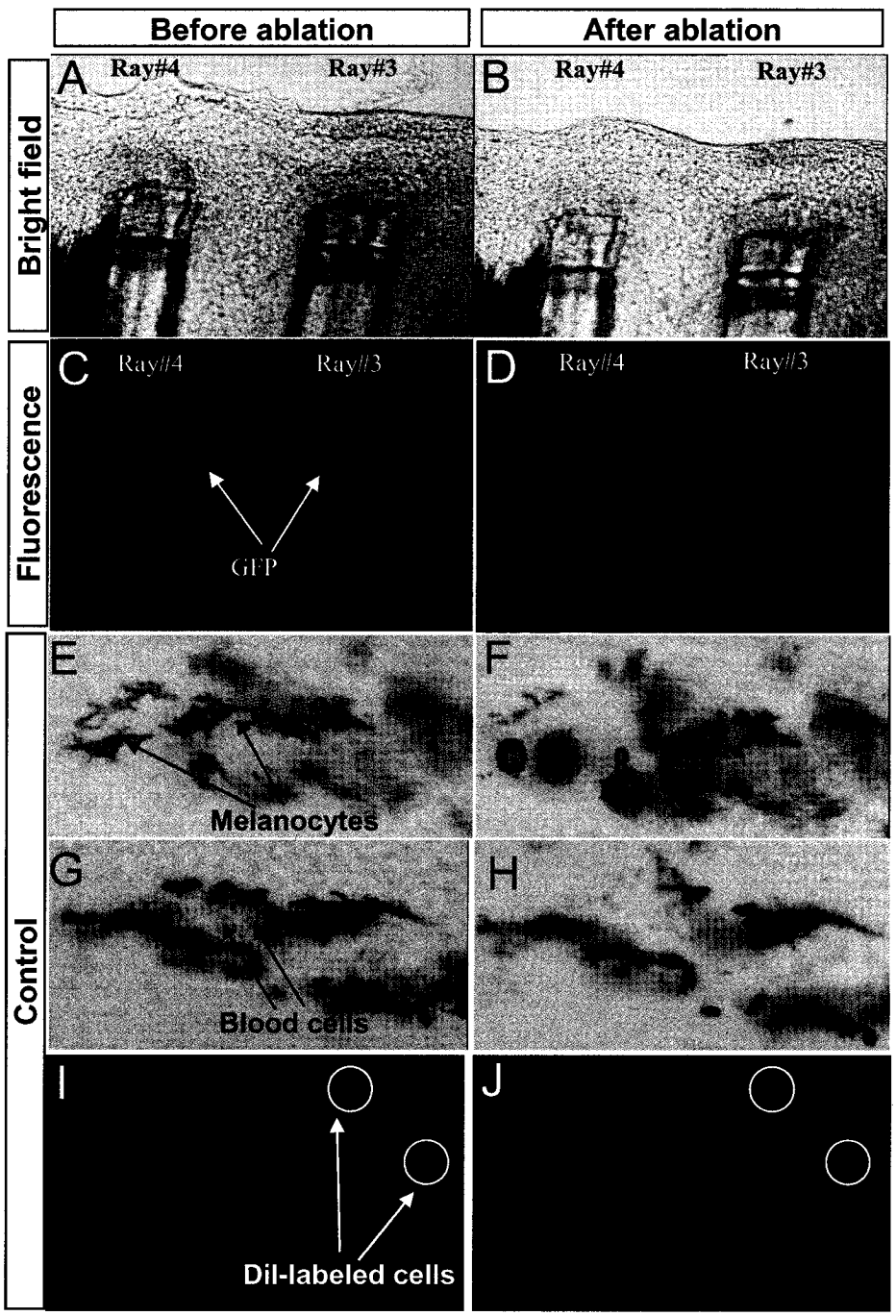
Before ablation
After ablation
Bright field
Fluorescence
Control
A
Ray#4
Ray#3
B
Ray#4
Ray#3
C
Ray#4
Ray#3
GFP
D
Ray#4
Ray#3
E
Melanocytes
F
G
Blood cells
H
I
Dil-labeled cells
J

Figure 11

Figure 11: Verification of the method of laser cell ablation on regenerate.

Pictures taken before (A, C, E, G, I) and after (B, D, F, H J) laser ablation of different cell types of the fin. GFP-expressing cells in two rays of the *2.2shh:gfp*ABC#15 transgenic line were ablated at 2dpa. After laser cell ablation, GFP fluorescence disappeared (D) while no damage to the tissue is visible (B). Controls showing successful ablation of melanocytes (E, F), blood cells (G, H) and DiI-labeled epithelial cells (G, H). Arrows indicate the cell types of interest.

A

B

C

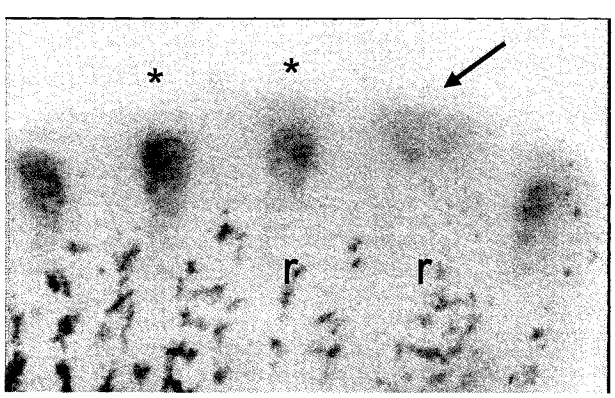

Figure 12

Figure 12: Shh transcripts are absent in the rays in which laser cell ablation has been performed.

The three pictures show the same fin. **A**, before laser ablation; **B**, immediately after laser ablation; **C**, The fin was fixed immediately after ablation and processed for *in situ* hybridization with *shh* anti-sense RNA probe. Red arrows indicate the targeted ray. r: ray. Asterisks in C indicate control rays showing normal expression of *shh.*

c. Ablation of *shh*-expressing cells induces a branching delay of the fin rays

Prior to examining the effects of cell ablation on ray branching, the variations in branching morphogenesis under normal conditions of regeneration were determined. Caudal fin of fish were amputated and the position of the first branching point of the corresponding dorsal and ventral rays (Figure 13A) of the same fin was compared at 21dpa. 63.30% (n=30) pairs of corresponding dorsal and ventral rays showed a difference of less than 1 segment in the position of their branching points, 36.63% showed a difference of 1~2 segments, while only 0.07% showed a difference of more than 2 segments (Figure 13B). Therefore, in the experiments described below, a difference greater than or equal to 2 segments in branching position between a dorsal and the corresponding ventral ray, was considered significant.

All experiments of laser ablation were performed using the *2.2shh:gfp*ABC#15 transgenic fish. *Shh:gfp*-expressing cells in 5 consecutive rays of one lobe of the caudal fin regenerate were ablated at 3dpa and the corresponding rays on the other lobe were used as internal control. Cell ablation was not performed on the lateral-most ray (first ray from the side), because this ray does not bifurcate. I chose to perform laser ablation on regenerates at 3dpa because 1) the regenerates at 2dpa are more fragile than that at 3dpa, and therefore have more chance to be damaged during the procedure and 2) a larger number of *shh*-expressing cells are present at 3dpa than at 2dpa and therefore ablating *shh*-expressing cells at this stage will lead to a more severe effect.

After laser ablation, regeneration was recorded in a time course analysis (data not shown). At 20 days post laser ablation (dpl), branching was delayed in the rays where laser ablation has been performed compared to control (Figure 14A). 42% (n=55) rays showed a branching delay of more than 2 segments (Figure 14B). There was no sign of significant growth delay or any other defect.

These observations support the hypothesis that *shh*-expressing cells are involved in patterning the ray branches, but they do not mean that the delay of branching is only due to the absence of *shh* transcripts. The role of Hh in branching morphogenesis suggested by the cell ablation experiments can be confirmed if inhibition or interference with Hh signaling induces similar defects in the regenerating fin. Therefore, we set out to explore the role of hip, a hedgehog antagonist, during zebrafish fin regeneration.

A

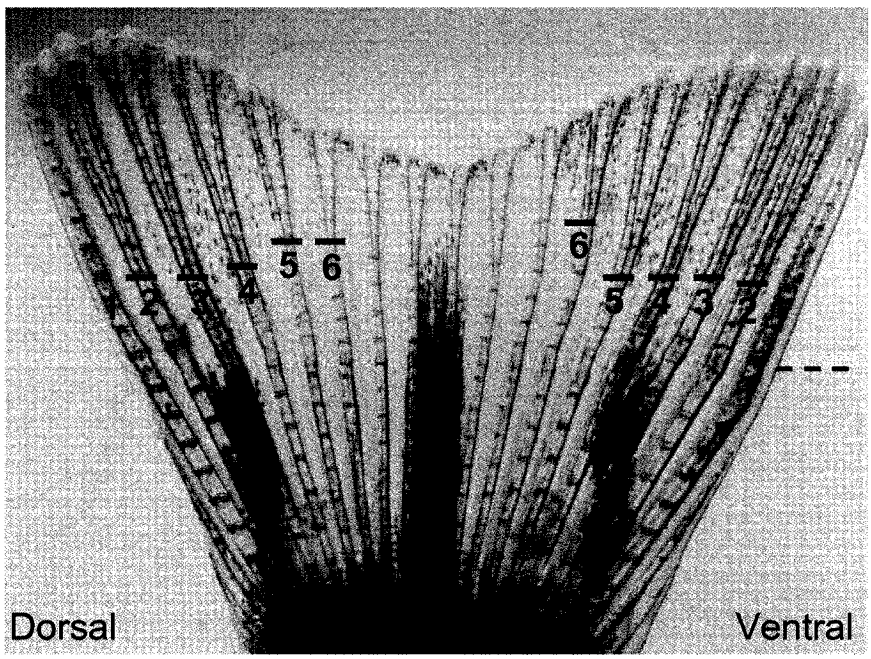
Dorsal
Ventral
Level of amputation

B

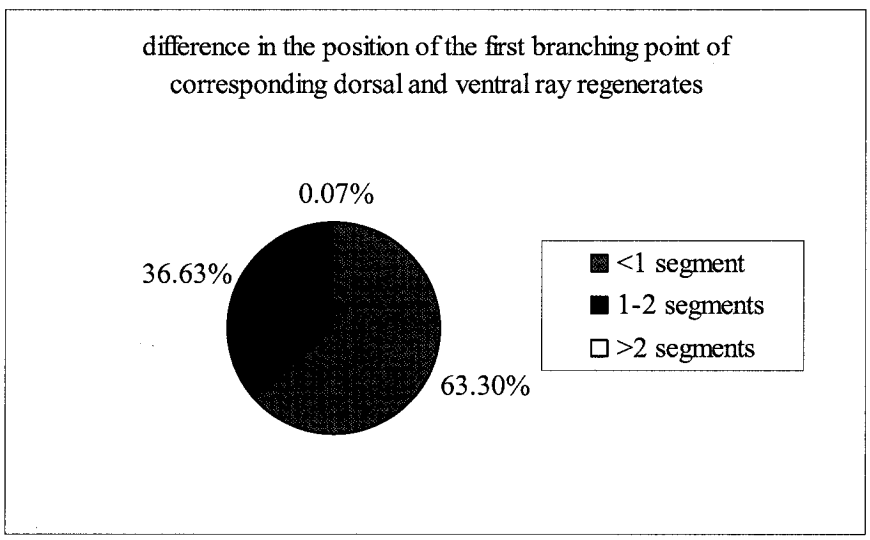
difference in the position of the first branching point of corresponding dorsal and ventral ray regenerates
0.07%
36.63%
63.30%
<1 segment
1-2 segments
>2 segments

Figure 13

Figure 13: Branching morphology in the normal regenerates.

A: Caudal fins of fish of the *2.2shh:gfp* ABC#15 transgenic line were amputated below the first branching point and regenerates were observed at 21dpa. The positions of the first branching points between the corresponding rays of the dorsal and ventral lobes were compared. The red lines indicate the position of the first branching point of each ray. **B**: Only 0.07% of the rays showed a difference in branching points greater than 2 segments. Therefore, in the experiments hereafter, a difference greater than or equal to 2 segments, in the position of the branching points, was considered significant.

A

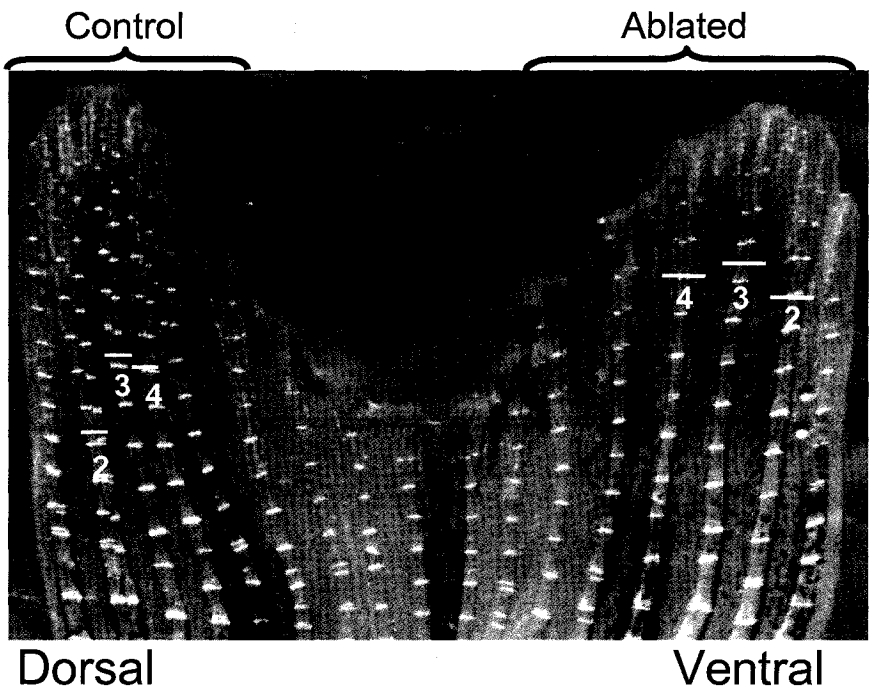
Control
Ablated
4
3
2
3
4
2
Dorsal
Ventral

B

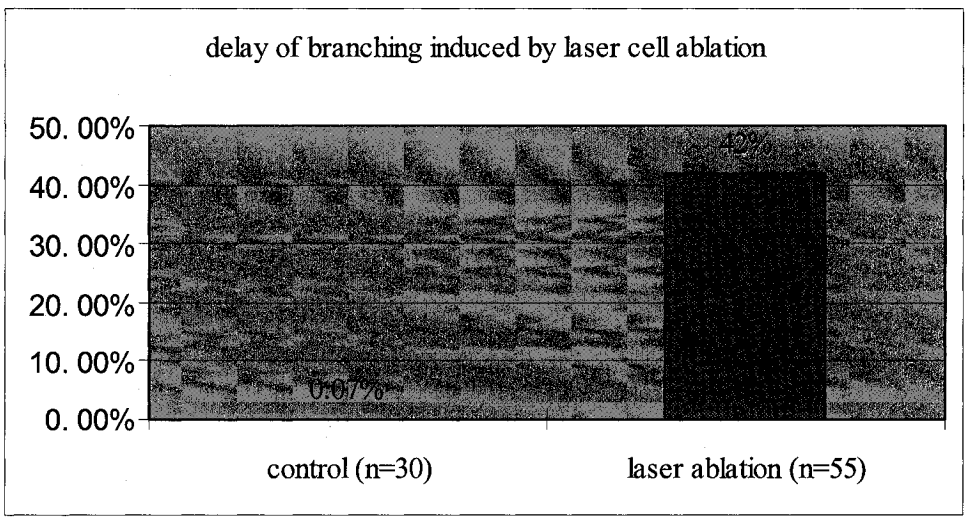
delay of branching induced by laser cell ablation
50. 00%
40. 00%
30. 00%
20. 00%
10. 00%
0. 00%
42%
0.07%
control (n=30)
laser ablation (n=55)

Figure 14

Figure 14: Laser ablation of the *shh*-expressing cells induces a delay of ray branching during fin regeneration.

A: Fin at 20 dpl (days post laser ablation) of the *shh:gfp*-expressing cells . The yellow lines indicate the bifurcation points in rays 2, 3, 4 in the control and ablated sides of the fin, respectively. **B**: 42% of the rays (n=55) in which laser cell ablation was performed showed a branching delay of more than 2 segments, compared to 0.07% in non-ablated control fish (n=30), demonstrating a defect in branching morphogenesis of the regenerative rays.

Part II: role of *hip*, a hedgehog antagonist, in the patterning of the fin rays during fin regeneration

a. Cloning of the zebrafish *hedgehog-interacting-protein* (*hip*) cDNA

A blast search in the Ensembl zebrafish genome database (http://www.sanger.ac.uk/Projects/D_rerio/) was performed to retrieve the sequence of the zebrafish *hedgehog-interacting protein* (*hip*) gene using the sequence of the mouse *hip* cDNA (Chuang and McMahon, 1999) as a query. The zebrafish *hip* gene is located on chromosome 1, and is composed of 13 exons. No duplicate of *hip* gene was found in the zebrafish genome. Primers (forward: 5' ATGAAGCATTTGAAATTTGTGCT 3'; reverse: 5' TTAAACAATATAACTAGTGAGGTCCA 3') were designed to amplify the entire coding region of *hip* using an RT-PCR approach based on the sequence of the *hip* transcript provided by Ensembl. The cDNA of the coding region of *hip* was cloned from mRNA of 20dpf and 40dpf zebrafish larvae. The coding region of *hip* cDNA is 2082bp long and 99.7% identical to the zebrafish sequence predicted by Ensembl. The deduced protein sequence is 66.6% and 66.3% identical to that of the human and mouse hip proteins, respectively, and the region between the amino acid residues 270 and 442 is highly conserved between zebrafish and mammals (89% identity). Scanning of hip protein sequence by SignalP 3.0 Server on-line program revealed a signal peptide of 22aa. The cleavage site of this signal peptide is highly conserved in zebrafish, human and mouse hip precursors. The 22aa transmembrane domain found at the C-terminal end of mouse hip protein is highly conserved in zebrafish hip protein (77.3%) (Figure 15).

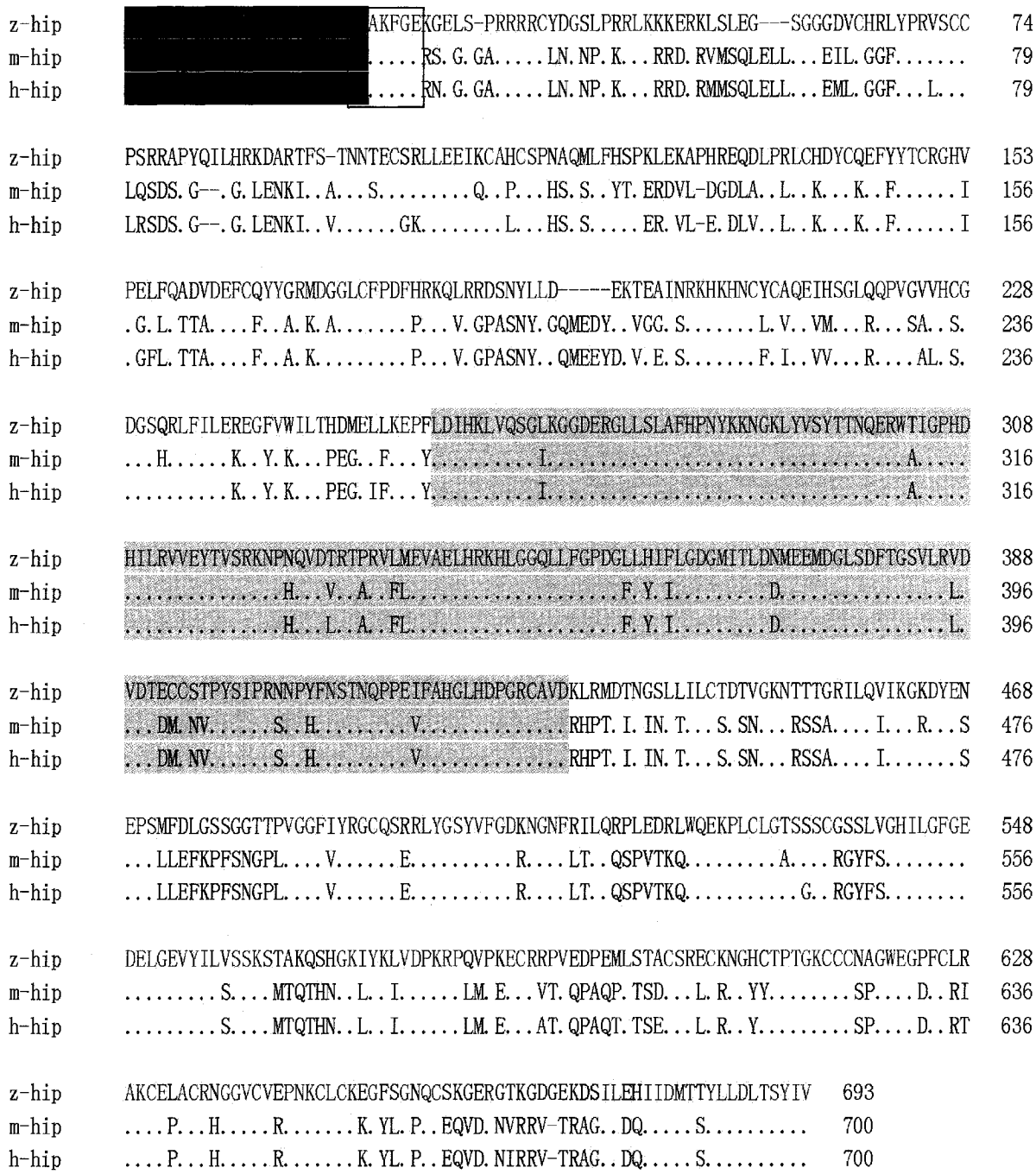
z-hip AKFGEKGELS-PRRRRCYDGSLPRRLKKKERKLSLEG---SGGGDVCHRLYPRVSCC 74
m-hip .....RS.G.GA.....LN.NP.K...RRD.RVMSQLELL...EIL.GGF..... 79
h-hip .....RN.G.GA.....LN.NP.K...RRD.RMMSQLELL...EML.GGF...L... 79
z-hip PSRRAPYQILHRKDARTFS-TNNTECSRLLEEIKCAHCSPNAQMLFHSPKLEKAPHREQDLPRLCHDYCQEFYYTCRGHV 153
m-hip LQSDS.G--.G.LENKI..A...S.....Q..P...HS.S..YT.ERDVL-DGDLA..L..K...K..F.....I 156
h-hip LRSDS.G--.G.LENKI..V.....GK.....L...HS.S.....ER.VL-E.DLV..L..K...K..F.....I 156
z-hip PELFQADVDEFCQYYGRMDGGLCFPDFHRKQLRRDSNYLLD-----EKTEAINRKHKHNCYCAQEIHSGLQQPVGVVHCG 228
m-hip .G.L.TTA....F..A.K.A.....P...V.GPASNY.GQMEDY..VGG.S.....L.V..VM...R...SA..S. 236
h-hip .GFL.TTA....F..A.K.....P...V.GPASNY..QMEEYD.V.E.S.....F.I..VV...R....AL.S. 236
z-hip DGSQRLFILEREGFVWILTHDMELLKEPFLDIHKLVQSGLKGGDERGLLSLAFHPNYKKNGKLYVSYTTNQERWTIGPHD 308
m-hip ...H.....K..Y.K...PEG..F...Y.....I.....A..... 316
h-hip .....K..Y.K...PEG.IF...Y.....I.....A..... 316
z-hip HILRVVEYTVSRKNPNQVDTRTPRVLMEVAELHRKHLGGQLLFGPDGLLHIFLGDGMITLDNMEEMDGLSDFTGSVLRVD 388
m-hip .....H...V..A..FL.....F.Y.I.....D.....L. 396
h-hip .....H...L..A..FL.....F.Y.I.....D.....L. 396
z-hip VDTECCSTPYSIPRNNPYFNSTNQPPEIFAHGLHDPGRCAVDKLRMDTNGSLLILCTDTVGKNTTTGRILQVIKGKDYEN 468
m-hip ...DM.NV.....S..H.....V.....RHPT.I.IN.T...S.SN...RSSA....I...R...S 476
h-hip ...DM.NV.....S..H.....V.....RHPT.I.IN.T...S.SN...RSSA....I.....S 476
z-hip EPSMFDLGSSGGTTPVGGFIYRGCQSRRLYGSYVFGDKNGNFRILQRPLEDRLWQEKPLCLGTSSSCGSSLVGHILGFGE 548
m-hip ...LLEFKPFSNGPL....V.....E.....R....LT..QSPVTKQ.....A....RGYFS..... 556
h-hip ...LLEFKPFSNGPL....V.....E.....R....LT..QSPVTKQ.....G..RGYFS..... 556
z-hip DELGEVYILVSSKSTAKQSHGKIYKLVDPKRPQVPKECRRPVEDPEMLSTACSRECKNGHCTPTGKCCCNAGWEGPFCLR 628
m-hip .....S....MTQTHN..L..I.....LM.E...VT.QPAQP.TSD...L.R..YY.....SP....D..RI 636
h-hip .....S....MTQTHN..L..I.....LM.E...AT.QPAQT.TSE...L.R..Y.....SP....D..RT 636
z-hip AKCELACRNGGVCVEPNKCLCKEGFSGNQCSKGERGTKGDGEKDSILEHIIDMTTYLLDLTSYIV 693
m-hip ....P...H.....R.....K.YL.P..EQVD.NVRRV-TRAG..DQ.....S..... 700
h-hip ....P...H.....R.....K.YL.P..EQVD.NIRRV-TRAG..DQ.....S..... 700

Figure 15

Figure 15: Alignment of the deduced amino acid sequences of the zebrafish hip (z-hip), mouse hip (m-hip), and human hip (h-hip).

Residues conserved between z-hip, m-hip and h-hip are shown in red in the z-hip sequence and are shown as dots in m-hip and h-hip sequences. Residues conserved only in m-hip and h-hip are shown in green. Similar residues are shown in blue. The putative protein sequence of hip is 66.3% and 66.6% identical to that of m-hip and h-hip, respectively, while the region from residue 270 to 442 (shaded region) is highly conserved between zebrafish and mammals (89% identity). The putative signal peptide predicted by SignalP 3.0 Server on-line is highlighted in blue, and the box indicates the highly conserved region around the cleavage site. The hydrophobic membrane-anchoring domain at the C-terminus is highlighted in yellow. This domain is highly conserved between zebrafish and mammals (77.3% identity).

b. Expression of *hip* during fin regeneration

Hip expression during fin regeneration was examined by *in situ* hybridization using a *hip* anti-sense RNA probe. Caudal fins of wild type adult zebrafish were amputated and the regenerates were cut off and fixed at different time points, and then processed for in situ hybridization on whole-mount samples or frozen transverse sections.

In situ hybridization on frozen sections of regenerates of 1dpa showed a ubiquitous week expression in the mesenchymal cells of the regenerates (data not shown). Since no detection of *hh* expression was reported at these stages, it is possible that this staining is an artifact. However, it is possible that a low level of *hh* gene expression may not have been detected by *in situ* hybridization. Moreover, we cannot rule out the possibility that factors other than those involved in the Hh signaling pathway can regulate *hip* transcription. The presence of *hip* and *hh* transcripts in fin regenerates at the early stages of fin regeneration will be examined by RT-PCR in the future.

In situ hybridization on whole mount regenerates at 4dpa showed that *hip* is expressed in the distal end of each fin ray (Figure 16A, black arrow). At a more proximal level of the regenerate, *hip* domain of expression becomes gradually restricted to the middle region of the lepidotrichia (Figure 16A). *In situ* hybridization on transverse sections revealed that in the distal blastema, *hip* is ubiquitously expressed in the blastema cells (Figure 16B, black arrows) and show a higher expression level in two groups of cells, one on each side of the fin ray, located in the middle of the scleroblasts cell layers (the bone matrix-secreting cells) (Figure 16B, yellow arrows).

On sections at a more proximal level, *hip* expression is restricted to a subset of scleroblasts, again located in the center of the scleroblasts lining the inside boundary of the regenerating hemirays and, to cells located around the actinotrichia (Figure 16C). It is important to note that at 4dpa, there is no obvious indication of the formation of a bifurcation when observing the structure of the ray tissue on the sections (Figure 16B and C). We therefore hypothesize that *hip* expression in these subsets of cells blocks shh and ihha signaling. This would prevent bone formation at this particular region, which in turn would induce the formation of ray branches.

At 6dpa, two ray branches are visible even on whole-mount fin samples (left panel, Figure 17). *Hip* expression on whole-mount fin regenerates at 6dpa is similar to that at 4dpa. *In situ* hybridization on transverse sections of fin regenerates shows that *hip* is still ubiquitously expressed in the distal blastema cells (Figure 17A) and at a more proximal level, *hip* expression is concentrated in cells surrounding the actinotrichia including the scleroblasts (Figure 17B). At even more proximal levels of the regenerate where the two branches of the lepidotrichia are already fully formed, the expression domain of *hip* is restricted to the lateral limits of the hemirays of the two branches and to the tissue between the two newly formed branches (Figure 17C). Finally, in sections performed below the bifurcation point, *hip* may be expressed around blood vessels; however, this remains to be verified (Figure 17D).

It was reported that before a lepidotrichia bifurcation becomes visible, the domain of expression of *shh* segregates into two, prefiguring the position of the future branches (Laforest et al., 1998). Here I show that *hip* is specifically expressed in subsets of

cells located at the future branching point, in the region separating the two sub-domains of expression of *shh*. This suggests that *hip* might be one of the factors that lead to or maintain the separation of the *shh*-expressing domains during regeneration that may allow the branching of the fin ray.

4dpa

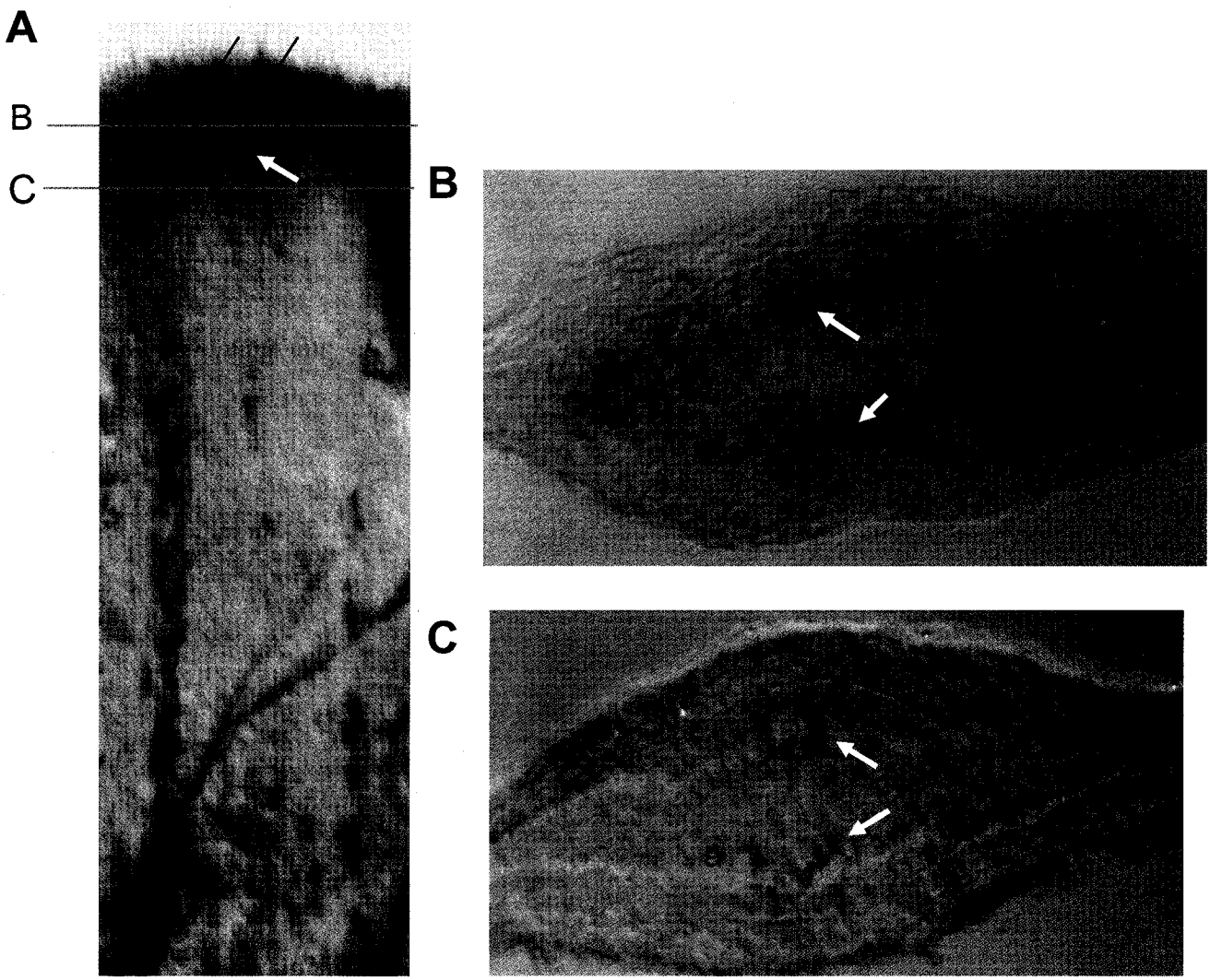

Figure 16

Figure 16: *Hip* expression in fin regenerates at 4dpa

Hip expression detected by *in situ* hybridization with *hip* anti-sense RNA probe on whole mount (**A**) and transverse sections (**B**, **C**) of fin regenerates at 4dpa. **B** and **C** show transverse sections at the levels indicated by blue lines in **A**. **A**: *Hip* is ubiquitously expressed in the distal blastema (black arrows). The domain of expression becomes restricted to the middle region of the fin ray in more proximal regions of the regenerate (yellow arrow). **B**: *hip* is expressed in mesenchymal cells in the distal blastema in a diffuse way (black arrows). Two groups of cells which are likely to be scleroblasts show a higher expression level of *hip* (yellow arrows). Red brackets indicate the epithelial layer. **C**: *hip* expression is restricted to two small groups of cells (yellow arrows) close to the actinotrichia. The red arrow indicates the bone matrix that has been deposited in the epithelial-mesenchymal boundary. Interestingly, the groups of cells indicated by yellow arrows in **B** and **C** are located at the site of the future branching points. e: epithelial layer; a: actinotrichia.

6dpa

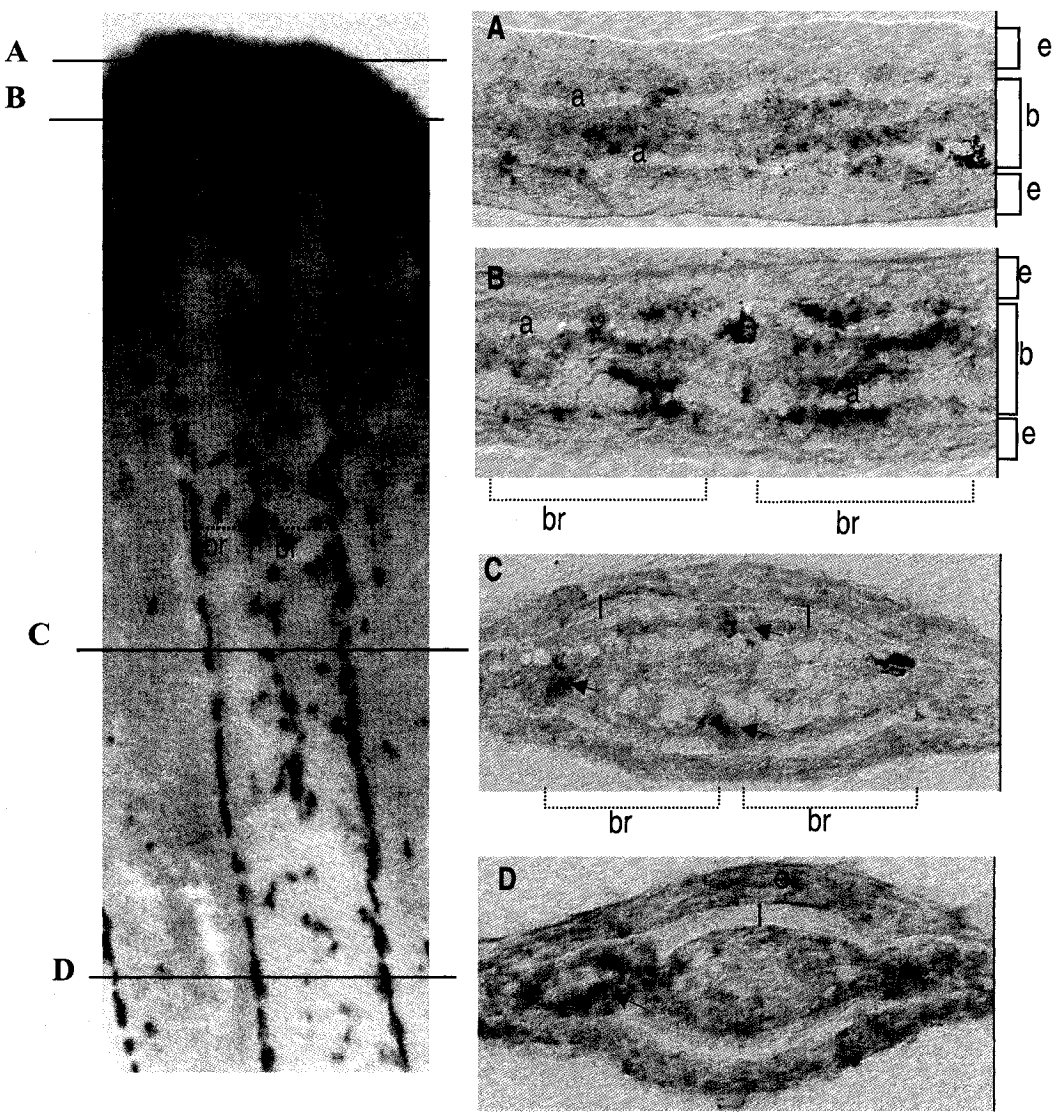

Figure 17

Figure 17: *Hip* expression in fin regenerates at 6dpa.

Hip expression in the two branches of one regenerating fin ray at 6dpa detected by in situ hybridization on whole mount (left panel) and transverse sections (right panels). The black lines in the left panel indicate the level of sections showed in the right panel.

A. *hip* is ubiquitously expressed in the mesenchymal cells in the distal blastema. **B.** *hip* is expressed in the scleroblasts and in the cells surrounding the actinotrichia. **C.** In more proximal regions, *hip* expression is restricted to the central region between the 2 ray branches and the lateral limits of the newly formed branches. **D**: at even more proximal levels where the lepidotrichia is fully formed, *hip* is expressed around a hole which judging by the position is very likely to be a blood vessel. This remains to be further investigated.

a: actinotrichia; b: blastema; br: branch of a ray; e: epidermis; l: lepidotrichia; red arrows indicate the expression region of *hip* in **C** and **D**.

c. *Hip o*verexpression induces a branching delay of the fin rays

To investigate the role of hip during fin regeneration, I analyzed the effect of hip overexpression in the fin regenerates on the regeneration process and ray patterning using the method of local cell transfection described by Quint et al (Quint et al., 2002). Briefly, it has been shown that plasmid DNA constructs microinjected into the blastema of the fin regenerate can transfect between 30 to 100 cells. The microinjection technique by itself does not affect the regeneration process as shown by the normal regeneration of rays injected with pEGFP-N1 (refer to Appendix II), an EGFP-expressing constructs (see control rays in the experiments described below and Quint et al., 2002).

Because hip is a membrane protein and because the technique of *in vivo* transfection has a limited transfection efficiency, a soluble form of Hip was made to enhance the effect of such overexpression. Since truncation of the last 22 amino acids of the mouse hip protein resulted in a soluble and biologically functional form of hip (Chuang and McMahon, 1999), and since this region presents a high degree of identity with the corresponding sequence of the zebrafish hip protein, a similar truncated form of the zebrafish protein was generated.

The coding region of *hip* cDNA without the last 66bp was amplified by PCR using the following primers: forward primer: 5' ATGAAGCATTTGAAATTTGTGCT 3'; reverse primer: 5' GTCTTTCTCACCGTCCCCTT 3'. This generated a truncated *hip* cDNA, named Δ*hip* (Figure 18A). The Δ*hip* cDNA was then inserted into an

expression vector under the control of the CMV promoter (Figure 18A).

Zebrafish caudal fins were amputated and microinjection of plasmid constructs was performed at 3dpa. The Δ*hip* construct was microinjected into the blastema of 6 rays of the ventral lobe, and a control construct, EGFP under the control of the CMV promoter (Quint et al, 2002), was microinjected into the blastema of the 6 corresponding rays of the dorsal lobe (Figure 18B). Approximately 30ng of plasmid DNA was microinjected into the blastema of each fin ray. EGFP expression in the regenerates was examined 1day post injection (dpi) (Figure 18C). GFP fluorescence showed that the cells of the regenerates were efficiently transfected. Fin regeneration was then observed during the following days. When branching of the regenerating rays was analyzed, the lateral-most rays were not included in the measurements and calculations since they do not bifurcate; but when the growth of the regenerates was examined, all 6 pairs of injected rays were included in the statistical analysis.

As described in the section about laser cell ablation, a difference of 2 segments or more in the position of the branching points of the corresponding dorsal and ventral rays was considered as significant. The position of the branching points of the fin rays was usually measured at 10dpa, i.e. 7dpi. However, in some cases when not all the injected rays had yet formed branches, I continued to follow the regeneration until the branching points of the corresponding dorsal and ventral rays were visible. 44% (n=250) of the Δhip-injected rays showed a significant delay of branching (Figure 19A and B), while 0.07% (n=30) of the control rays showed branching delay.

In some of the overexpression experiments, a growth delay of the *Δhip*-injected rays was also observed (Figure 20A). The length of the fin rays was measured at 11dpa (i.e. 8dpi) and the growth delay was calculated by the following formula:

$$\text{Average delay of growth} = \frac{1}{n}\sum^{n}\frac{Ld - Lv}{Ld} \times 100\%$$

n= total number of Δhip-injected rays

Ld and Lv represent the length of a dorsal ray and of the corresponding ventral ray, respectively.

The calculated average growth delay induced by *hip* overexpression is 11% (P= 0.00026). For comparison, in non-injected control fish, a growth delay between dorsal and ventral rays was observed in 4% of the rays (Figure 20B). This growth delay might be due to the occasional high efficiency of cell transfection of the injected plasmid, which leads to a more robust inhibition of Hh. This result is reminiscent of the growth arrest observed after inhibition of hh signaling by cyclopamine although the growth defect is much more moderate (Quint et al., 2002).

A

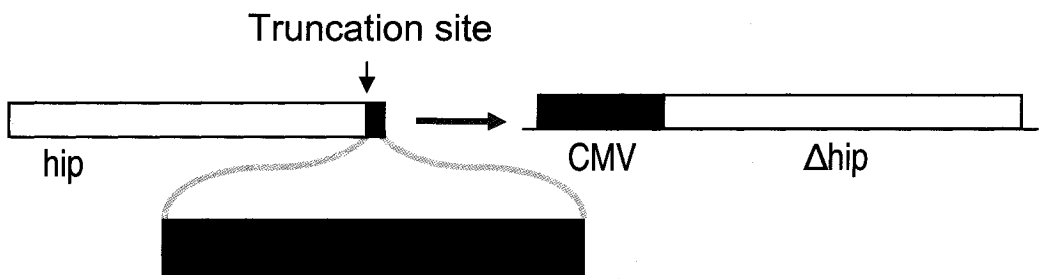

B

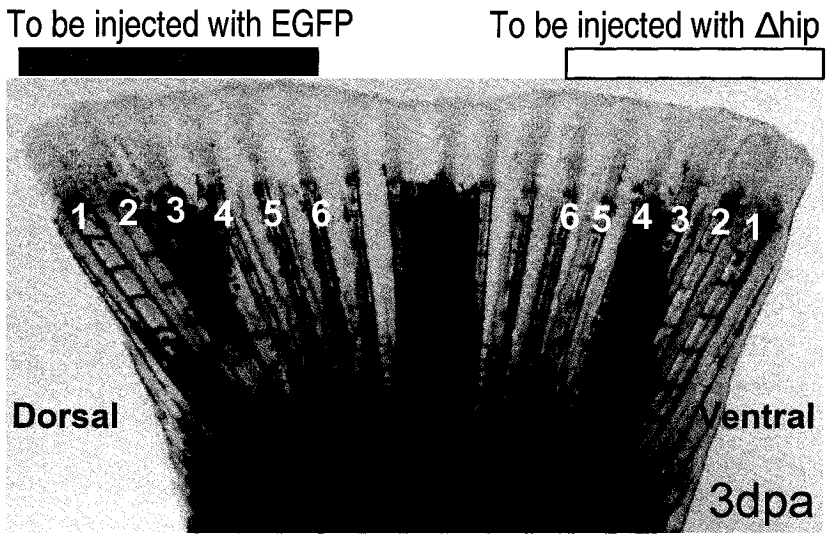

C

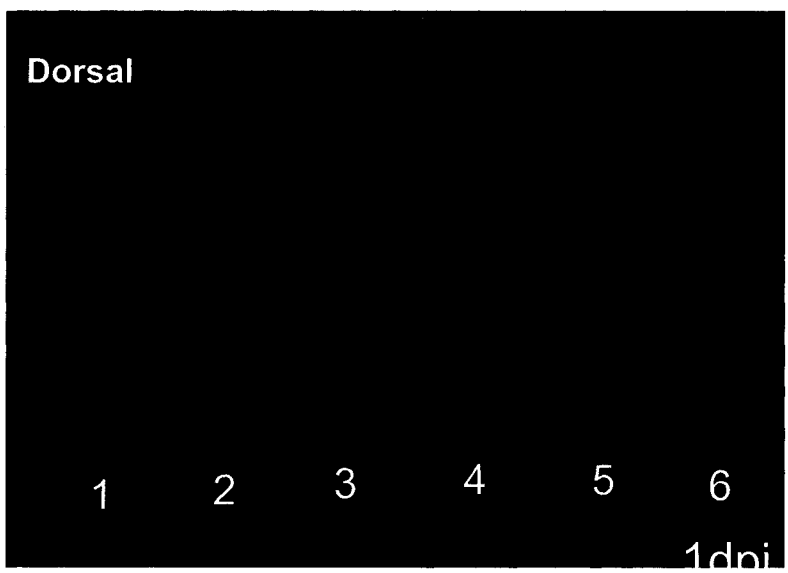

Figure 18

Figure 18: The method of *hip* overexpression.

A: Schematic representation of the CMV:Δ *hip* construct used in over-expression experiments. The coding region of the last 22aa membrane binding site was truncated to generate a soluble form of hip, named Δhip. The cDNA of Δhip was inserted into a modified pCMV5 vector (Quint et al., 2002) under the control of CMV promoter, making the Δhip construct (refer to Appendix II). **B**: Design of the Δ *hip* overexpression experiment. Δhip construct was microinjected into the 6 ventral rays of the regenerates at 3dpa, while the pEGFP-N1 (refer to Appendix II) was injected at the same time into the corresponding 6 dorsal rays as control. **C**: The pEGFP-N1 injected rays were examined at 1day post injection (dpi). The green fluorescence indicates the cells that are transfected by the EGFP construct. Numbers in B and C indicate ray numbers.

A

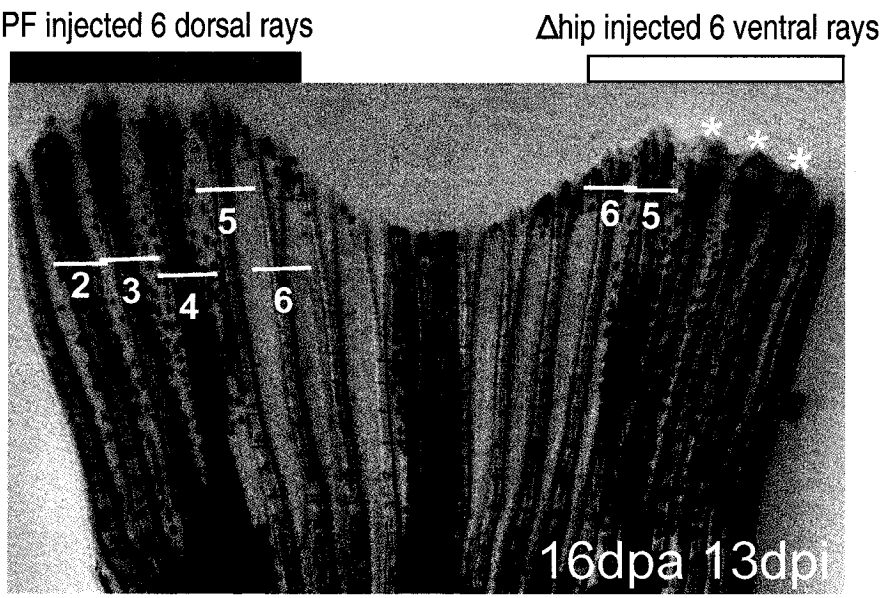
GPF injected 6 dorsal rays
Δhip injected 6 ventral rays
2
3
4
5
6
6
5
16dpa 13dpi

B

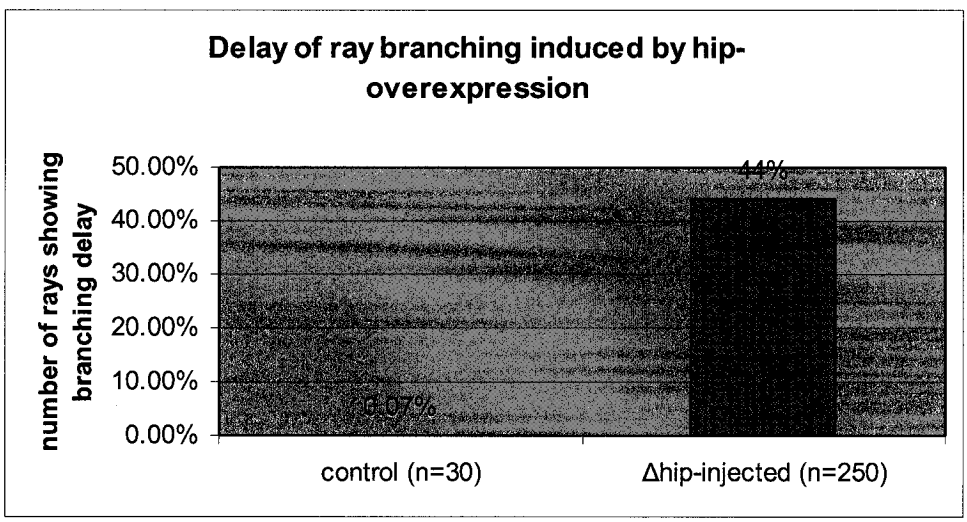
Delay of ray branching induced by hip-overexpression
number of rays showing branching delay
50.00%
40.00%
30.00%
20.00%
10.00%
0.00%
44%
3.07%
control (n=30)
Δhip-injected (n=250)

Figure 19

Figure 19: *Hip* overexpression induces a delay of ray branching during fin regeneration.

A: Δ *hip*-injected rays show delayed bifurcation at 16dpa 13dpi when compared to the conrol EGFP-injected rays. The white lines indicate the origin of bifurcations in ray 2-6 injected with EGFP construct (left side) or Δ hip construct (right side). Note: only rays #5 and #6 show a bifurcation in this fin after Δ hip injection and their formation is delayed when compared to the corresponding rays on the EGFP-injected side. **B**: 44% of the rays (n=250) in which *hip* is overexpressed showed a delay of branching, while 0.07% (n=30) of the rays in non-injected control fish show a delay of ray branching.

A

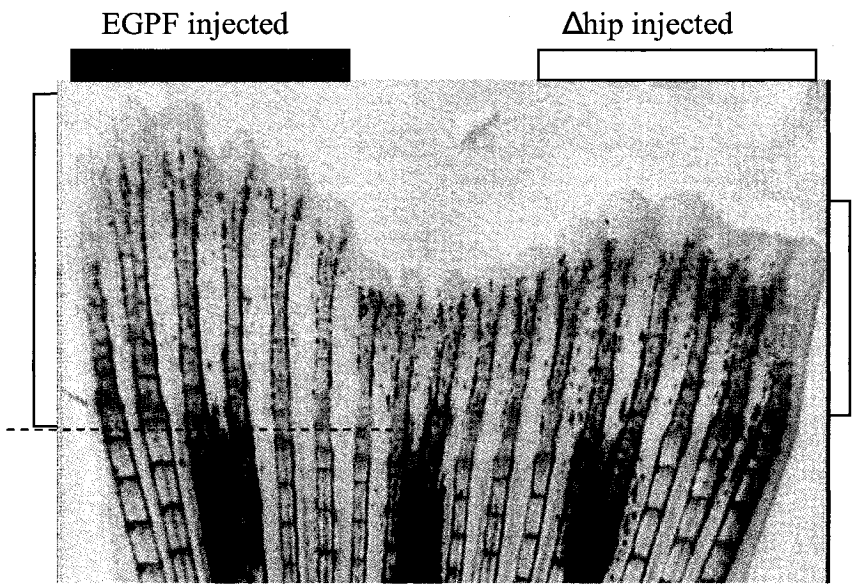
EGPF injected
Δhip injected

B

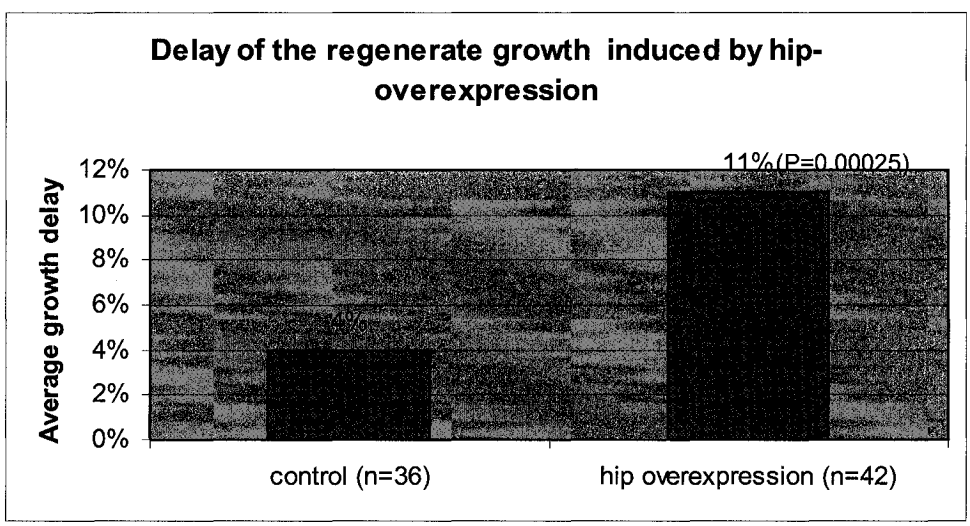
Delay of the regenerate growth induced by hip-overexpression
Average growth delay
12%
10%
8%
6%
4%
2%
0%
11%(P=0.00025)
4%
control (n=36)
hip overexpression (n=42)

Figure 20

Figure 20: *Hip* overexpression induces a delay of growth during fin regeneration.

A: Δ hip injected rays showed a growth delay compared to the EGFP-injected rays. Dotted line indicates the level of amputation. Brackets on the left and right sides of the picture indicate the length difference of the rays after EGFP or Δ hip injections,respectively. **B**: The regenerates were examined at 11dpa 8dpi and the injected rays were measured. The length of a dorsal ray is termed Ld, and the length of its corresponding ventral ray is termed Lv. All 6 pairs of injected rays were measured in each fish. Percentage of difference in the length of the rays was calculated by the following formula:

$$\text{Average delay of growth} = \frac{1}{n}\sum^{n}\frac{Ld - Lv}{Ld} \times 100\%$$

Average growth delay in all the *hip*-injected rays is 11% (P= 0.00026), which is significant compared to 4% in non-injected control rays.

d. Overexpression of Δ*hip* affects the expression of genes important for patterning the regenerates and bone deposition.

To investigate the molecular events which lead to the delay of ray branching induced by the overexpression of Δ*hip* in the regenerates, I examined the expression of selected gene markers by whole mount in situ hybridization. Δ*hip* overexpression was performed as described above at 3dpa on fish of the 2.2*shh:gfp* ABC#15 transgenic line. Fluorescence imaging before injection (Figure 21A and B) and at 1dpi (Figure 21C and D) showed that the *shh:gfp* expression remained the same, indicating that the overexpression of Δ*hip* has no obvious effect on the expression of *shh.* At 8dpa, i.e. 5dpi, the expression domain of GFP in all the rays separated into two sub-domains, suggesting that the rays were going to branch (Figure 21E and F). At 11dpa, i.e. 8dpi, the 5 control EGFP-injected dorsal rays already showed very clear bifurcation, and *shh:gfp* expression was observed in each branch. In contrast, only two of the 5 Δ*hip*-injected ventral rays showed sign of branching although GFP was expressed in two subdomains as in the control rays (Figure 21G and H). As hip is known to interfere with hh signaling by direct binding to hh proteins, we did not expect to observe an effect on the endogenous *shh* transcript expression or GFP expression in the *shh:gfp* transgenic line. In contrast, hip overexpression should affect the expression of downstream targets of hh signaling. The expression of *ptc1,* the receptor and transcriptional target of shh signaling, was therefore examined after *hip* overexpression.

During fin regeneration, *ptc1* is expressed at the same proximal-distal level as *shh* (Laforest et al., 1998). As *shh,* the expression domain of *ptc1* divides into two before

ray branching. At 11dpa, 8 dpi, in the control EGFP-injected dorsal rays the expression domain of *ptc1* was clearly separated and the ray branches were starting to be visible (Figure 22A), while in the Δ*hip*-injected ventral rays the expression domain of *ptc1* remained undivided or just started to show sign of division (Figure 22B). This result indicates that although *shh* expression remained unchanged, Δhip interfered with shh signaling, therefore affecting *ptc1* expression. The improper spatial expression of *ptc1* could possibly lead to the unsuccessful induction of downstream signals finally affecting the proper expression of genes that are responsible for bone deposition.

The above proposal was supported by the expression analysis of Type X Collagen (*col10a1),* a scleroblast marker (Avaron et al., 2006). At 8dpa 5dpi, the expression domain of *col10a1* was clearly separated in the control EGFP-injected dorsal rays, prefiguring the ray branching (Figure 22C), while it remained undivided in the *Δhip*-injected ventral rays (Figure 22B). Since Collagen X is an important component of the lepidotrichia, this delay of division of *col10a1* expression domain would then lead to the delay of ray branching.

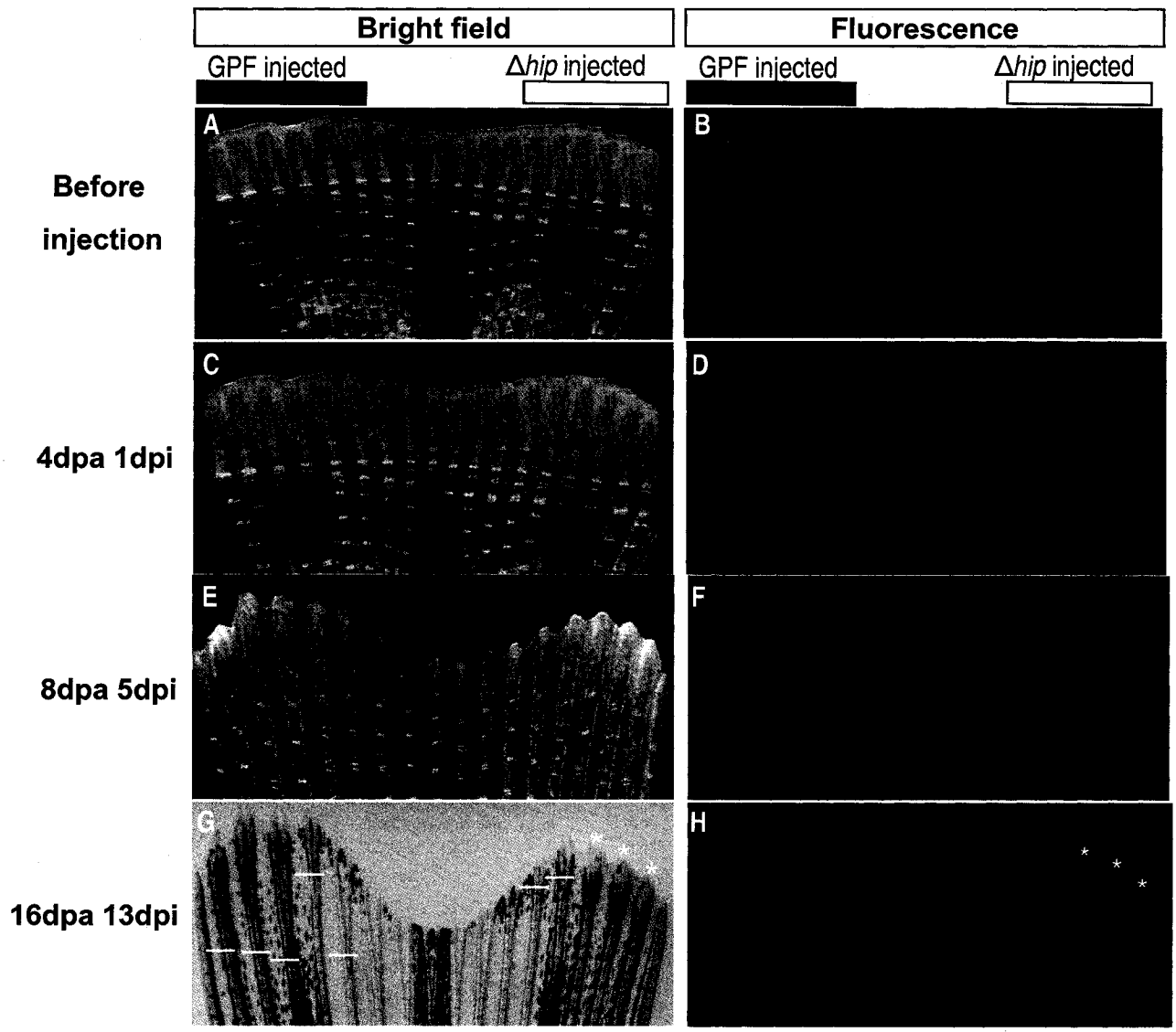
Bright field
Fluorescence
GPF injected
Δhip injected
GPF injected
Δhip injected
Before injection
4dpa 1dpi
8dpa 5dpi
16dpa 13dpi
A
B
C
D
E
F
G
H

Figure 21

Figure 21: The overexpression of *Δhip* had no obvious effect on the expression level of *shh:gfp*.

Despite the inhibition of branching formation following *Δhip* overexpression, the GFP domain of expression (i.e. *shh* domain of expression) divides into two subdomains in each fin ray. The eight panels show the same fin of a *shh:gfp* ABC#15 transgenic fish observed before injection (A,B), at 1dpi (C,D), 5dpi (E,F) and 13 dpi (G,H) in bright field (A,C,E,G) and under fluorescence microscope (B,D,F,H). The right rays were injected with *Δhip1* construct and the left rays with the control construct. **A,B**: pictures taken before injection, showing the regenerates and the *shh:gfp* expression domain on each fin ray. **C,D**: at 1dpi, the *shh:gfp* expression domain remained the same showing no effect due to the overexpression of *Δhip*. **E,F**: at 5 dpi, two GFP-subdomains are visible in each fin ray suggesting the imminent formation of a bifurcation. However, 8 days later (13 dpi), while all the control rays effectively formed bifurcations, only two *Δhip*-injected rays show a bifurcation whose formation is delayed (G). The white horizontal lines in G indicate the origin of bifurcation in the injected rays. The white stars in G and H indicate the three rays in each panel as examples of a GFP domain subdivision not accompanied by branching formation.

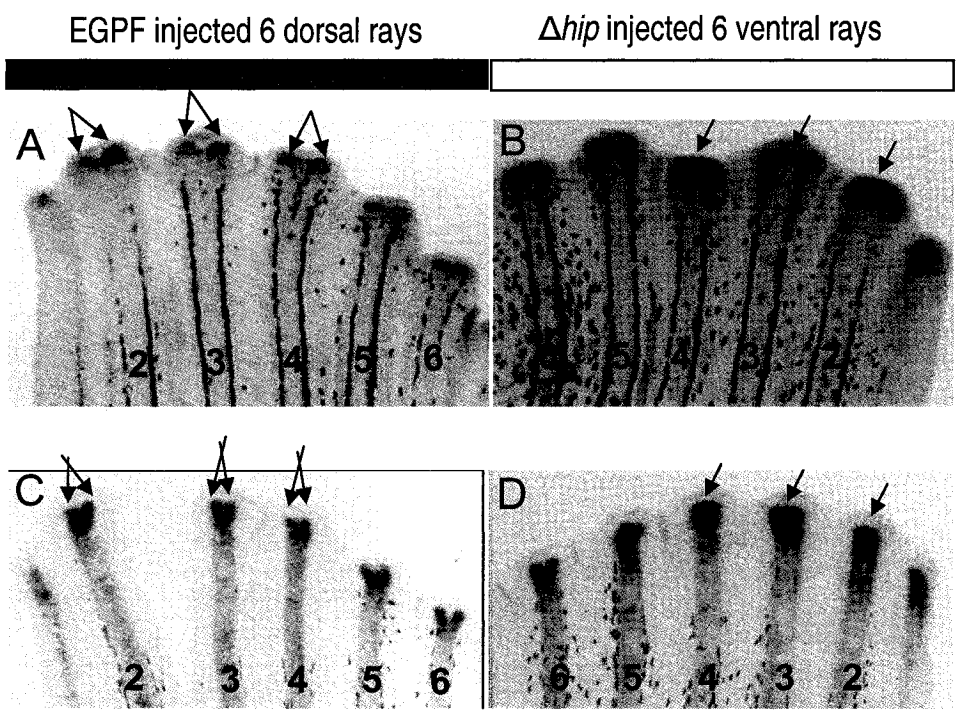
EGPF injected 6 dorsal rays
Δhip injected 6 ventral rays
ptc1
col10a1
A
B
C
D
2
3
4
5
6
6
5
4
3
2

Figure 22

Figure 22: The separation of the expression domain of *ptc1* and *col10a1* is delayed due to the overexpression of *Δhip.*

A and B: *Ptc1* expression in rays of the dorsal and ventral lobes, respectively, of the same fin regenerates at 11dpa (i.e. 8dpi). C and D: *col10a1* expression in the rays of the dorsal and ventral lobes, respectively, of the same fin regenerates at 8dpa (i.e. 5dpi). The 6 dorsal rays shown in A and C have been injected with the EGFP construct and the 6 ventral rays shown in B and D have been injected with Δhip construct. *Ptc1* (A) and *col10al* (C) expression in the control rays is observed in two distinct subset of cells in each fin ray while there is not a clear subdivision of the expression domain of *ptc1* (B) and *col10a1* (D) in most of the Δhip-injected rays. Coupled arrows in A and C indicates the subdivision of the expression domain of *ptc1* and *col10a1*, and arrows in B and D indicate the expression domain of *ptc1* and *col10a1* that still remain unseparated.

Discussion

Zebrafish caudal fin is considered to be a good model to study epimorphic regeneration. Fin regeneration depends on the formation of a blastema, a tissue consisting of undifferentiated and proliferating mesenchymal cells. As the regeneration proceeds, cells located in the proximal part of the blastema differentiate into various cell types to reconstruct the missing part of the fins. Little is known about the signals that regulate the differentiation of the blastemal cells. However, a few factors have been shown to regulate the formation of the lepidotrichia. During fin regeneration, *shh* is expressed in a subset of cells of the basal epithelial layer located just at the level of new bone-matrix deposition in each regenerating fin ray. *Ptc1,* which encodes the receptor of shh, is expressed in the same cells as *shh,* plus adjacent scleroblasts, the cells that release bone matrix for the formation of the lepidotrichia. *Bmp2b* is expressed in the same cells as *shh,* and in a subset of *ptc1*-expressing cells. Before the formation of a bifurcation of the regenerating lepidotrichia, expression domains of *shh, bmp2b* and *ptc1* separate into two, prefiguring the position of the lepidotrichia branches (Laforest et al., 1998). Ectopic expression of *shh* in the tissue between two branches of the regenerating rays induced ectopic expression of *ptc1* and bone fusion between the two sister rays (Quint et al., 2002). These experiments suggested that shh is involved in bone formation during fin regeneration. It has recently been shown that the zebrafish ortholog of the tetrapod *Indian hedgehog* gene, *ihha,* is expressed in the newly differentiated scleroblasts overlapping the *ptc1*-expressing cells and at the same longitudinal level as the *shh*-expressing cells (Avaron et al., 2006). Studies in mammals showed that Ihh is required for the cartilage formation during embryonic development (St-Jacques et al., 1999; Colnot et al., 2005),

suggesting that ihha may play a direct role in bone formation during fin regeneration. Based on these findings, we proposed that the role of shh in bone formation during zebrafish fin regeneration is patterning bone morphogenesis, rather than directly regulating the bone deposition. Two approaches were used to test this hypothesis.

1. Inhibition of shh signaling by removing the shh-expressing cells during fin regeneration

a. laser ablation of shh-expressing cells induces delay of ray branching during fin regeneration

If the above hypothesis is correct, disruption of shh signaling by removing *shh*-expressing cells in the regenerates would induce a defect in bone patterning. To target the *shh*-expressing cells in regenerates *in vivo*, the zebrafish *shh:gfp*ABC#15 transgenic line in which GFP expression recapitulates endogenous expression of *shh* was utilized. Ablation of the *shh*-expressing cells by a laser beam induces a significant delay of ray branching during fin regeneration, without affecting the growth of the fin regenerates. This result supports the hypothesis that *shh*-expressing cells are involved in patterning bone formation during fin regeneration.

b. The technique of laser cell ablation

In the current study, the laser cell ablation was used to study fin regeneration for the first time. The method of laser cell ablation has been previously successfully applied in zebrafish embryos and larvae to study the functions of specific cell types *in vivo*. Laser Ablation of the GFP-expressing optic tectum induces defects in the visuomotor

behaviors of zebrafish larvae (Roeser and Baier, 2003), and laser ablation of the cardiac premigratory neural crest at the three- to four-somite stage resulted in failure of the heart tube to undergo looping (Li et al., 2003). Based on the laser ablation experiment described in these publications, a method suitable for adult live fish was established. Since the purpose of utilizing laser cell ablation is to kill the designated cells, two major issues regarding this technique have to be addressed: 1) the efficiency (whether the targeted cells are actually killed) and 2) the specificity (whether only the targeted cells are killed).

The efficiency of this method was confirmed. In the current study, *shh:gfp*-expressing cells were targeted in the guidance of GFP fluorescence. After the laser pulses were applied, the disappearance of GFP fluorescence could be due to the destruction of the cell or simply photobleaching of GFP fluorescence. To determine whether the cells were effectively killed, control experiments were performed. Various cell types, such as melanocytes, blood cells and DiI-labeled cells in the regenerates were successfully ablated by this method. Furthermore, *shh* transcripts were undetectable by *in situ* hybridization after the ablation of the *shh:gfp*-expressing cells, confirming the efficiency of the method of laser cell ablation in regenerating fin. *In situ* hybridization may be less sensitive than e.g. Reserse Transcriptase-PCR in detecting transcripts, therefore it is possible that there was still small amount of *shh* transcripts remaining after laser ablation was performed. However, a dramatic decrease in *shh* transcripts has been shown by *in situ* hybridization, which ought to be enough to induce morphological defects.

As for whether only the *shh:gfp*-expressing cells are ablated with the adopted method, more work needs to be done. The purpose of our experiments was to remove only the *shh:gfp*-expressing cells in the regenerates. However, laser is thought to exert its effect in the tissue by generating heat and free radicals, both of which can spread between cells. So it is possible that this method also destroyed the cells above or beneath the basal layer of epithelia, such as scleroblasts. It is further possible that other connections to and from the *shh*-expressing cells were secondarily affected. This is an intrinsic problem of many lesion-inducing techniques, such as surgical, genetic manipulation, or toxin injection. The effect of the laser cell ablation in regenerates was quite mild (ray branching was delayed but bone growth was not affected), therefore the lesion in the scleroblasts induced by the laser treatment, if any, is presumed to be tolerable. The intactness of scleroblasts after laser ablation will be confirmed in the future work by examining the expression of *ihha* and *col10a1*, scleroblast markers in the regenerating fin.

c. The limitation of the experiment of laser cell ablation

Despite the clear effect observed on ray branching, the laser cell ablation approach may present some limitations for the interpretation of the results. Besides *shh*, there are other factors expressed in the ablated cells that may be involved in tissue patterning as well. One of such factors is the Lymphoid Enhancer Factor 1, lef1 (Poss et al., 2000). Lef1 is a member of the Wnt signaling pathway. Targeted inactivation of Lef-1 abrogates the formation of organs that depend on epithelial-mesenchymal tissue interactions, such as mammary glands, whiskers, teeth, and body hair during mouse embryonic development (van Genderen et al., 1994). Requirement for Lef1 expression in both mesenchymal and epithelial tissue has been demonstrated

(Kratochwil et al., 1996). During zebrafish fin regeneration, lef1 was proposed to play a similar role as shh in patterning the skeleton (Poss et al., 2000), as suggested by the observation that *lef1* is expressed in the same cells as *shh* and treatment of fin regenerates with retinoic acid or the synthetic Fgfr1 inhibitor SU5402 down-regulates the expression of *lef1* in epidermis, similar to their effects on *shh* expression. Therefore, the defect in bone formation during fin regeneration induced by laser ablation of *shh*-expressing cells may not necessarily be due to only the inhibition of shh signaling, but also to the disruption of Wnt signaling. Many other unknown signals might be present in these *shh*-expressing cells and might play a role in bone patterning as well. To further investigate the role of shh signaling in bone patterning during fin regeneration, hip, an hh signaling antagonist was overexpressed in the fin regenerates.

2. Overexpression of *hip*, an hh signaling antagonist, in the fin regenerate

a. *Hip*-overexpressing induces delay of ray branching during fin regeneration

To inhibit shh signaling during fin regeneration *in vivo*, the zebrafish cDNA encoding the *hedgehog interacting protein* (*Hip*), an antagonist of Hh signaling, was cloned and overexpressed in regenerating fins. Analysis of *hip* expression during fin regeneration revealed that when ray branches form, *hip* transcripts are detected between the two new branches in the scleroblasts. This restricted domain of expression presumably creates a zone that will be less responsive to hh signal, a situation that would be expected if hh is involved in branching morphogenesis. To inhibit hh signaling in the

regenerates *in vivo, hip* was overexpressed in the regenerates by injecting a *hip*-expressing construct in the blastema at 3dpa. *Hip*-injected rays exhibited a significant delay of branching, similar to that observed in the laser cell ablation experiments.

This result also supports the hypothesis that hh signaling is involved in patterning the ray branches. However, the overexpression of *hip* in the fin regenerates blocks not only shh but also ihha signaling. During long bone development in mammals, *Ihh* is expressed in pre-hypertrophic and early hypertrophic chondrocytes and can directly stimulate chondrocyte proliferation and osteoblast lineage, suggesting that Ihh is an important regulator of chondrocyte proliferation and differentiation (St-Jacques et al., 1999; Long et al., 2004; Colnot et al., 2005). *Ihha*, the zebrafish ortholog of the mammalian *Ihh*, is expressed in the scleroblasts during fin regeneration, suggesting its role in the formation of lepidotrichia. Therefore, the delay of ray branching induced by *hip*-overexpression can be due to the disruption of ihha and/or shh signaling. Nevertheless, shh has been shown to be involved in the branching morphogenesis in other systems such as lung (van Tuyl and Post, 2000; Hu and Rosenblum, 2003; Miller et al., 2004), prostate (Pu et al., 2004), and salivary glands (Jaskoll et al., 2004). In these systems, *shh* is expressed in the epithelial layer and directing epithelial-mesenchymal interactions via its receptor ptc1 expressed in the adjacent mesenchymal cells, a situation similar to the ray branching during fin regeneration. No similar role has been reported for ihha. Results from these other studies favor the hypothesis that shh signaling may have a more important role in bone patterning.

b. Shh signaling may control ray branching by directing the site of scleroblast differentiation during fin regeneration

How shh exerts its function in bone patterning during fin regeneration remains to be further investigated. One possibility is that shh signaling may be necessary to define the region of bone deposition, by determining the position of scleroblast differentiation, as suggested by the findings that ectopic expression of *shh* in the fin regenerates induces ectopic bone depostion only at the right position, i.e. in the space between the basal epithelial cells and the mesenchymal cells, but not, for example, in the middle of the blastema cells (Quint et al., 2002). The current work showed that, in the *2.2shh:gfp*ABC#15 transgenic fish, although *hip*-injected rays were not undergoing any branching, GFP expression domain in these rays was nevertheless divided into two domains as the control rays. However, the *ptc1*-expressing cells in these *hip*-injected rays remained in one domain. The cells expressing *col10a1,* a lepidotrichia component and scleroblast marker, in the *hip*-injected rays remained in one group as well. These observations suggest that the delay of branching induction is due to a defect of shh signal transmission to the target cells, i.e. the differentiating scleroblasts expressing *ptc1* in the blastema, rather than a defect in the *shh* transcription. Probably, this disruption of shh transmission results in the failure in directing scleroblast differentiation at two separated sites, which in turn lead to a defect in the bone branching.

Alternatively, these results may suggest that shh signaling regulates the branching morphogenesis by mediating the migration of differentiated scleroblasts to the proper sites where lepidotrichia is to be formed. Shh has been shown to act as an axonal

chemo-attractant collaborating with netrin-1 in midline axon guidance (Charron et al., 2003). It is further suggested that shh would first act as a chemo-attractant for the commissural axons guidance through its receptor complex Ptc1 and Smo. Later, as these receptors are no longer expressed, *hip* expression is transiently up-regulated and may mediate the repulsive effect of shh observed on the postcommissural axons (Bourikas et al., 2005). However, other studies have also suggested that shh arrests the migration of trigeminal precursors in the head of chick embryo *in vivo* (Fedtsova et al., 2003) and restricts migration of chick neural crest cells *in vitro* (Testaz et al., 2001). More evidence is required for determining the potential role of shh in mediating cell migration during zebrafish fin regeneration.

In summary, the results of the current work suggest that shh signaling is involved in patterning the ray branching during zebrafish fin regeneration. Ihha signaling may also be involved in this process. However, based on the distinct roles of Shh and Ihh in branching morphogenesis of many organs and chondrocyte differentiation and proliferation, respectively, revealed in mammals, ihha may play a more direct role in regulating scleroblast differentiation and/or proliferation rather than in bone patterning. Shh may influence ray branching by mediating the site of scleroblast differentiation or migration of differentiated scleroblasts.

3. *Hip*-overexpression occasionally induced growth delay of the regenerates

Besides the ray branching delay, in some cases of *hip*-overexpression experiments, a

significant growth delay of the regenerates was also observed. It is possible that, in these cases, the blastema cells were more efficiently transfected by the *hip*-expressing plasmid. The higher expression level of hip would then lead to a more severe disruption of hh signaling, which in turn affected other signaling pathways that are responsible for the growth of regenerates.

A stronger regenerative growth arrest effect was observed in the cyclopamine-treated regenerating fin (Quint et al., 2002). Cyclopamine is a steroidal alkaloid that blocks hh signal transduction by directly binding to Smo (Taipale et al., 2000; Chen et al., 2002). Exposing the regenerating fin to cyclopamine resulted in the inhibition of the regenerate outgrowth, reduction of cell proliferation, abolition of *ptc1* expression and an expansion, followed by a reduction, in the domains of *shh* expression.

Treatment of fish with solanidine, another steroidal alkaloid resembling cyclopamine but having no effect on hh signaling, did not alter fin regeneration suggesting that steroidal alkaloids such as solanidine and cyclopamine did not have obvious toxic effects and did not harm the fish at the doses used in these experiments (5-10 μM). However, one cannot exclude the possibility that the severe defects following cyclopamine treatment may partially reflect a secondary effect of cyclopamine because the amputated fish were maintained in the water containing cyclopamine for 1-5 days. For example, one can envisage that the regeneration defect may be due to an insufficient nutrient-intake and/or failure of angiogenesis in the regenerates.

In this context, the *hip*-overexpression experiment described in the present work may represent a better way to inhibit hh signaling than cyclopamine since it allows a local disruption of hh signaling and gives the possibility to use non-injected rays as internal controls. The growth delay induced by *hip*-overexpression further confirms that hh signaling is involved in the control of the regenerate outgrowth. The underlying molecular events that lead to the regenerative growth defect induced by *hip*-overexpression remain to be revealed. Moreover, because of the strong inhibition effect of cyclopamine on growth of the regenerate, we have not previously been able to observe the effect of an inhibition of hh signaling on ray branching. In contrast, *hip*-overexpression having a milder effect than cyclopamine on the growth of the regenerate, gave us the opportunity to reveal the role of hh signaling in patterning the ray branching.

4. Model for the molecular mechanism of ray branching morphogenesis during zebrafish fin regeneration

Based on the previous study and results of the current work, a model for the signal cascades that regulate the branching morphogenesis during zebrafish fin regeneration can be proposed (Figure 23). Shh is secreted by cells in the basal epithelial layer and transmitted to the adjacent mesenchymal cells in the blastema, inducing the expression of *ptc1* and *bmp2b* in these cells. Shh signal is sequestered by Hip. The mesenchymal cells responsive to shh signal differentiate into scleroblasts and secrete bone matrix to form the lepidotrichia. Then, the *shh*-expressing cells separate into two domains that in turn, signal to the differentiating scleroblasts to segregate into two groups, prefiguring the bifurcation of the lepidotrichia. *Hip* is expressed in the cells

between the two groups of differentiating scleroblasts and block hh signaling, contributing to the formation of branches.

This model explains the delay of ray branching induced by ablation of *shh*-expressing cells and *hip*-overexpression. The ablation of *shh*-expressing cells removes the source of shh signal while overexpression of *hip* blocks the transmission of shh signal to its target cells. Both the experiments prevent the reception of shh signal by the differentiating scleroblasts. Therefore, the scleroblasts are maintained in one group, which in turn leads to the delay of ray branching.

One important issue to address to understand branching morphogenesis, but is beyond the scope of this thesis, is to determine how the *shh*-expressing region separates into two before formation of the ray bifurcation. Several hypotheses can be proposed: 1) *shh* expression could be downregulated in cells in the middle of the *shh* domain of expression; 2) *shh*-expressing cells could migrate laterally to form two sub-groups; 3) cell proliferation could be triggered in some cells located in the center of the domain of expression of *shh* to form the division.or 4) cells located at the center of the *shh*-expressing region could undergo apoptosis. In the future, more work is required to investigate these hypotheses or explore other possibilities to unravel the mechanism(s) of the segregation of the *shh*-expressing cells before ray branching.

A

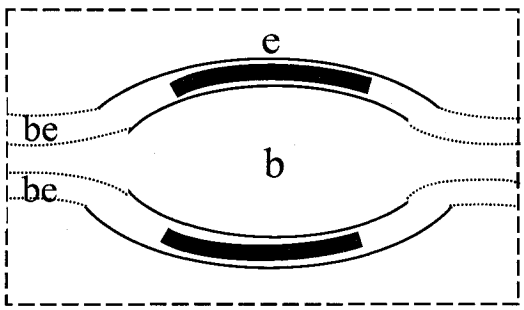

Expression region of *shh*

Expression region of *hip*

Expression region of *ptc-1* and *bmp2b*

B

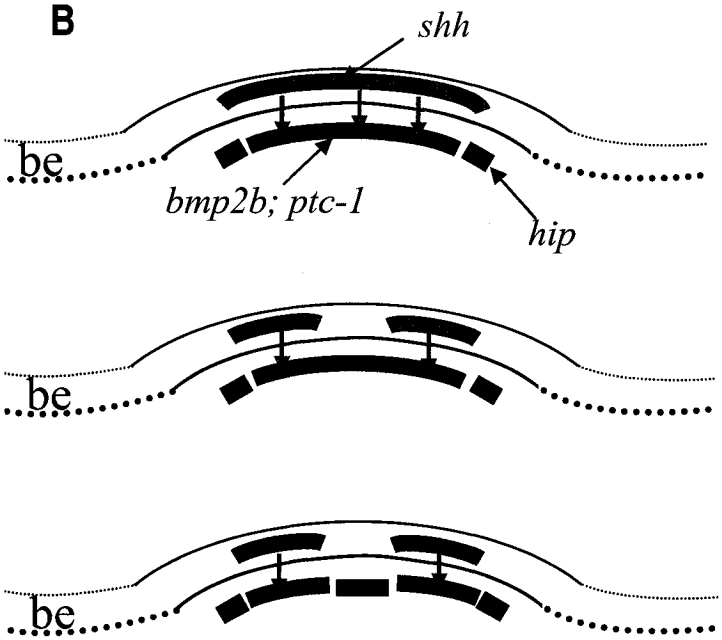

shh-expressing cells in the basal epithelial layer signal to the scleroblasts which express *bmp2b* and *ptc-1*; shh signaling to the lateral sides is limited by *hip* expression

↓

Subdivision of *shh* domain of expression prior to the formation of a branching point

↓

Local upregulation of *hip* expression and local inhibition of *bmp2b* leading to a gap in bone matrix deposition.

C

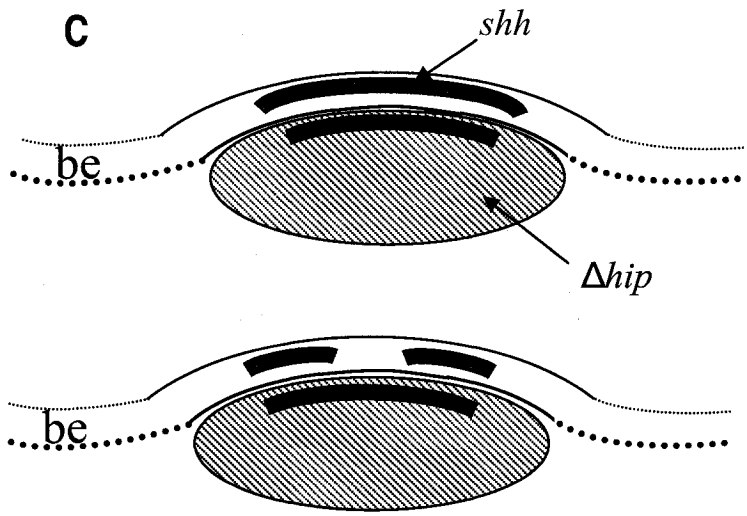

Overexpression of Δ*hip* in the blastema restricts the action of shh on the scleroblasts

↓

Although *shh* domain of expression divides into two domains, this does not lead to the division of *bmp2b* and *ptc-1* domain of expression → no formation of bifurcation

Figure 23: Model for the molecular mechanism of ray branching morphogenesis during zebrafish fin regeneration

A: Schematic representation of a cross section of a fin ray showing *shh* expression (red) in the basal epidermal layer on both sides of the ray, before branching. **Note:** only half of the ray is shown on the following drawings. **B.** Possible cascade of events leading to *hip* upregulation in the centre of a ray and branching morphogenesis. **C.** inhibition of branching morphogenesis following *Δhip* injection in the blastema. e: epithelia; be: basal epithelial layer; b: blastema.

References:

Affolter M, Bellusci S, Itoh N, Shilo B, Thiery JP, Werb Z. 2003. Tube or not tube: remodeling epithelial tissues by branching morphogenesis. Dev Cell 4:11-18.

Akimenko MA, Johnson SL, Westerfield M, Ekker M. 1995. Differential induction of four msx homeobox genes during fin development and regeneration in zebrafish. Development 121:347-357.

Akimenko MA, Mari-Beffa M, Becerra J, Geraudie J. 2003. Old questions, new tools, and some answers to the mystery of fin regeneration. Dev Dyn 226:190-201.

Amores A, Force A, Yan YL, Joly L, Amemiya C, Fritz A, Ho RK, Langeland J, Prince V, Wang YL, Westerfield M, Ekker M, Postlethwait JH. 1998. Zebrafish hox clusters and vertebrate genome evolution. Science 282:1711-1714.

Avaron F, Hoffman L, Guay D, Akimenko MA. 2006. Characterization of two new zebrafish members of the hedgehog family: atypical expression of a zebrafish indian hedgehog gene in skeletal elements of both endochondral and dermal origins. Dev Dyn 235:478-489.

Berghmans S, Jette C, Langenau D, Hsu K, Stewart R, Look T, Kanki JP. 2005. Making waves in cancer research: new models in the zebrafish. Biotechniques 39:227-237.

Bitgood MJ, McMahon AP. 1995. Hedgehog and Bmp genes are coexpressed at many diverse sites of cell-cell interaction in the mouse embryo. Dev Biol 172:126-138.

Bitgood MJ, Shen L, McMahon AP. 1996. Sertoli cell signaling by Desert hedgehog

regulates the male germline. Curr Biol 6:298-304.

Bornemann DJ, Duncan JE, Staatz W, Selleck S, Warrior R. 2004. Abrogation of heparan sulfate synthesis in Drosophila disrupts the Wingless, Hedgehog and Decapentaplegic signaling pathways. Development 131:1927-1938.

Bourikas D, Pekarik V, Baeriswyl T, Grunditz A, Sadhu R, Nardo M, Stoeckli ET. 2005. Sonic hedgehog guides commissural axons along the longitudinal axis of the spinal cord. Nat Neurosci 8:297-304.

Briscoe J, Chen Y, Jessell TM, Struhl G. 2001. A hedgehog-insensitive form of patched provides evidence for direct long-range morphogen activity of sonic hedgehog in the neural tube. Mol Cell 7:1279-1291.

Bumcrot DA, Takada R, McMahon AP. 1995. Proteolytic processing yields two secreted forms of sonic hedgehog. Mol Cell Biol 15:2294-2303.

Butler EG. 1935. Studies on limb regeneration in X-rayed *Ambystoma* larvae. Anat. Rec. 62:295-307.

Byrd N, Becker S, Maye P, Narasimhaiah R, St-Jacques B, Zhang X, McMahon J, McMahon A, Grabel L. 2002. Hedgehog is required for murine yolk sac angiogenesis. Development 129:361-372.

Chang BE, Blader P, Fischer N, Ingham PW, Strahle U. 1997. Axial (HNF3beta) and retinoic acid receptors are regulators of the zebrafish sonic hedgehog promoter. EMBO J 16:3955-3964.

Chang DT, Lopez A, von Kessler DP, Chiang C, Simandl BK, Zhao R, Seldin MF, Fallon JF, Beachy PA. 1994. Products, genetic linkage and limb patterning activity of

a murine hedgehog gene. Development 120:3339-3353.

Charron F, Stein E, Jeong J, McMahon AP, Tessier-Lavigne M. 2003. The morphogen sonic hedgehog is an axonal chemoattractant that collaborates with netrin-1 in midline axon guidance. Cell 113:11-23.

Chen JK, Taipale J, Cooper MK, Beachy PA. 2002. Inhibition of Hedgehog signaling by direct binding of cyclopamine to Smoothened. Genes Dev 16:2743-2748.

Chiang C, Litingtung Y, Lee E, Young KE, Corden JL, Westphal H, Beachy PA. 1996. Cyclopia and defective axial patterning in mice lacking Sonic hedgehog gene function. Nature 383:407-413.

Chuang PT, Kawcak T, McMahon AP. 2003. Feedback control of mammalian Hedgehog signaling by the Hedgehog-binding protein, Hip1, modulates Fgf signaling during branching morphogenesis of the lung. Genes Dev 17:342-347.

Chuang PT, McMahon AP. 1999. Vertebrate Hedgehog signalling modulated by induction of a Hedgehog-binding protein. Nature 397:617-621.

Clark AM, Garland KK, Russell LD. 2000. Desert hedgehog (Dhh) gene is required in the mouse testis for formation of adult-type Leydig cells and normal development of peritubular cells and seminiferous tubules. Biol Reprod 63:1825-1838.

Cobourne MT, Sharpe PT. 2002. Expression and regulation of hedgehog-interacting protein during early tooth development. Connect Tissue Res 43:143-147.

Coelho CN, Sumoy L, Kosher RA, Upholt WB. 1992. GHox-7: a chicken homeobox-containing gene expressed in a fashion consistent with a role in patterning events during embryonic chick limb development. Differentiation 49:85-92.

Colnot C, de la Fuente L, Huang S, Hu D, Lu C, St-Jacques B, Helms JA. 2005. Indian hedgehog synchronizes skeletal angiogenesis and perichondrial maturation with cartilage development. Development 132:1057-1067.

Coulombe J, Traiffort E, Loulier K, Faure H, Ruat M. 2004. Hedgehog interacting protein in the mature brain: membrane-associated and soluble forms. Mol Cell Neurosci 25:323-333.

Coutelle O, Blagden CS, Hampson R, Halai C, Rigby PW, Hughes SM. 2001. Hedgehog signalling is required for maintenance of myf5 and myoD expression and timely terminal differentiation in zebrafish adaxial myogenesis. Dev Biol 236:136-150.

Currie PD, Ingham PW. 1996. Induction of a specific muscle cell type by a hedgehog-like protein in zebrafish. Nature 382:452-455.

Denef N, Neubuser D, Perez L, Cohen SM. 2000. Hedgehog induces opposite changes in turnover and subcellular localization of patched and smoothened. Cell 102:521-531.

Desbordes SC, Sanson B. 2003. The glypican Dally-like is required for Hedgehog signalling in the embryonic epidermis of Drosophila. Development 130:6245-6255.

Drummond IA. 2005. Kidney development and disease in the zebrafish. J Am Soc Nephrol 16:299-304.

Dyer MA, Farrington SM, Mohn D, Munday JR, Baron MH. 2001. Indian hedgehog activates hematopoiesis and vasculogenesis and can respecify prospective neurectodermal cell fate in the mouse embryo. Development 128:1717-1730.

Echelard Y, Epstein DJ, St-Jacques B, Shen L, Mohler J, McMahon JA, McMahon AP. 1993. Sonic hedgehog, a member of a family of putative signaling molecules, is implicated in the regulation of CNS polarity. Cell 75:1417-1430.

Ekker SC, McGrew LL, Lai CJ, Lee JJ, von Kessler DP, Moon RT, Beachy PA. 1995. Distinct expression and shared activities of members of the hedgehog gene family of Xenopus laevis. Development 121:2337-2347.

Ekker SC, Ungar AR, Greenstein P, von Kessler DP, Porter JA, Moon RT, Beachy PA. 1995. Patterning activities of vertebrate hedgehog proteins in the developing eye and brain. Curr Biol 5:944-955.

Fedtsova N, Perris R, Turner EE. 2003. Sonic hedgehog regulates the position of the trigeminal ganglia. Dev Biol 261:456-469.

Fu M, Lui VC, Sham MH, Pachnis V, Tam PK. 2004. Sonic hedgehog regulates the proliferation, differentiation, and migration of enteric neural crest cells in gut. J Cell Biol 166:673-684.

Geraudie J, Landis WJ. 1982. The fine structure of the developing pelvic fin dermal skeleton in the trout *Salmo gairdneri*. Am J Anat 163:141-156.

Glise B, Miller CA, Crozatier M, Halbisen MA, Wise S, Olson DJ, Vincent A, Blair SS. 2005. Shifted, the *Drosophila* ortholog of Wnt inhibitory factor-1, controls the distribution and movement of Hedgehog. Dev Cell 8:255-266.

Goetz JA, Suber LM, Zeng X, Robbins DJ. 2002. Sonic Hedgehog as a mediator of long-range signaling. Bioessays 24:157-165.

Goodrich LV, Johnson RL, Milenkovic L, McMahon JA, Scott MP. 1996.

Conservation of the hedgehog/patched signaling pathway from flies to mice: induction of a mouse patched gene by Hedgehog. Genes Dev 10:301-312.

Gorfinkiel N, Sierra J, Callejo A, Ibanez C, Guerrero I. 2005. The *Drosophila* ortholog of the human Wnt inhibitor factor Shifted controls the diffusion of lipid-modified Hedgehog. Dev Cell 8:241-253.

Greenspoon S, Patel CK, Hashmi S, Bernhardt RR, Kuwada JY. 1995. The notochord and floor plate guide growth cones in the zebrafish spinal cord. J Neurosci 15:5956-5965.

Haas H. 1962. Studies on mechanisms of joint and bone formation in the skeletal rays of fish fins. Dev Biol 5:1-34.

Han C, Belenkaya TY, Wang B, Lin X. 2004. *Drosophila* glypicans control the cell-to-cell movement of Hedgehog by a dynamin-independent process. Development 131:601-611.

Hu MC, Rosenblum ND. 2003. Genetic regulation of branching morphogenesis: lessons learned from loss-of-function phenotypes. Pediatr Res 54:433-438.

Hutchin ME, Kariapper MS, Grachtchouk M, Wang A, Wei L, Cummings D, Liu J, Michael LE, Glick A, Dlugosz AA. 2005. Sustained Hedgehog signaling is required for basal cell carcinoma proliferation and survival: conditional skin tumorigenesis recapitulates the hair growth cycle. Genes Dev 19:214-223.

Hynes M, Stone DM, Dowd M, Pitts-Meek S, Goddard A, Gurney A, Rosenthal A. 1997. Control of cell pattern in the neural tube by the zinc finger transcription factor and oncogene Gli-1. Neuron 19:15-26.

Incardona JP, Gruenberg J, Roelink H. 2002. Sonic hedgehog induces the segregation of patched and smoothened in endosomes. Curr Biol 12:983-995.

Ingham PW, McMahon AP. 2001. Hedgehog signaling in animal development: paradigms and principles. Genes Dev 15:3059-3087.

Jaskoll T, Leo T, Witcher D, Ormestad M, Astorga J, Bringas P, Jr., Carlsson P, Melnick M. 2004. Sonic hedgehog signaling plays an essential role during embryonic salivary gland epithelial branching morphogenesis. Dev Dyn 229:722-732.

Johnson SL, Weston JA. 1995. Temperature-sensitive mutations that cause stage-specific defects in Zebrafish fin regeneration. Genetics 141:1583-1595.

Koleva M, Kappler R, Vogler M, Herwig A, Fulda S, Hahn H. 2005. Pleiotropic effects of sonic hedgehog on muscle satellite cells. Cell Mol Life Sci 62:1863-1870.

Kratochwil K, Dull M, Farinas I, Galceran J, Grosschedl R. 1996. Lef1 expression is activated by BMP-4 and regulates inductive tissue interactions in tooth and hair development. Genes Dev 10:1382-1394.

Krauss S, Concordet JP, Ingham PW. 1993. A functionally conserved homolog of the *Drosophila* segment polarity gene hh is expressed in tissues with polarizing activity in zebrafish embryos. Cell 75:1431-1444.

Laforest L, Brown CW, Poleo G, Geraudie J, Tada M, Ekker M, Akimenko MA. 1998. Involvement of the sonic hedgehog, patched 1 and bmp2 genes in patterning of the zebrafish dermal fin rays. Development 125:4175-4184.

Laufer E, Nelson CE, Johnson RL, Morgan BA, Tabin C. 1994. Sonic hedgehog and Fgf-4 act through a signaling cascade and feedback loop to integrate growth and

patterning of the developing limb bud. Cell 79:993-1003.

Lee J, Platt KA, Censullo P, Ruiz i Altaba A. 1997. Gli1 is a target of Sonic hedgehog that induces ventral neural tube development. Development 124:2537-2552.

Lee JJ, von Kessler DP, Parks S, Beachy PA. 1992. Secretion and localized transcription suggest a role in positional signaling for products of the segmentation gene hedgehog. Cell 71:33-50.

Li Y, Zhang H, Choi SC, Litingtung Y, Chiang C. 2004. Sonic hedgehog signaling regulates Gli3 processing, mesenchymal proliferation, and differentiation during mouse lung organogenesis. Dev Biol 270:214-231.

Li YX, Zdanowicz M, Young L, Kumiski D, Leatherbury L, Kirby ML. 2003. Cardiac neural crest in zebrafish embryos contributes to myocardial cell lineage and early heart function. Dev Dyn 226:540-550.

Lo DC, Allen F, Brockes JP. 1993. Reversal of muscle differentiation during urodele limb regeneration. Proc Natl Acad Sci U S A 90:7230-7234.

Long F, Chung UI, Ohba S, McMahon J, Kronenberg HM, McMahon AP. 2004. Ihh signaling is directly required for the osteoblast lineage in the endochondral skeleton. Development 131:1309-1318.

Mabee PM, Bird NC. 2001. A preliminary description of the anatomy and development of the zebrafish axial skeleton. ZFIN Direct Data Submission.

Macdonald R, Barth KA, Xu Q, Holder N, Mikkola I, Wilson SW. 1995. Midline signalling is required for Pax gene regulation and patterning of the eyes. Development 121:3267-3278.

Machold R, Hayashi S, Rutlin M, Muzumdar MD, Nery S, Corbin JG, Gritli-Linde A, Dellovade T, Porter JA, Rubin LL, Dudek H, McMahon AP, Fishell G. 2003. Sonic hedgehog is required for progenitor cell maintenance in telencephalic stem cell niches. Neuron 39:937-950.

Makino S, Whitehead GG, Lien CL, Kim S, Jhawar P, Kono A, Kawata Y, Keating MT. 2005. Heat-shock protein 60 is required for blastema formation and maintenance during regeneration. Proc Natl Acad Sci U S A 102:14599-14604.

Marigo V, Johnson RL, Vortkamp A, Tabin CJ. 1996. Sonic hedgehog differentially regulates expression of GLI and GLI3 during limb development. Dev Biol 180:273-283.

Miller LA, Wert SE, Clark JC, Xu Y, Perl AK, Whitsett JA. 2004. Role of Sonic hedgehog in patterning of tracheal-bronchial cartilage and the peripheral lung. Dev Dyn 231:57-71.

Mohler J, Vani K. 1992. Molecular organization and embryonic expression of the hedgehog gene involved in cell-cell communication in segmental patterning of *Drosophila*. Development 115:957-971.

Morgan TH. 1901. Regeneration. The Macmillan Company, New York.

Muller F, Chang B, Albert S, Fischer N, Tora L, Strahle U. 1999. Intronic enhancers control expression of zebrafish sonic hedgehog in floor plate and notochord. Development 126:2103-2116.

Mullor JL, Guerrero I. 2000. A gain-of-function mutant of patched dissects different responses to the hedgehog gradient. Dev Biol 228:211-224.

Muneoka K, Sassoon D. 1992. Molecular aspects of regeneration in developing vertebrate limbs. Dev Biol 152:37-49.

Murciano C, Fernandez TD, Duran I, Maseda D, Ruiz-Sanchez J, Becerra J, Akimenko MA, Mari-Beffa M. 2002. Ray-interray interactions during fin regeneration of *Danio rerio*. Dev Biol 252:214-224.

Nechiporuk A, Keating MT. 2002. A proliferation gradient between proximal and msxb-expressing distal blastema directs zebrafish fin regeneration. Development 129:2607-2617.

Nusslein-Volhard C, Wieschaus E. 1980. Mutations affecting segment number and polarity in *Drosophila*. Nature 287:795-801.

Odelberg SJ. 2005. Cellular plasticity in vertebrate regeneration. Anat Rec B New Anat 287:25-35.

Odelberg SJ, Kollhoff A, Keating MT. 2000. Dedifferentiation of mammalian myotubes induced by msx1. Cell 103:1099-1109.

Olsen CL, Hsu PP, Glienke J, Rubanyi GM, Brooks AR. 2004. Hedgehog-interacting protein is highly expressed in endothelial cells but down-regulated during angiogenesis and in several human tumors. BMC Cancer 4:43.

Parmantier E, Lynn B, Lawson D, Turmaine M, Namini SS, Chakrabarti L, McMahon AP, Jessen KR, Mirsky R. 1999. Schwann cell-derived Desert hedgehog controls the development of peripheral nerve sheaths. Neuron 23:713-724.

Pepinsky RB, Zeng C, Wen D, Rayhorn P, Baker DP, Williams KP, Bixler SA, Ambrose CM, Garber EA, Miatkowski K, Taylor FR, Wang EA, Galdes A. 1998.

Identification of a palmitic acid-modified form of human Sonic hedgehog. J Biol Chem 273:14037-14045.

Poleo G, Brown CW, Laforest L, Akimenko MA. 2001. Cell proliferation and movement during early fin regeneration in zebrafish. Dev Dyn 221:380-390.

Porter JA, von Kessler DP, Ekker SC, Young KE, Lee JJ, Moses K, Beachy PA. 1995. The product of hedgehog autoproteolytic cleavage active in local and long-range signalling. Nature 374:363-366.

Porter JA, Young KE, Beachy PA. 1996. Cholesterol modification of hedgehog signaling proteins in animal development. Science 274:255-259.

Poss KD, Keating MT, Nechiporuk A. 2003. Tales of regeneration in zebrafish. Dev Dyn 226:202-210.

Poss KD, Shen J, Keating MT. 2000. Induction of lef1 during zebrafish fin regeneration. Dev Dyn 219:282-286.

Poss KD, Shen J, Nechiporuk A, McMahon G, Thisse B, Thisse C, Keating MT. 2000. Roles for Fgf signaling during zebrafish fin regeneration. Dev Biol 222:347-358.

Pu Y, Huang L, Prins GS. 2004. Sonic hedgehog-patched Gli signaling in the developing rat prostate gland: lobe-specific suppression by neonatal estrogens reduces ductal growth and branching. Dev Biol 273:257-275.

Quint E, Smith A, Avaron F, Laforest L, Miles J, Gaffield W, Akimenko MA. 2002. Bone patterning is altered in the regenerating zebrafish caudal fin after ectopic expression of sonic hedgehog and bmp2b or exposure to cyclopamine. Proc Natl Acad Sci U S A 99:8713-8718.

Ramirez-Weber FA, Kornberg TB. 1999. Cytonemes: cellular processes that project to the principal signaling center in *Drosophila* imaginal discs. Cell 97:599-607.

Riddle RD, Johnson RL, Laufer E, Tabin C. 1993. Sonic hedgehog mediates the polarizing activity of the ZPA. Cell 75:1401-1416.

Roelink H, Augsburger A, Heemskerk J, Korzh V, Norlin S, Ruiz i Altaba A, Tanabe Y, Placzek M, Edlund T, Jessell TM, et al. 1994. Floor plate and motor neuron induction by vhh-1, a vertebrate homolog of hedgehog expressed by the notochord. Cell 76:761-775.

Roeser T, Baier H. 2003. Visuomotor behaviors in larval zebrafish after GFP-guided laser ablation of the optic tectum. J Neurosci 23:3726-3734.

Sambrook J, Russell D. 2001. Molecular Cloning. Cold Spring Harbor, New York: Cold Spring Harbor Laboratory Press.

Santamaria JA, Becerra J. 1991. Tail fin regeneration in teleosts: cell-extracellular matrix interaction in blastemal differentiation. J Anat 176:9-21.

Santos-Ruiz L, Santamaria JA, Ruiz-Sanchez J, Becerra J. 2002. Cell proliferation during blastema formation in the regenerating teleost fin. Dev Dyn 223:262-272.

Sasaki H, Hui C, Nakafuku M, Kondoh H. 1997. A binding site for Gli proteins is essential for HNF-3beta floor plate enhancer activity in transgenics and can respond to Shh in vitro. Development 124:1313-1322.

Sasaki H, Nishizaki Y, Hui C, Nakafuku M, Kondoh H. 1999. Regulation of Gli2 and Gli3 activities by an amino-terminal repression domain: implication of Gli2 and Gli3 as primary mediators of Shh signaling. Development 126:3915-3924.

Schauerte HE, van Eeden FJ, Fricke C, Odenthal J, Strahle U, Haffter P. 1998. Sonic hedgehog is not required for the induction of medial floor plate cells in the zebrafish. Development 125:2983-2993.

Singer M. 1954. Induction of regeneration of the forelimb of the postmetamorphic frog by augmentation of the nerve supply. J. Exp. Zool 126: 419-472.

Sire JY, Akimenko MA. 2004. Scale development in fish: a review, with description of sonic hedgehog (shh) expression in the zebrafish (*Danio rerio*). Int J Dev Biol 48:233-247.

Song K, Wang Y, Sassoon D. 1992. Expression of Hox-7.1 in myoblasts inhibits terminal differentiation and induces cell transformation. Nature 360:477-481.

St-Jacques B, Hammerschmidt M, McMahon AP. 1999. Indian hedgehog signaling regulates proliferation and differentiation of chondrocytes and is essential for bone formation. Genes Dev 13:2072-2086.

Strahle U, Blader P, Henrique D, Ingham PW. 1993. Axial, a zebrafish gene expressed along the developing body axis, shows altered expression in cyclops mutant embryos. Genes Dev 7:1436-1446.

Strahle U, Blader P, Ingham PW. 1996. Expression of axial and sonic hedgehog in wildtype and midline defective zebrafish embryos. Int J Dev Biol 40:929-940.

Streisinger G, Walker C, Dower N, Knauber D, Singer F. 1981. Production of clones of homozygous diploid zebrafish (*Brachydanio rerio*). Nature 291:293-296.

Tabata T, Eaton S, Kornberg TB. 1992. The *Drosophila* hedgehog gene is expressed specifically in posterior compartment cells and is a target of engrailed regulation.

Genes Dev 6:2635-2645.

Taipale J, Chen JK, Cooper MK, Wang B, Mann RK, Milenkovic L, Scott MP, Beachy PA. 2000. Effects of oncogenic mutations in Smoothened and Patched can be reversed by cyclopamine. Nature 406:1005-1009.

Tanaka EM. 2003. Cell differentiation and cell fate during urodele tail and limb regeneration. Curr Opin Genet Dev 13:497-501.

Tashiro S, Michiue T, Higashijima S, Zenno S, Ishimaru S, Takahashi F, Orihara M, Kojima T, Saigo K. 1993. Structure and expression of hedgehog, a *Drosophila* segment-polarity gene required for cell-cell communication. Gene 124:183-189.

Testaz S, Jarov A, Williams KP, Ling LE, Koteliansky VE, Fournier-Thibault C, Duband JL. 2001. Sonic hedgehog restricts adhesion and migration of neural crest cells independently of the Patched- Smoothened-Gli signaling pathway. Proc Natl Acad Sci U S A 98:12521-12526.

Umehara F, Tate G, Itoh K, Yamaguchi N, Douchi T, Mitsuya T, Osame M. 2000. A novel mutation of desert hedgehog in a patient with 46,XY partial gonadal dysgenesis accompanied by minifascicular neuropathy. Am J Hum Genet 67:1302-1305.

van Genderen C, Okamura RM, Farinas I, Quo RG, Parslow TG, Bruhn L, Grosschedl R. 1994. Development of several organs that require inductive epithelial-mesenchymal interactions is impaired in LEF-1-deficient mice. Genes Dev 8:2691-2703.

van Tuyl M, Post M. 2000. From fruitflies to mammals: mechanisms of signalling via the Sonic hedgehog pathway in lung development. Respir Res 1:30-35.

Viviano C, Horton C, Maden M, Brockes J. 1995. Synthesis and release of 9-cis retinoic acid by the urodele wound epidermis. Development:3753-3762.

Vortkamp A, Lee K, Lanske B, Segre GV, Kronenberg HM, Tabin CJ. 1996. Regulation of rate of cartilage differentiation by Indian hedgehog and PTH-related protein. Science 273:613-622.

Warburton D, Bellusci S, De Langhe S, Del Moral PM, Fleury V, Mailleux A, Tefft D, Unbekandt M, Wang K, Shi W. 2005. Molecular mechanisms of early lung specification and branching morphogenesis. Pediatr Res 57:26R-37R.

Westerfield M. 1995. The zebrafish Book. University of Oregon Press.

White JA, Boffa MB, Jones B, Petkovich M. 1994. A zebrafish retinoic acid receptor expressed in the regenerating caudal fin. Development 120:1861-1872.

Whitehead GG, Makino S, Lien CL, Keating MT. 2005. fgf20 is essential for initiating zebrafish fin regeneration. Science 310:1957-1960.

Yuasa T, Kataoka H, Kinto N, Iwamoto M, Enomoto-Iwamoto M, Iemura S, Ueno N, Shibata Y, Kurosawa H, Yamaguchi A. 2002. Sonic hedgehog is involved in osteoblast differentiation by cooperating with BMP-2. J Cell Physiol 193:225-232.

Zardoya R, Abouheif E, Meyer A. 1996. Evolution and orthology of hedgehog genes. Trends Genet 12:496-497.

Zardoya R, Abouheif E, Meyer A. 1996. Evolutionary analyses of hedgehog and Hoxd-10 genes in fish species closely related to the zebrafish. Proc Natl Acad Sci U S A 93:13036-13041.

Zeng X, Goetz JA, Suber LM, Scott WJ, Jr., Schreiner CM, Robbins DJ. 2001. A freely diffusible form of Sonic hedgehog mediates long-range signalling. Nature 411:716-720.

Appendix I: Synthesis of RNA probes.

List of the restriction enzymes used to linearize each plasmid of interest and the type of RNA polymerase needed in order to synthesize an anti-sense RNA probe.

Plasmid names	Vector	Size of the probe	Restriction enzyme for linearization	RNA polymerase
Shh	pBS	2.5kb	EcoRI	T7
Ptc1	pBS	1.15kb	BamHI	T3
Hip	pDrive	2.0kb	HindIII	T7
Col10a1	pCRII	713b	XhoI	Sp6

Appendix II: Construct maps

- *Δhip* expression construct:

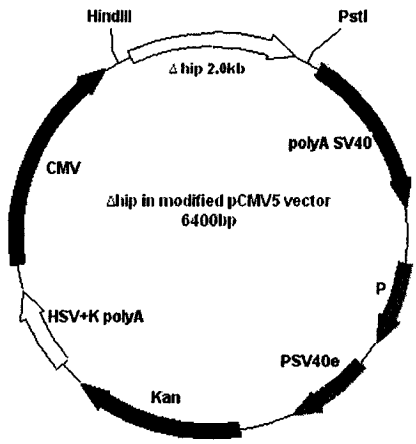

Full length *hip* cDNA is inserted in a modified version of pCMV5 vector (Department of Molecular and General Biochemistry, University of Texas, Southwestern Medical Center) at the restriction sites of *HindIII* and *PstI* under the control of the CMV promoter and followed by the SV40 polyA signal. For a description of the generation of the modified version of pCMV5 vector see Quint et al. (2002).

Control EGFP construct:

pEGFP-N1 encodes the Enhanced Green Fluorescence Protein (EGFP) which has been optimized for brighter fluorescence and higher expression than GFP. The expression of EGFP is under the control of the CMV promoter, making it a valid control for the Δhip expression construct.